THE UNIVERSITY OF MICHIGAN

INDUSTRY PROGRAM OF THE COLLEGE OF ENGINEERING

# CAVITATION DAMAGE TESTS WITH WATER IN A CAVITATING VENTURI

Frederick G. Hammitt
Visvaldis Biss
Paul T. Chu
Vincent F. Cramer
Richard D. Ivany
Robert D. Pehlke
M. John Robinson
Clarence A. Siebert

April, 1962

IP-562

ACKNOWLEDGEMENTS

The authors wish to acknowledge the contributions of the following research personnel of the University of Michigan, all of whom in addition to the authors, made significant contributions to the investigation: J. Brigham, L. Barinka, D. Goodell, R. Radius, E. Rupke.

The financial support of the NASA is acknowledged, and sincere thanks extended to William Wingstedt and Ronald Patterson of the Micrometrical Manufacturing Company for their assistance in the operation of that company's Linear Proficorder. Thanks are also extended to the company management for the loan of that machine.

FOREWORD

Cavitation has long been a serious problem for manufacturers and users of all forms of fluid-handling equipment, and all submerged marine appurtenances. On the other hand, cavitation has served useful purposes in various recent applications having to do with cleaning apparatus.

From a very general viewpoint, cavitation is merely one aspect of two-phase flow, and thus is closely related to boiling heat transfer and condensation phenomena, which are of great and rapidly increasing importance in modern technology. It is not possible at present to present a realistic theoretical treatment of the two-phase flow problem. However, research investigations either from the viewpoint of cavitation or of boiling heat transfer will assist toward this end.

As a purely fluid-dynamic phenomenon, cavitation is important because the efficiency of most fluid-handling components is reduced by its presence. However, it may be of even greater importance as a damaging mechanism to these components. It is this latter aspect of the phenomenon with which this report deals. In the past, cavitation-damage research has been much less emphasized than the fluid-dynamic performance aspect.

TABLE OF CONTENTS

TABLE OF CONTENTS (CONT'D)

LIST OF TABLES

LIST OF FIGURES

LIST OF FIGURES ( CONT'D )

LIST OF FIGURES (CONT'D)

# I. INTRODUCTION

An initial series of cavitation damage tests using water with carbon steel, stainless steel, aluminum, and plexiglass as test materials has been completed. Damage was produced on small test samples exposed to a cavitating field in a conical venturi diffuser. Test durations ranged up to 150 hours, and water velocities to 95 feet per second. It is the purpose of this report to present a summary of the observations which were made on the formation and nature of cavitation damage, and a compilation of the quantity of damage produced as a function of the flow and material parameters. These are then discussed in the light of the results of previous investigators.

Two major approaches have been followed in these studies:

i) Mechanism and Damage Form Study

Metallographic studies were conducted to trace the formation and development of pits on the damaged surface, and to observe the resulting changes in microstructure in the pitted areas. Also, the detailed configuration of the damaged portion has been in some cases, studied by a high precision "Linear Proficorder" which can measure the depth and contour of typical pits.[4,44]* Using the above approaches, a qualitative study of the form of the damage has been made.

ii) Gross Damage Measurements

Since the damage is in the form of surface pitting, its quantity is related to the number and size of the pits, and,

* Refer to numbers of items listed in Bibliography.

consequently, to the weight loss of the test specimens. The number of pits in various size categories has been tabulated using low power magnification (100x). The weight loss has then been calculated from an approximate relation between mean pit diameter and pit volume, which was obtained statistically from the proficorder analysis.[4,44]

A radioactive tracer technique has also been developed to measure the weight loss,[45] and thus to check the values calculated from pit counts as well as the general trends which were indicated. In addition, direct weighing of the test specimens has been utilized where feasible. Generally an accurate determination of weight loss has not been possible in the water tests because of the limited material damage encountered during reasonable durations.

## II. WORK OF PREVIOUS INVESTIGATORS PRESENT STATE OF KNOWLEDGE

A considerable literature on cavitation damage exists. This can be divided into categories according to the method of production of the damage and the methods of observation of the damage produced. Methods of damage production include:

i) Field operation of full scale machines.

ii) Laboratory operation of cavitating flow devices as venturis, modified venturis, test specimens in fluid tunnels, etc.

iii) Devices which impact a fluid jet upon a test specimen producing damage similar to that of "true cavitation."

iv) Laboratory operation of devices producing a high frequency pressure oscillation in the fluid. In this category, magnetostrictive and ultra-sonic devices are included.

All of the above produce a similar form of pitting. It is difficult, however, in most of these cases, to relate results in a quantitative fashion to results actually observed in operating machines. The methods are arranged in approximate order of similarity to actual operating results in the above tabulation.

Examination of the damage is generally of one or both of the following types:

i) Gross measurements, as weight loss or surface appearance.

ii) Detailed surface examination employing techniques of metallography, and x-ray diffraction.

The first approach is certainly the most common, but of limited usefulness.

At the present time, the general state of knowledge of this subject might be summarized in the following terms:

i) Mechanical-impact forces generated by bubble implosions are a substantial, and in some cases, the only substantial, cause of the observed pitting.

ii) In many cases corrosion or other chemical effects are significantly involved.

iii) In some cases the damage of the metal at the surface resembles fatigue-type failure. Cracks of the fatigue-type have been photographed, as well as slip-lines indicative of plastic distortion beneath pitted regions.

iv) In some cases, the pitting appears to be the result of single implosions which form symmetrical crater-like depressions, surrounded by a rim of raised metal.

v) The quantity of damage ( in terms of weight loss ) is generally decreased as the hardness or tensile strength of the material is increased, provided, at least, that this is not accomplished by increasing the susceptibility to corrosion. Also, there may be additional complicating factors which are significant to a lesser extent.

vi) Prediction of damage from a knowledge of the fluid, flow, and material parameters is not presently possible. Also, a reliable correlation between results obtained from oscillator-type devices or impact devices, and flowing systems is not available.

There are in addition many theories, indications, observations, etc., relating to the cavitation damage phenomenon, but the above summarizes those aspects upon which it is believed that general agreement can be obtained.

A. Specific Investigations

Investigations of cavitation damage date from the early 1900's when its effects were first noted upon propellers of naval vessels. Those investigations attained a very precise character in the early and mid-1930's with the work in Germany of Schroter,(40) Nowotny,(27) and others. Schroeter developed a technique, using a modified venturi, for rapidly producing damage in a flowing system. This device was later utilized in this country by Boetcher(3) and Mousson(24) at the laboratories of the Safe Harbor Water Power Corporation.* At approximately the same time an investigation by Hunsaker, Spannhake, and others,(12) using a more conventional venturi was underway at MIT. The work of Boetcher and Mousson particularly was developed to a considerable degree in the direction of metallographic examinations of the damaged specimens. This included the photographic observation of apparent fatigue lines in the surface, of slip lines beneath the deformed area, and of a small "slab" of material, presumably loosened by fatigue, and about to be peeled from the surface by the through-velocity. Tests with copper were made to determine the effect of grain size with the tentative result that a large-grained specimen suffered a weight loss eleven times that of a small-grained specimen. Both were of equal hardness and

* Conestoga, Pennsylvania

neither appeared corroded. In addition, gross information regarding the effects of hardness, fluid velocity, time, etc., were presented.

The somewhat parallel investigation at MIT concentrated more on a description of the flow phenomena in the venturi and produced little in the way of damage results.

While these investigations shed much light on the nature of the cavitation pitting process, they do not allow any prediction of the degree of damage to be expected from a cavitation regime described in terms of the flow parameters. Also, they seem to ignore the observable formation of craters presumably by single-bubble actions (as opposed to fatigue).

From about this period, almost until the present, detailed metallographic studies appear to have been somewhat neglected except for the group at CIT where use was made of x-ray diffraction techniques and tests were run on single-crystal materials [Plesset,[30] Ellis[5]] to demonstrate that plastic deformation occurred very early in the damage process. However, there is some recent work more or less of a confirmatory type as far as the earlier investigations are concerned by Rao et al.,[37] Leith,[20] and Wheeler.[46] There is also the work which has been started in the present University of Michigan investigation.

Nonetheless, there has been no dearth of cavitation research during the above period. The major portion of the research, however, has been concerned with fluid-dynamic effects, bubble dynamics, acoustics, etc. Theoretical bubble dynamics are, of course, of major importance to an understanding of the cavitation damage process, and considerable progress has been made in this field, especially the work of

Plesset,[30,31] and Naude and Ellis,[25] and Knapp and Hollander.[16] However, the present report is not concerned primarily with this aspect which will be discussed in subsequent documents.

Cavitation damage research from the mid-1930's to the early 1960's has largely been divided into the two following categories:

i) Gross damage results produced by piezoelectric oscillators, magnetostrictors, etc., or impacting jets, (References 11, 14, 20, 39, and 46 are typical) wherein the objective was the determination of the relative cavitation resistance of different materials, and of the same materials under different conditions of the macroscopic mechanical properties such as hardness, tensile strength, etc. While much data of this type has resulted, there has always been the question of its applicability to flowing systems with "conventional" cavitation.

ii) Single-pit observations by Knapp,[17,18] on fully-annealed aluminum specimens which were exposed to a cavitating field in a water tunnel and later imbedded in a turbine blade in a field test. These observations emphasized the single-blow formation of symmetrical craters. Data was presented on the effects of through-velocity which showed an approximate dependence on velocity to the 6th power.* This great

* An alternative formulation has been suggested by Ackeret[1] wherein, following Honegger, it is suggested that Wgt. Loss = (V - Const.)$^2$, reflecting the observation in some cases of a "threshhold velocity".

sensitivity to velocity has been confirmed by Hobbs[11] using a jet-impact device (5th power variation), and Kerr[15] reporting on the erosion of a radioactive paint from water-turbine blades in field tests (5th to 7th power variation). However, as will be discussed later, the results from the present University of Michigan investigation show smaller values of "best-fit" exponents, which depend considerably on variations in the test parameters and materials.

An interesting recent contribution to this general field is that of Rao et al.[37] An idealized model has been proposed in an attempt to predict the degree of damage to be expected from a given flow regime in a given geometry. This involves an assumption of energy available per bubble to be applied to the deformation of the metal surface, based on an assumed uniform bubble size prior to collapse, and an assumed frequency of bubble generation based on the observations of Hunsaker[12] that the Strouhal number, $fL/V_o$ could be considered a constant ($L$ is the length of the cavitating region, $f$ the frequency of bubble generation in the region, and $V_o$ the unperturbed through-velocity). While these assumptions appear to be considerably oversimplified, an interesting approach is afforded.

Many of the previous investigators have observed or assumed an "incubation period" during which no damage was produced, and then a fairly linear variation of weight loss with time, at least until very gross damage resulted. This is explained on the basis of a required

preconditioning before the fatigue limit is reached at a given location on the surface, and actual material failure occurs. (Of course, this should not be anticipated if single-blow cratering is the mechanism of major importance.) As will be explained in a later section, this is somewhat at variance with the observations of the present investigation, and may have resulted in part from an inability in the previous investigations to detect small weight losses with available weighing techniques. An exception to the investigations showing an incubation period is that by Kerr[15] where the decrease in radioactivity from a paint containing radioisotopes and applied to the blades of an hydraulic turbine in service, was measured. A continuous increasing loss from the time of the initiation of the test was observed.

The previous discussions have been generally based on the hypothesis that damage results from the application of mechanical forces to the material, perhaps aided in some cases by corrosion. However, other theories have been advanced from time to time which have not been entirely disproved. A review of the evidence, pro and con, relating to these various theories may be desirable.

## B. Evidence for Mechanical Action Hypotheses

The assumption that cavitation damage is caused by very high (local as well as transient) pressures, generated by the collapse of bubbles, either substantially empty or filled with condensible vapor, as the bubbles are swept into a region of sufficiently high external pressure to cause collapse, dates from Lord Rayleigh's[38] pioneering analysis. Considering merely the balance between pressure and inertial

forces, he showed that an infinite pressure would exist at the point of final collapse if the fluid were incompressible. If the compressibility of a conventional liquid were considered, pressures still well in excess of the ultimate stress of most materials were likely.

An earlier and less comprehensive analysis by Parsons and Cook[28] had visualized the inrush of liquid into a collapsing bubble against a small solid sphere at the center. The resulting pressures were of the order of magnitude derived by Rayleigh. Both models of course consider a water-hammer type phenomenon.

In a subsequent analysis, Beeching[2] added the effect of surface tension to the Rayleight model, showing that in most cases this was not of major importance, even toward the end of the collapse. Typical pressures at the seat of collapse, according to his model, ranged from 100,000 to 1,000,000 psi.

A further modification was made by Silver,[41] who introduced various approximations to provide for the removal of the latent heat through the surrounding liquid as the bubble collapse was completed. He postulated that the final collapse would in fact be controlled by the rate of condensation of the vapor, which was in turn controlled by the removal of latent heat. On this basis the calculated final pressures were on the order of 10,000 psi, sufficient to cause fatigue-type damage to certain materials, and not to others. However, the theoretical model appears very approximate, so that it is questionable whether the numbers so derived should be considered as realistic. However, the mechanisms suggested certainly must be considered.

Additional theoretical analyses have been made by Plesset,[30] Poritsky,[34] and Gilmore.[6] Various simplifying assumptions are made in all cases, but the results generally confirm those previously quoted, i.e.: there is a likelihood of the development of local and transient pressures of sufficient magnitude to damage almost any material. The papers by Poritsky[34] and Gilmore[6] are of especial interest in their discussion of the fact that for spherically symmetrical laminar flow the equation of motion does not contain the viscosity. This apparent paradox is resolved by noting that the pressure boundary condition for the fluid adjacent to the cavity is affected. The mean pressure at this point is not the principal normal stress in the radial direction, but is increased over the pressure in the cavity (even assuming negligible surface tension) by the shear stress which is proportional to viscosity.

It is apparent from the preceding discussion, that the difficulty in obtaining meaningful appraisals of the pressures which might be generated in bubble collapse stems from uncertainties as to that portion of the collapse in which the radius is approaching zero. In this connection the following points may be made:

i) While the assumptions of thermodynamic equilibrium, zero surface tension, incompressible liquid phase, inviscid fluid, and spherical symmetry may be tenable for relatively large bubbles (this was demonstrated experimentally by Knapp and Hollander whose high-speed motion pictures of bubble collapse approximately matched Rayleigh's calculations), it is not at all certain that any of these

assumptions are valid at the end of collapse. However, it is in just this portion of the collapse that the pressures necessary to cause structural damage must originate.

ii) The assumed model of a spherical collapse may not be realistic at least toward the end of collapse. The possibility of a non-spherical collapse was postulated by Kornfeld and Suvorov[19] and shown to be mathematically possible by Plesset,[33] who demonstrated the instability of a spherical collapse. In a certain configuration, non-spherical collapses were actually photographed by Naude and Ellis.[25] Of course, none of this can be taken as proof that non-spherical collapses are generally the case.

Experimentally, it has been shown (Plesset and Ellis,[31] Ellis,[5] Poulter,[35] and others) that damage can be caused with liquids and materials which are chemically inert to each other, at least under ordinary circumstances. However, as will be discussed later, if there is the possibility of very high temperatures at the seat of collapse, the assumption of chemical inertness may not be justified. Nevertheless, it seems fairly strongly indicated that the mechanical action is at least one of the major contributory mechanisms to cavitation damage. However, the available tests do not prove that it is the only such mechanism.

It has also been observed experimentally, that large, symmetrical craters are formed in cavitation regions (although the damage is not

exclusively of this type). Such craters have been reported by Knapp[17] in tests on fully-annealed aluminum with water, and have been observed by the present investigators (discussed in detail later) in tests with water on aluminum, carbon steel, and austenitic stainless steel. The symmetry of these craters, and their lack of change through subsequent testing, strongly suggests that they are the result of a single blow, presumably implying the existence of a transient pressure well in excess of the yield strength of the material (order of 35,000 psi for the stainless steel).

Finally, stress patterns have been observed in photoelastic material by Naude and Ellis,[25] at the seat of collapse of bubbles which were photographed simultaneously. Pressures resulting from a similar test were measured with a piezo-electric crystal by Jones et al,[13] indicating stresses of the magnitude required to explain the observed damage effects ($\sim$ 150,000 psi.).[13]

In summary, the evidence clearly seems to indicate that under some conditions at least, pressures are generated at the site of bubble collapse of sufficient magnitude to cause the pitting which is observed. However, it is not indicated, nor does it seem true, that other factors do not in some cases also contribute significantly to the formation of damage.

## C. Alternative and/or Complimentary Damage Hypotheses

Several damage hypotheses which can be considered as alternative and/or complimentary to the mechanical action hypothesis are listed

below:

i) Conventional corrosion

ii) Accelerated corrosion caused by local high temperatures induced by bubble collapse. Such corrosion may be a result of dissociation[42] of the fluid under high temperature, or simply increased chemical potentials.

iii) Accelerated corrosion due to galvanic action resulting from changes in galvanic potentials due to cold-work[29] or to thermoelectric action resulting from local heating.[26]

iv) Local weakening of material due to high local temperatures caused by bubble collapse.[47]

v) Liquid penetration into small crevices under high pressure, subsequently exploding particles from surface when pressure is released.[35] A related hypothesis suggested in the same reference is the penetration of hydrogen, from the dissociation of water under high temperature and pressure, into crevices in the material, causing hydrogen-embrittlement and subsequent failure in steels.

It is impossible to prove at the present time that any of the above may not be significant and it is obvious that some of them are important under certain conditions. For example, it seems clear that, with certain materials, susceptibility to corrosion is certainly a factor in determining damage rates in a cavitating flow. An obvious instance is the development of pitting around certain portions of the running gear

of ships in sea-water, where velocities appear in some cases to be too low to cause significant cavitation damage in the absence of corrosion. As discussed in recent papers by Prieser and Tytell,[36] and Lichtman, et al.,[22] it is not surprising that the pitting is largely suppressed by relatively low level cathodic protection. As another example, tests conducted in the present investigation using carbon steel in water showed the formation of corrosion products around the pitted areas, clearly implying a type of stress-corrosion, thus apparently weakening the material and increasing the rate of wear in the cavitating flow regime. Present work at CIT[32] is aimed at evaluating this effect by subjecting specimens to periodic bursts of (magnetostrictive) cavitation while they are maintained continuously under water. It is found that the rate of damage is a function not only of the duration of the cavitation, but also of the portion of the total exposure time to the fluid which it represents.

It is noted that many of the mechanisms listed above depend upon the existence of a local high temperature at the point of damage. As often suggested in the past, such a temperature would result if, in the final stages of collapse, the bubble were filled with a non-condensible gas which would then be compressed to high pressure. In the present absence of quantitative numbers, it seems probable that heat transfer rates would not be sufficient to remove the heat fast enough to prevent the collapse becoming virtually adiabatic. This would be the case even though the bubble contained only the vapor phase of the liquid, since condensation of the vapor (even if it were permissible to assume thermodynamic

equilibrium over such a rapid transient) would require the maintenance of sufficiently low temperature in the surrounding liquid, and hence adequate heat transfer rates from the vicinity.

An apparent difficulty of damage hypotheses related to the above mechanism, if it is assumed that the test material reaches a high temperature, is the transfer of sufficient heat from the gas to the solid. Such transfer would contradict the assumption of an adiabatic collapse. There also appears to be a difficulty related to the large discrepancy in volumetric specific heat and conductivity between the solid and the gas.

If the mechanism relates only to the heating of the vapor itself, or the immediately adjacent liquid, resulting in dissociation or increased chemical potential, the above objections may not be valid.

A somewhat similar mechanism has been hypothesized by Wheeler,[46] wherein he suggests that a high local temperature is created in the solid by the deformation energy received from the collapsing bubble. If such a high temperature in fact existed, it could be responsible for a weakening of the material, allowing greater deformation than otherwise expected from a given imposed pressure, or for increased corrosion.

At present, all the high-temperature theories remain merely hypotheses since no confirmatory measurements have been made. This appears to be a difficult task due to the extremely local and transient nature of the anticipated phenomenon. However, in this connection it is interesting to note that discoloration, similar in appearance to "temper blueing" has been noted in the present, as well as several of the past[23,32,46] investigations.

## III. THE EXPERIMENTAL PROCEDURE

### A. General

The detailed construction of the overall test facility has been previously described.[10] However, those details especially pertinent to the damage program are repeated here for convenience.

A cavitating field is generated in the diffusing section of the damage test venturi (Figure 1, 2) where a pair of specimen holders (Figure 3) are located. Test condition; i.e.: degree of cavitation (see Appendix A), flow rate, temperature, and static pressure can be varied independently over a wide range. The specimen is approximately 3/4" x 1/16" x 1/2" in size and is tapered front and back to present a reasonably stream-lined profile (Figure 4 and 5) to minimize the cavitation induced locally by the test section. The area of the portion exposed to cavitation is approximately 3/4" x 1/16" on the polished face and 3/4" x 3/16" on each side.

### B. Preparation of Specimens

The procedure for preparation of the specimens is as follows. Twelve specimens, milled to the desired size, are placed in a steel fixture. The controlled surface, (Figures 4 and 5), after milling, is polished with a set of abrasive wheels of increasing fineness. A fine diamond polish is applied last. For the stainless steel specimens, syntron polishing for about an hour is used. However, for the carbon steel and aluminum samples, this last step often causes so-called "syntron defect" (formation of wavy surface due to the fine polish) and is therefore omitted. The polished specimens are then screened by examination

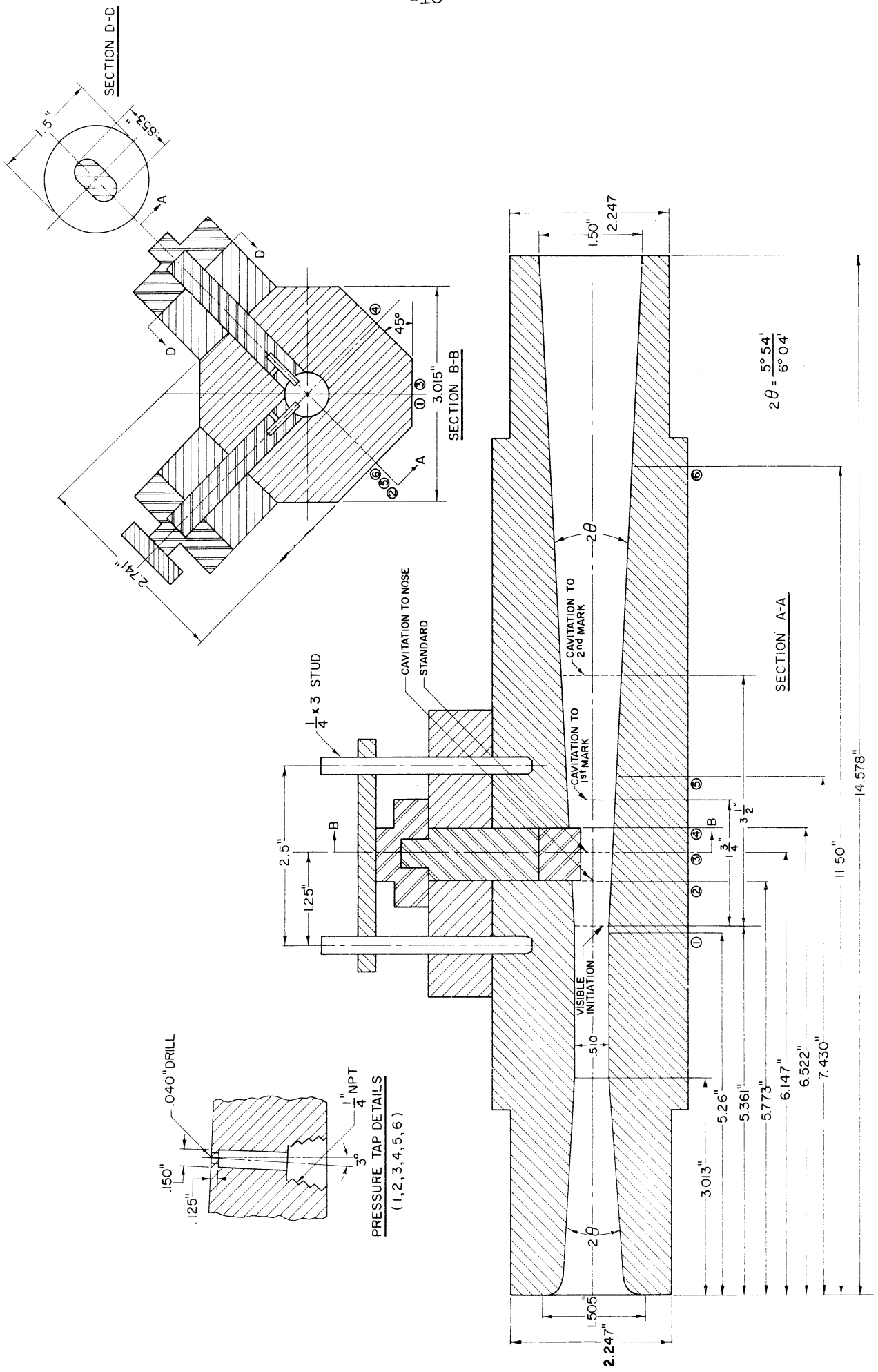


Figure 1. Drawing of the damage test venturi showing location of specimens and specimen holders. The dotted lines represent location of cavitation termination for various degrees of cavitation.

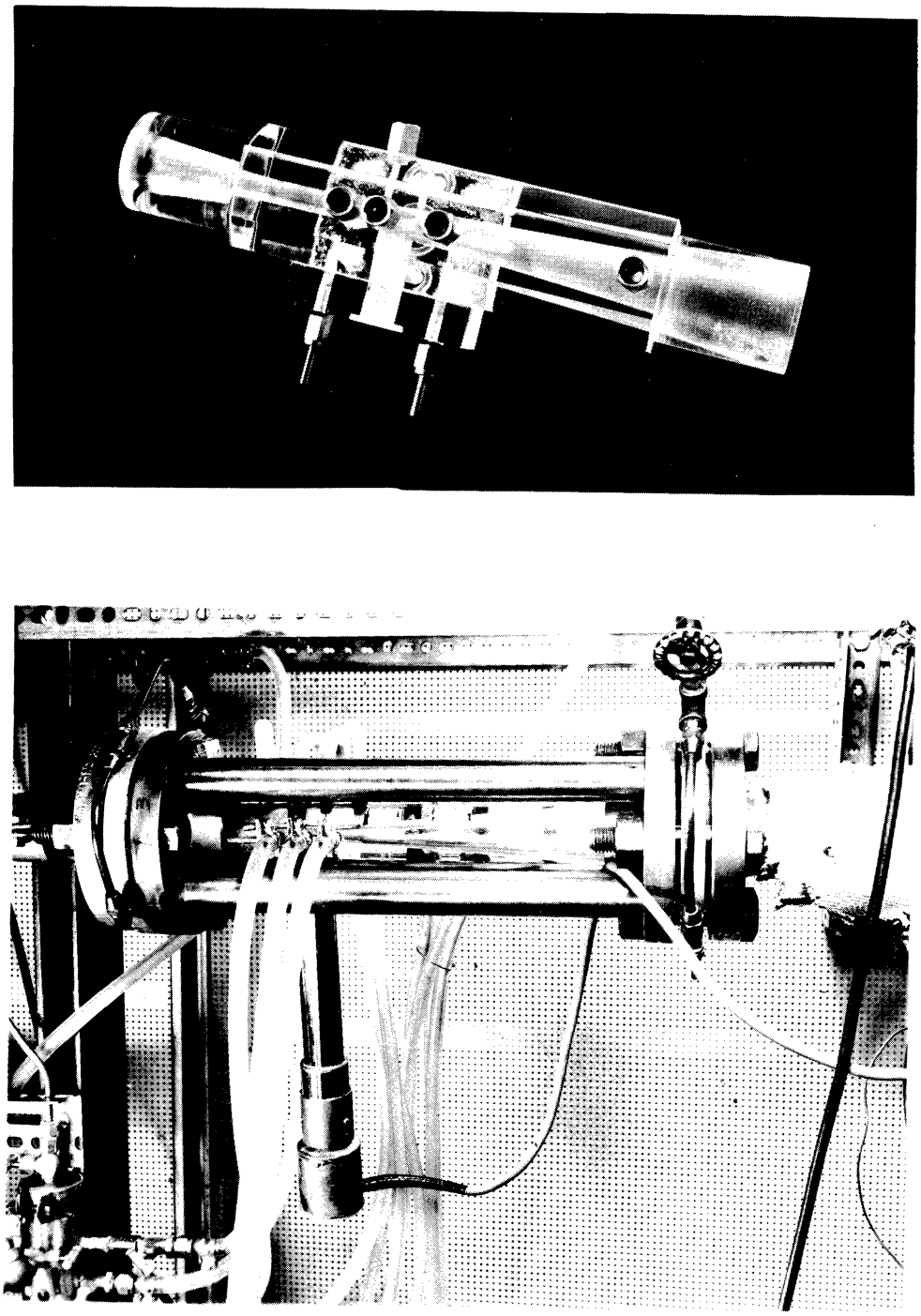

Figure 2. Photograph of damage test venturi (upper) and of venturi installed in test facility (lower)

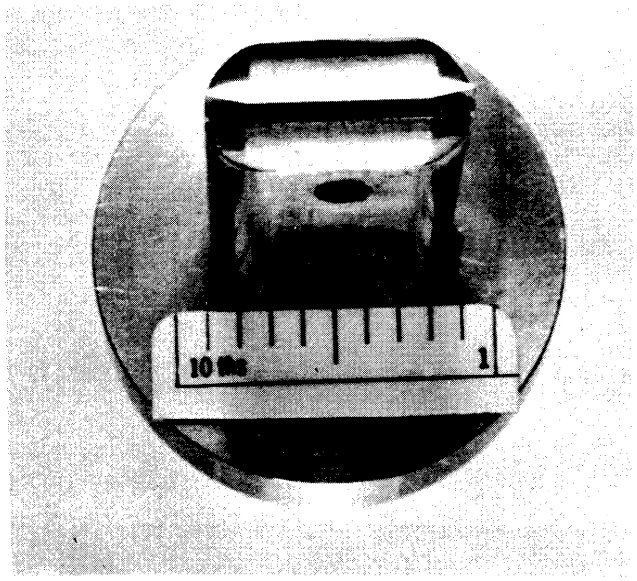

Figure 3. Photograph of specimen holder with test specimen in place.

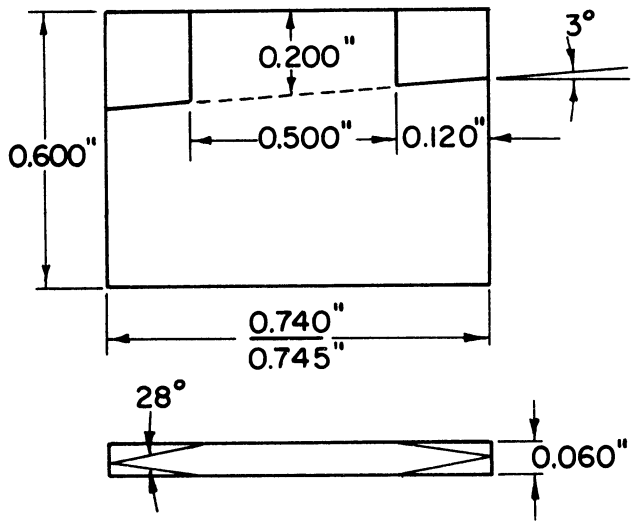


Figure 4. Drawing of test specimen.

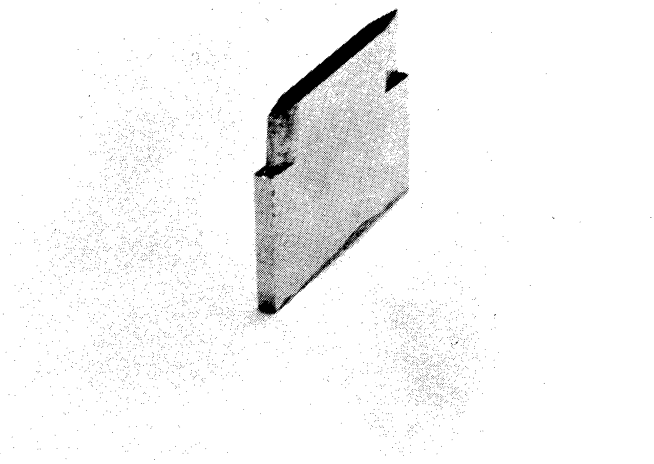

Figure 5. Photograph of test specimen. The upper shadowed surface is the polished surface.

under a 100x metallographic microscope. Those specimens with more than about fifteen small (~1 mil) pits away from the edges, or with numerous irregularities along the edges, are rejected, and returned for re-polishing. If they are accepted for test, the initial pit count is tabulated according to pit size.

The specimens in the holder protrude approximately 0.2 inches into the stream from the wall of the diffuser with the controlled surface parallel to the axis of the venturi (Figure 1 and 4). They are exposed in a prescribed cavitating field (degree of cavitation, temperature, and velocity) for a measured length of time, after which the controlled surface is examined under the optical system used initially for pit-counting and classification. Generally, only the polished surface has been examined for pitting, although it is only about 1/9 the total exposed area. Hence weight loss calculations using extrapolations based on the polished surface can only be considered semi-quantitative at best.

Some arbitrarily chosen localities (chosen to illustrate interesting pits, etc.) are photographed at the time of pit counting in order to observe the development of local damage. The specimen is then returned to the venturi for additional exposure to the cavitation field. About sixty specimens have been tested in this fashion in water.

C. Pit Counting Procedure

The pit counting and tabulating process is admittedly subject to error. It is fortunate, however, that the major portion of the weight loss derives from the large pits,* which can be counted quite reliably.

* An example of the relative significance of large and small pits has been given previously.(44)

Thus, in the early stages of the test when the number of pits is small, visual counting is quite precise. As the experiment proceeds, the large pits are still countable to high accuracy, but a certain error is involved in the overall count due to the presence of very large numbers of small pits. A method for measuring the weight loss to a very high accuracy so that a comparison can be made (at least for one or two check points) and the percent of error from visual counting estimated is extremely desirable but very difficult to attain.

The microscope used for pit-counting is equipped with a micrometer eyepiece (with accurate grid lines) for classifying the pits. The pits have been classified into various categories; i.e.: small (less than 1.5 mil average diameter), large (between 1.5 and 3.0 mil), and very large (from 3.0 to 10.0 mil) etc. Very seldom has a pit larger than 10.0 mil been found, although in some cases eventual superposition of pits produces a single depression of such dimensions. The pits are not necessarily circular, although in a significant proportion of cases nearly circular craters occur as will be discussed later.

In general, it is possible to assign an approximate representative diameter to each pit.

## D. Test Parameters

### 1. General

At least five physical variables are of practical interest; i.e.: temperature, air content, throat velocity, cavitation condition, and local pressure (only two out of the last three variables are independent in a fixed geometry). However, the effect of the condition of the water has

not yet been fully investigated. With only one exception, the temperature of the water has been about 70°F, and in most cases, the water has been approximately saturated with air but has been settled over a long period so that entrained air is minimized. A single run was made with substantial entrained air and compared directly to another run wherein the water had been de-aerated to about 50% saturation at STP. Within the small range of air content and temperature variation, and within the precision of the results, few conclusions on the effects of the variation of these variables can be drawn. The main emphasis to date has been the study of the damage rate as a function of degree of cavitation and throat velocity, using tap water (pH~10) at room temperature as the medium. Five degrees of cavitation (see Appendix A) have been used covering a range from incipient to well-developed cavitation, extending well beyond the trailing edge of the specimen. The velocity has been varied from a minimum of 55 fps to a maximum of 100 fps.* The definition of degree of cavitation is given in Appendix A and illustrated in Figure 1. The conditions of the various runs are listed in Table I.

2. Actual Flow at Test Specimen

As a first approximation it has been assumed that the flow conditions felt by the test specimen are the same as those generally existing at the applicable axial position in the venturi; i.e.: the flow is essentially one-dimensional. Since the test specimens block only about 8% of the flow area, it has been assumed as a first approximation that

* Minimum is controlled by the requirement of diffusing from throat pressure up to pump sump pressure (about atmospheric) and maximum by available pump head at maximum pump speed.

TABLE I

LISTING OF CAVITATION RUNS AND DAMAGE DATA

CAVITATION DAMAGE DATA PROCESSING ... TESTS

| RUN NO. | | CONTROLLED SURFACE PERCENT DAMAGED AREA | EXTRAPOLATED WEIGHT LOSS *10E-08 GRS. | EXTRAPOLATED WEIGHT LOSS *10E-08 GRS. | ORIGINAL DATA Small | Large | Very Large | Vol. Loss/Area $cm^3/cm^2 \times 10^6$ | Cavitation Condition | Throat Velocity ft/sec |
|---|---|---|---|---|---|---|---|---|---|---|
| 326.001 | | .7320E 00 | .1105E 04 | .9599E 04 | 105.00 | 41.00 | 2.00 | 5.63 | Standard | 97.2 ft/sec |
| 326.003 | | .4164E 01 | .3344E 04 | .2906E 05 | 2490.00 | 60.00 | 5.00 | 17.05 | " | " |
| 326.012 | | .3711E 01 | .6691E 04 | .5814E 05 | 590.00 | 149.00 | 17.00 | 34.11 | " | " |
| 323.001 | | .3864E 00 | .5733E 03 | .4981E 04 | 56.00 | 22.00 | 1.00 | 2.92 | " | " |
| 323.003 | | .2211E 01 | .1865E 04 | .1621E 05 | 1290.00 | 33.00 | 3.00 | 9.51 | " | " |
| 323.012 | | .3628E 01 | .6376E 04 | .5540E 05 | 640.00 | 143.00 | 16.00 | 32.5 | " | " |
| 310.001 | * | .2131E 00 | .4019E 03 | .3492E 04 | 2 00 | 10.00 | 1.00 | 2.05 | Standard | 64.7 ft/sec |
| 309.001 | * | .8 48 01 | 5 E | 6599E 03 | 24.00 | 5.00 | .00 | 0.387 | " | " |
| 306.001 | † | .2142E 00 | .3855E 03 | .3350E 04 | 38.00 | 8.00 | 1.00 | 1.97 | Standard | |
| 311.001 | † | .1074E 00 | .1025E 03 | .8905E 03 | 26.00 | 7.00 | .00 | 0.522 | " | |
| 314.035 | | .2966E 00 | .4779E 03 | .4152E 04 | 44.00 | 15.00 | 1.00 | 2.44 | Standard | 64.7 ft/sec |
| 315.035 | | .2632E 00 | .4391E 03 | .3815E 04 | 43.00 | 12.00 | 1.00 | 2.24 | | " |
| 318.035 | | .1054E 01 | .7834E 03 | .6807E 04 | 649.00 | 15.00 | 1.00 | 3.994 | Cav. to Nose | 64.7 ft/sec |
| 318.145 | | .8392E 00 | .1080E 04 | .9388E 04 | 259.00 | 33.00 | 2.00 | 5.508 | " | " |
| 318.265 | | .8145E 00 | .1011E 04 | .8787E 04 | 299.00 | 26.00 | 2.00 | 5.155 | " | " |
| 318.515 | | .1439E 01 | .3086E 04 | .2681E 05 | 139.00 | 50.00 | 9.00 | 15.73 | " | " |
| 319.035 | | .6071E 00 | .7300E 03 | .6343E 04 | 164.00 | 30.00 | 1.00 | 3.721 | " | " |
| 319.145 | | .8856E 00 | .1099E 04 | .9550E 04 | 296.00 | 33.00 | 2.00 | 5.603 | " | " |
| 319.265 | | .1310E 01 | .1895E 04 | .1386E 05 | 476.00 | 44.00 | 3.00 | 8.132 | " | " |
| 319.515 | | .1678E 01 | .3275E 04 | .2846E 05 | 236.00 | 61.00 | 9.00 | 16.70 | " | " |
| 316.035 | | .5754E 00 | .5397E 03 | .4689E 04 | 318.00 | 9.00 | 1.00 | 2.751 | First Mark | 64.7 ft/sec |
| 317.035 | | .3038E 00 | .1648E 03 | .1432E 04 | 200.00 | 5.00 | .00 | .8402 | " | " |
| 336.035 | | .8756E 00 | .8298E 03 | .7210E 04 | 387.00 | 29.00 | 1.00 | 4.230 | Visible | 64.7 ft/sec |
| 336.155 | | .1497E 01 | .1738E 04 | .1510E 05 | 557.00 | 92.00 | 3.00 | 8.859 | " | " |
| 336.275 | | .1953E 01 | .2125E 04 | .1846E 05 | 717.00 | 76.00 | 3.00 | 10.83 | " | " |
| 336.385 | | .1633E 01 | .2719E 04 | .2362E 05 | 407.00 | 52.00 | 7.00 | 13.86 | " | " |
| 336.508 | | .2790E 01 | .5123E 04 | .4452E 05 | 387.00 | 117.00 | 13.00 | 26.12 | " | " |

| | | | | | | | | | | |
|---|---|---|---|---|---|---|---|---|---|---|
| 335.035 | .7359E 00 | .6551E 03 | .5693E 04 | 395.00 | 15.00 | 1.00 | 3.340 | Visible | 64.7 ft/sec | |
| 335.155 | .5390E 00 | .6180E 03 | .5369E 04 | 195.00 | 20.00 | 1.00 | 3.150 | " | " | |
| 335.275 | .1442E 01 | .1665E 04 | .1447E 05 | 565.00 | 46.00 | 3.00 | 8.490 | " | " | |
| 335.385 | .7466E 00 | .1619E 04 | .1407E 05 | 110.00 | 19.00 | 5.00 | 8.254 | " | | |
| 335.508 | .1623E 01 | .3383E 04 | .2940E 05 | 230.00 | 49.00 | 10.00 | 17.25 | " | " | |
| 334.035 | .4228E 00 | .4950E 03 | .4301E 04 | 179.00 | 11.00 | 1.00 | 2.523 | Sonic | 64.7 ft/sec | |
| 333.035 | .2188E 00 | .1474E 03 | .1281E 04 | 115.00 | 7.00 | .00 | .7516 | " | " | |
| 304.001 | .2282E 00 | .4249E 03 | .3692E 04 | 15.00 | 12.00 | 1.00 | 2.166 | Standard | 64.7 ft/sec | |
| 304.003 | .2847E 00 | .4816E 03 | .4184E 04 | 26.00 | 16.00 | 1.00 | 2.455 | " | " | |
| 304.007 | .3507E 00 | .5504E 03 | .4783E 04 | 36.00 | 21.00 | 1.00 | 2.806 | " | " | |
| 304.015 | .4510E 00 | .6247E 03 | .5428E 04 | 82.00 | 25.00 | 1.00 | 3.185 | " | " | |
| 304.030 | .6118E 00 | .9464E 03 | .8223E 04 | 120.00 | 28.00 | 2.00 | 4.824 | " | " | |
| 304.045 | .8056E 00 | .1256E 04 | .1091E 05 | 210.00 | 28.00 | 3.00 | 6.401 | " | " | |
| 304.060 | .0000E 00 | .0000E 00 | .0000E 00 | .00 | .00 | .00 | - | " | " | |
| 304.075 | .1801E 01 | .2235E 04 | .1942E 05 | 590.00 | 69.00 | 4.00 | 11.39 | " | " | |
| 304.086 | .0000E 00 | .0000E 00 | .0000E 00 | .00 | .00 | .00 | - | " | " | |
| 304.098 | .0000E 00 | .0000E 00 | .0000E 00 | .00 | .00 | .00 | - | " | " | |
| 304.110 | .2050E 01 | .2601E 04 | .2260E 05 | 690.00 | 73.00 | 5.00 | 13.26 | " | " | |
| 304.127 | .2645E 01 | .5489E 04 | .4769E 05 | 350.00 | 85.00 | 16.00 | 27.98 | " | " | |
| 304.154 | .3495E 01 | .7654E 04 | .6651E 05 | 370.00 | 109.00 | 23.00 | 39.02 | " | " | |
| 305.001 | .7289E-01 | .8013E 02 | .6962E 03 | 7.00 | 6.00 | .00 | .4085 | Standard | 64.7 ft/sec | |
| 305.003 | .2074E 00 | .3912E 03 | .3399E 04 | 24.00 | 9.00 | 1.00 | 1.994 | " | " | |
| 305.007 | .2388E 00 | .4208E 03 | .3656E 04 | 32.00 | 11.00 | 1.00 | 2.145 | " | " | |
| 305.015 | .3259E 00 | .4813E 03 | .4182E 04 | 76.00 | 14.00 | 1.00 | 2.454 | " | " | |
| 305.030 | .6327E 00 | .8872E 03 | .7709E 04 | 205.00 | 20.00 | 2.00 | 4.523 | " | " | |
| 305.045 | .9522E 00 | .1332E 04 | .1157E 05 | 310.00 | 30.00 | 3.00 | 6.788 | " | " | |
| 305.060 | .0000E 00 | .0000E 00 | .0000E 00 | .00 | .00 | .00 | - | " | " | |
| 305.075 | .1757E 01 | .2735E 04 | .2376E 05 | 540.00 | 48.00 | 7.00 | 13.94 | " | " | |
| 305.086 | .0000E 00 | .0000E 00 | .0000E 00 | .00 | .00 | .00 | - | " | " | |
| 305.098 | .0000E 00 | .0000E 00 | .0000E 00 | .00 | .00 | .00 | - | " | " | |

| | | | | | | | | | |
|---|---|---|---|---|---|---|---|---|---|
| 305.110 | .2088E 01 | .3277E 04 | .2847E 05 | 560.00 | 69.00 | 8.00 | 16.70 | Standard | 64.7 ft/sec |
| 305.127 | .1901E 01 | .2967E 04 | .2578E 05 | 310.00 | 96.00 | 6.00 | 15.12 | " | " |
| 305.154 | .5199E 01 | .1292E 05 | .1122E 06 | 320.00 | 130.00 | 42.00 | 65.83 | " | " |
| 330.035 | .2470E 00 | .1673E 03 | .1453E 04 | 129.00 | 8.00 | .00 | 0.852 | Standard | 56.3 ft/sec |
| 330.145 | .1406E 01 | .8886E 03 | .7721E 04 | 799.00 | 38.00 | .00 | 4.53 | " | " |
| 330.275 | .6060E 00 | .7633E 03 | .6633E 04 | 129.00 | 34.00 | 1.00 | 3.89 | " | " |
| 330.535 | .1537E 01 | .3589E 04 | .3118E 05 | 88.00 | 50.00 | 11.00 | 18.29 | " | " |
| 329.035 | .3214E 00 | .2987E 03 | .2596E 04 | 86.00 | 20.00 | .00 | 1.52 | " | " |
| 329.145 | .1336E 01 | .1004E 04 | .8725E 04 | 598.00 | 55.00 | .00 | 5.12 | " | " |
| 329.275 | .6065E 00 | .5828E 03 | .5064E 04 | 143.00 | 40.00 | .00 | 2.97 | " | " |
| 329.535 | .1025E 01 | .1598E 04 | .1389E 05 | 129.00 | 58.00 | 3.00 | 8.15 | " | " |
| 342.005 | .6413E-01 | .7659E 02 | .6655E 03 | .00 | 6.00 | .00 | 0.390 | Zero Cav. | 56.3 ft/sec |
| 342.018 | .9051E-01 | .1041E 03 | .9049E 03 | 4.00 | 8.00 | .00 | 0.531 | " | " |
| 342.058 | .2482E 00 | .2777E 03 | .2413E 04 | 19.00 | 21.00 | .00 | 1.42 | " | " |
| 341.005 | .0000E 00 | .0000E 00 | .0000E 00 | .00 | .00 | .00 | - | " | " |
| 341.018 | .2378E-01 | .9596E 01 | .8338E 02 | 19.00 | .00 | .00 | 0.0489 | " | " |
| 341.058 | .0000E 00 | .0000E 00 | .0000E 00 | .00 | .00 | .00 | - | " | " |
| 332.035 | .3473E 00 | .3514E 03 | .3054E 04 | 64.00 | 25.00 | .00 | 1.79 | Standard | 76.6 ft/sec |
| 331.035 | .2002E 00 | .1737E 03 | .1510E 04 | 66.00 | 11.00 | .00 | 0.886 | " | " |
| 122.001 | .5844E 00 | .6870E 03 | .5969E 04 | 180.00 | 26.00 | 1.00 | 3.50 | Standard | 96.2 ft/sec |
| 118.001 | .5515E 00 | .6230E 03 | .5413E 04 | 205.00 | 20.00 | 1.00 | 3.18 | " | " |
| 119.001 | .3021E 00 | .4717E 03 | .4098E 04 | 57.00 | 14.00 | 1.00 | 2.40 | Standard | 64.7 ft/sec |
| 119.003 | .3416E 00 | .4961E 03 | .4310E 04 | 80.00 | 15.00 | 1.00 | 2.53 | " | " |
| 119.007 | .9257E 00 | .8670E 03 | .7533E 04 | 410.00 | 31.00 | 1.00 | 4.42 | " | " |
| 119.022 | .1243E 01 | .1235E 04 | .1073E 05 | 590.00 | 32.00 | 2.00 | 6.30 | " | " |
| 117.001 | .1400E 00 | .1326E 03 | .1152E 04 | 35.00 | 9.00 | .00 | 0.676 | " | " |
| 117.003 | .3122E 00 | .4757E 03 | .4134E 04 | 65.00 | 14.00 | 1.00 | 2.43 | " | " |
| 117.007 | .9031E 00 | .1106E 04 | .9612E 04 | 310.00 | 33.00 | 2.00 | 5.64 | " | " |
| 117.022 | .1699E 01 | .2460E 04 | .2137E 05 | 410.00 | 73.00 | 5.00 | 12.54 | " | " |
| 136.001 | .6471E-01 | .6837E 02 | .5941E 03 | 9.00 | 5.00 | .00 | 0.349 | Zero Cav. | 64.7 ft/sec |

| | | | | | | | | | |
|---|---|---|---|---|---|---|---|---|---|
| 130.001 | .5585E-01 | .4789E 02 | .4161E 03 | | | | 0.244 | Zero Cav. | 64.7 ft/sec |
| 210.005 min. | .1235E 01 | .2194E 04 | .1907E 05 | 19.00 | 3.00 | .00 | 11.19 | Standard | 96.2 ft/sec |
| 213.005 min. | .2763E 00 | .1537E 03 | .1336E 04 | 456.00 | 9.00 | 7.00 | 0.784 | " | " |
| 204.005 min. | .2923E 00 | .6569E 03 | .5708E 04 | 178.00 | 5.00 | .00 | 3.35 | " | " |
| 207.005 min. | .6830E 00 | .1379E 04 | .1198E 05 | 27.00 | 9.00 | 2.00 | 7.03 | " | " |
| 206.005 min. | .1831E 01 | .2065E 04 | .1794E 05 | 107.00 | 21.00 | 4.00 | 10.53 | " | 64.7 ft/sec |
| 203.005 min. | .2582E 00 | .5924E 03 | .5147E 04 | 968.00 | 20.00 | 5.00 | 3.02 | " | " |
| 212.005 min. | .8003E 00 | .1313E 04 | .1141E 05 | 51.00 | 3.00 | 2.00 | 6.69 | " | 55.0 ft/sec |
| 211.005 min. | .3072E-01 | .2085E 02 | .1811E 03 | 146.00 | 35.00 | 3.00 | 0.106 | " | " |
| | | | | 16.00 | 1.00 | .00 | | | |

NOTE: * Denotes Aereated Water

† Denotes 150°F

All other Runs at room temperature (cold, well settled).

Run Numbers are given as follows:

326.003

- Time duration of test in hours, except where noted
- Specimen number (even number = front location in venturi; odd number = rear location)
- Denotes material of specimen 1) Carbon Steel, 2) Aluminum (Type 6061-T6)
  See Table II for specifications 3) Stainless Steel (Type 302 )

Total specimen area exposed to fluid taken as 0.3362 $in.^2$

Definition of machine output notation

1. Damage Area

   .1831E 01 means $0.1831 \times 10^1$ %

2. Weight Loss

   Heading 10E - 08 GRS means $10^{-8}$ Grams

   Therefore, tabulated numbers are interpreted as follows:

   .1105E 04 means $(.1105 \times 10^4) \times 10^{-8}$, or $0.1105 \times 10^{-4}$ Grams

Size of Pits

Small means pit diameters $0.3 < D < 1.5$ mils
Large means pit diameters $1.5 < D < 3.0$ mils
Very Large means pit diameters $3.0 < D < 10$ mils

Note that these pit size designations differ somewhat from those of the very detailed tabulations in Table III.

the venturi flow is not significantly affected by the test specimens. This is essentially the case as far as the axial pressure profiles, as measured from wall taps, are concerned. The profiles for various cavitation conditions, with and without test specimens are compared in Figure 6 and 7 and where it is seen that the effect of the test specimens is not great.

However, the pressure coefficient of the test specimens themselves must be considered. Although they are fairly well streamlined, there must be significant local pressure depressions and increases due to their presence. The actual pressure gradients and velocities existing along the specimens must control the bubble collapses and the intensity of the resultant pressure waves. Because of the two-phase and three-dimensional nature of the flow, and the presence of a strong axial pressure gradient no reasonably precise estimates of the actual pressure perturbations caused by the specimens as a function of position along the surface seem possible. However, it is planned to make local pressure measurements on the specimens at different cavitation conditions to determine actual pressures. This has been postponed until the improved water facility is in operation. Eventually, it may become desirable to consider damage tests with a simpler flow geometry, wherein the local flow conditions can be more easily specified.

The appearance of cavitation pitting, in runs where the pressures as measured by the conventional venturi wall taps were considerably in excess of those corresponding to cavitation initiation in the absence of test specimens, indicates that the local pressure depressions due to

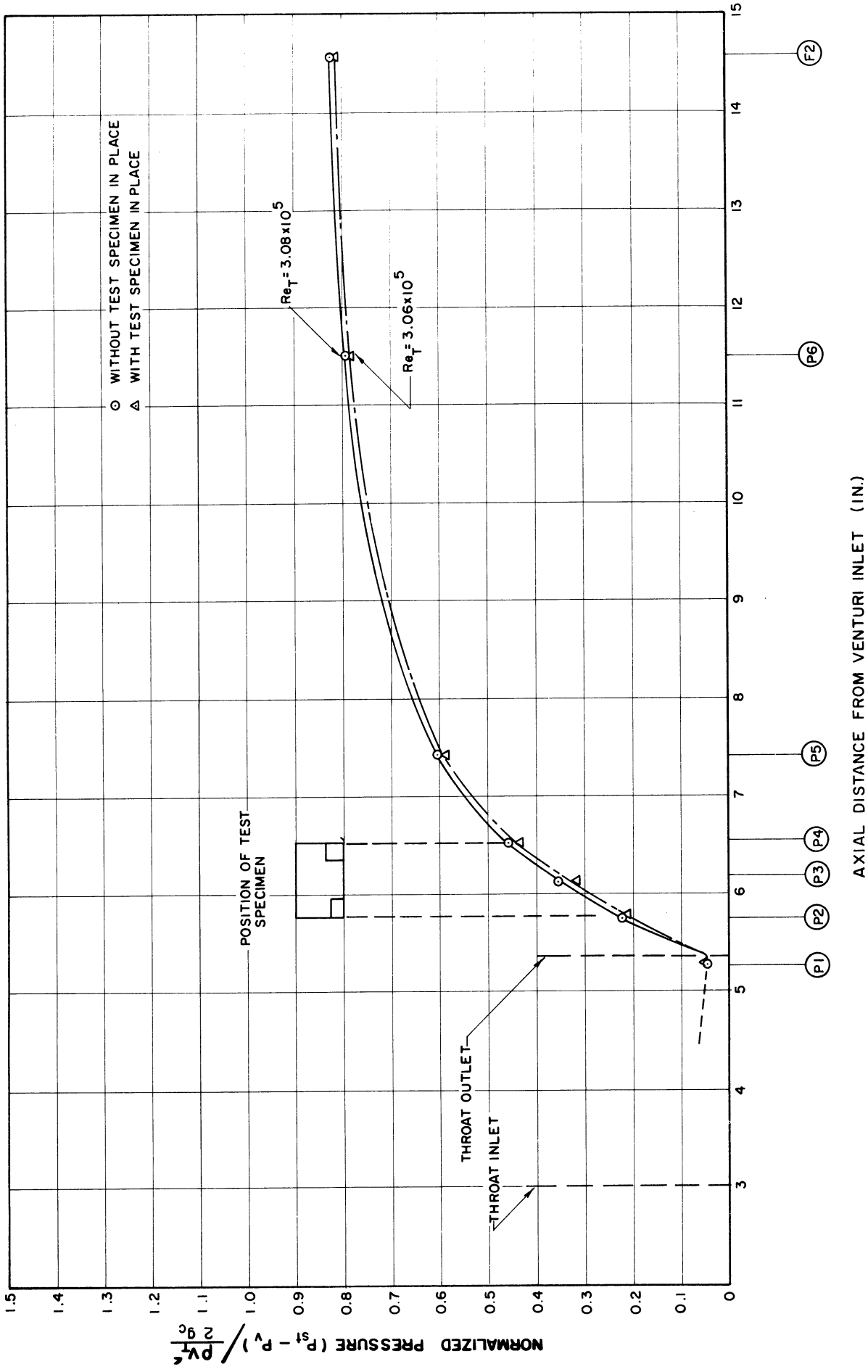


Figure 6. Normalized axial pressure profiles for "Visible Initiation", with and without test specimen in place.

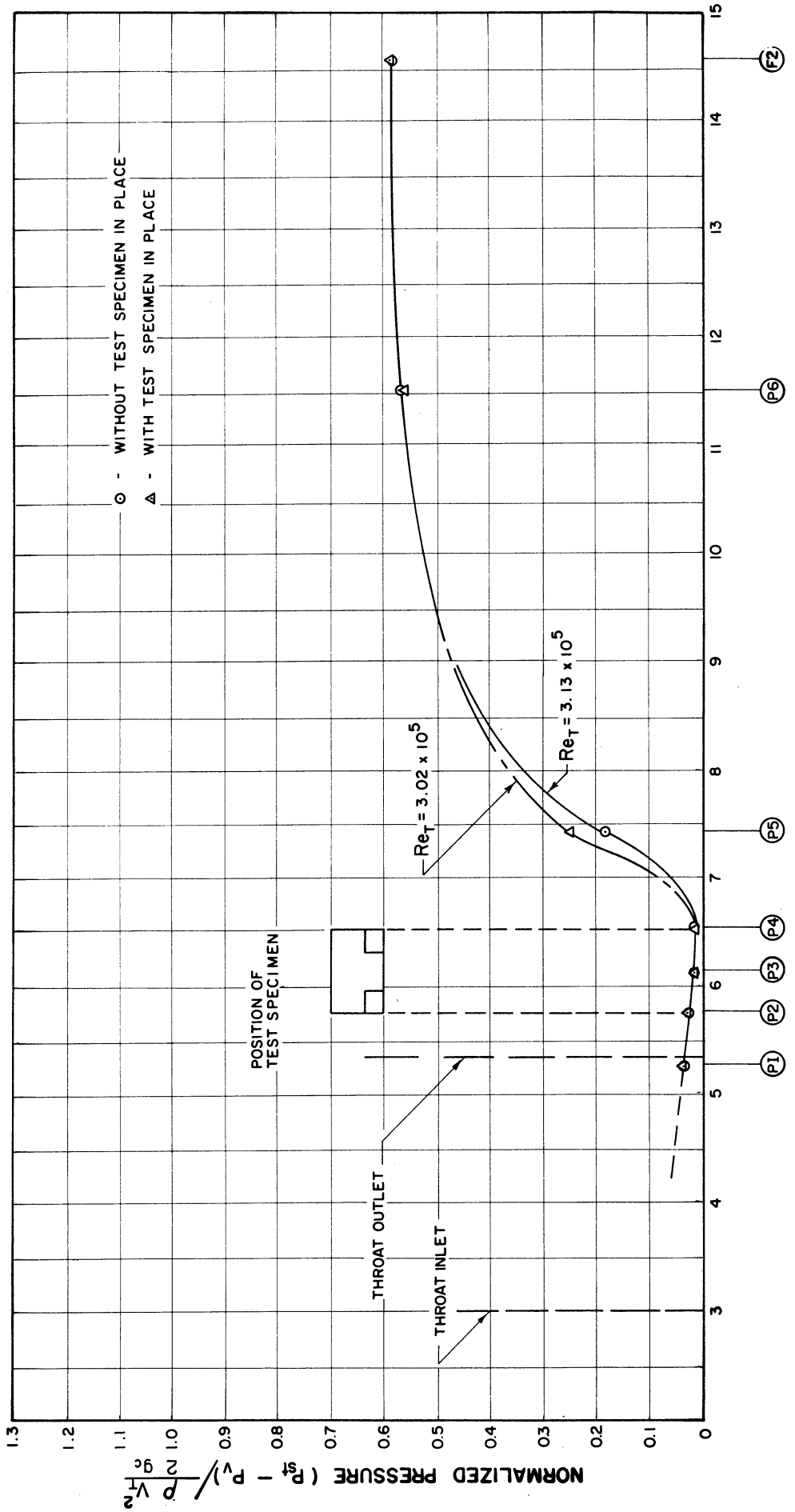


Figure 7. Normalized axial pressure profiles for "Cavitation to first Mark"; with and without test specimens in place.

the specimens themselves in this essentially single-phase flow regime are considerable. However, in most cases of interest, the main cavitating field is relatively well developed, so that single-phase calculations or measurements are not the primary problem.

### 3. Specifications of Test Specimen Materials

The test specimen dimensions are shown in Figure 4. The materials utilized were aluminum in two different conditions, low carbon steel, annealed austenitic stainless steel, and plexiglass (methyl-methacrylate). The applicable properties of the materials in the "as used" condition are listed in Table II.

TABLE II

TYPICAL MECHANICAL PROPERTIES OF MATERIALS TESTED

| Material | Condition | Tensile Strength psi | 0.2% Yield Strength psi | % Elong. in 2 in. | % Reduction in Area | Hardness | | Bending Fatigue Strength psi | Elastic Modulus |
|---|---|---|---|---|---|---|---|---|---|
| | | | | | | Measured Rockwell B | BHN | | |
| Stainless Steel Type 302 | Annealed | 98,000 | 37,000 | 55 | 65 | 76 | 140* | 35,000 @ $10^7$ cycles | 28 x $10^6$ |
| 1010 Carbon Steel | Annealed | 50,000 | 30,000 | 40 | 71 | 48 | 85* | 25,000 @ $10^7$ cycles | 28 x $10^6$ |
| Aluminum 1100-0(2S0) | Annealed | 13,000 | 5,000 | 35 | - | - | 23** | 5,500 @ $10^7$ cycles | 10 x $10^6$ |
| Aluminum 6061-T6(61-ST6) | Age Hardened | 45,000 | 40,000 | 12 | - | 57 | 90* | 13,500 @ $10^7$ cycles | 10 x $10^6$ |
| Plexiglass | - | 10,445* | - | 2-7 | - | - | M90-M100 Rockwell** | - | 0.4 x $10^6$* |

* Measured value or converted from measured value

** Typical value

## IV. OBSERVATIONS OF THE DAMAGE FORMATION

### A. General

Nearly 60 percent of the tests were on austenitic stainless steel, which was emphasized because of its high resistance to chemical reactions so that damage could be attributed almost solely to mechanical effects, and also because of its technological importance. However, enough tests were made on carbon steel to allow a meaningful comparison between these materials. Also, there were a few short duration tests on aluminum and plexiglass. (See Table I for listing of tests.) The aluminum tests were limited to short duration (5 minutes) because of the very rapid pitting.

It was noticed that there was no detectable damage on the plexiglass venturi even after many hours of exposure in various cavitating fields. Hence, a run was made with plexiglass test specimens to determine whether the flow geometry was such that the wall of the venturi would not be damaged per se because of its shape and position, or whether the lack of damage was due to the particular properties of plexiglass. Much less damage occurred on the test specimen than would have been encountered with stainless steel under similar conditions. The possible reasons are discussed in Section V.

### B. Specific Observations

#### 1. Pit Contours

Figures 8 through 17 show typical damaged regions on stainless steel, carbon steel, and aluminum specimens. It is noted generally that the pits have fairly regular contours so that they can be assigned a

(a)

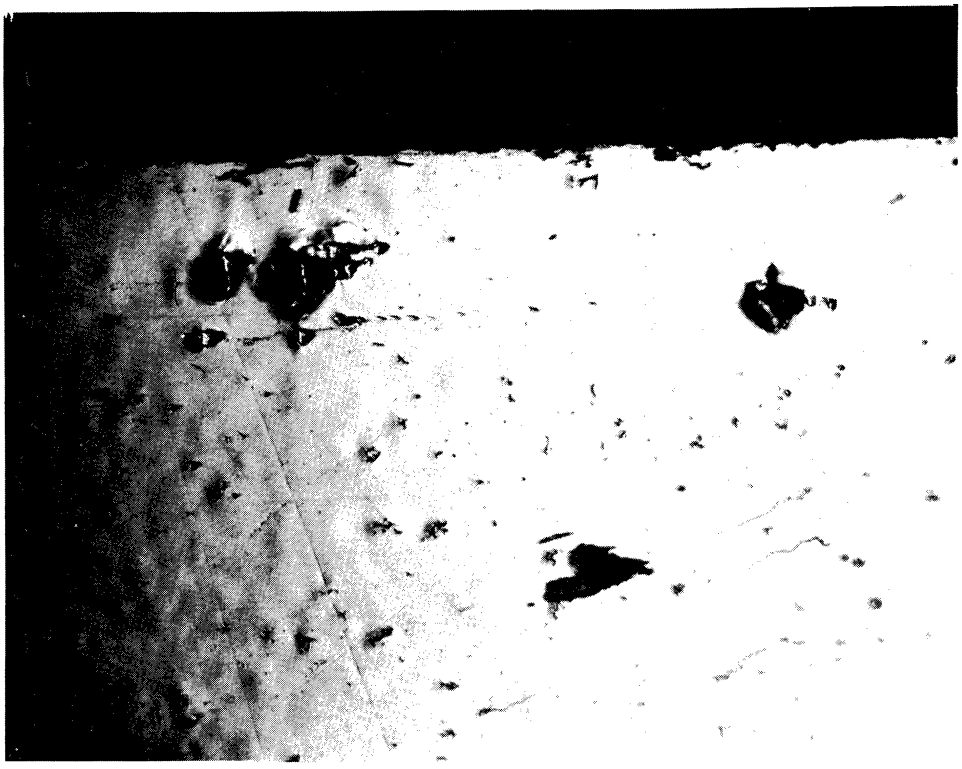

(b)

Figure 8. Typical cavitation damage on carbon steel. Carbon steel specimen 1-19, standard cavitation condition, 64.7 ft/sec. Location 1 (upper photo), after 22 hours; Location 2 (lower photo) after 3 hours, (X100).

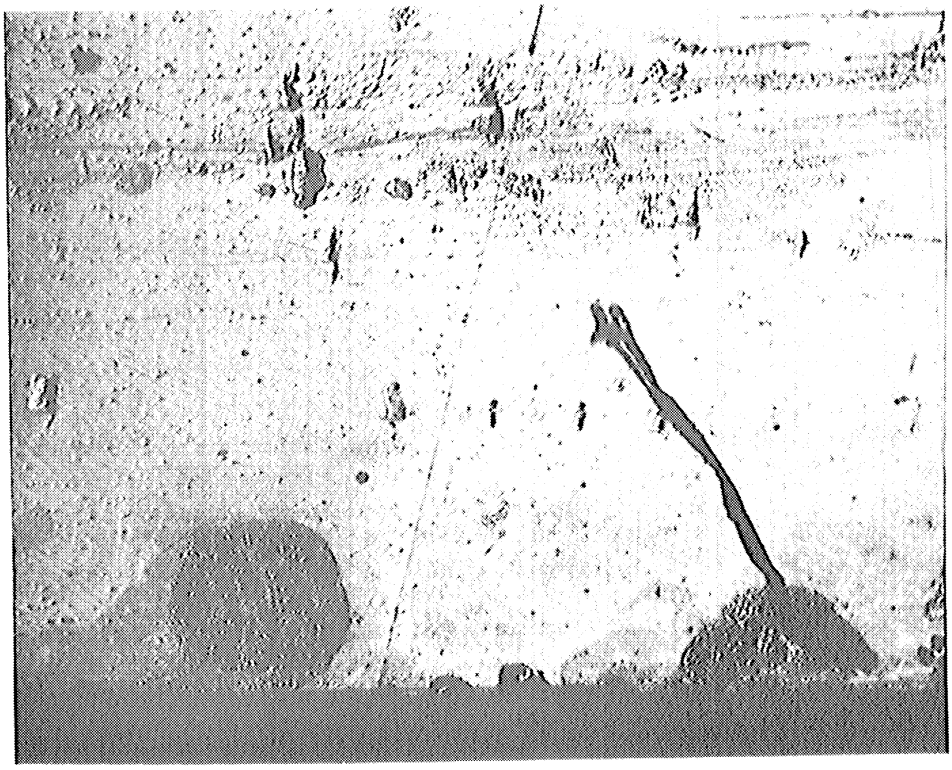

Figure 9. Typical cavitation damage on 6061-T6 (61-ST6) aluminum. Aluminum specimen number 2-3 after 5 minutes in test section, standard cavitation, throat velocity = 97.2 ft/sec. (X100).

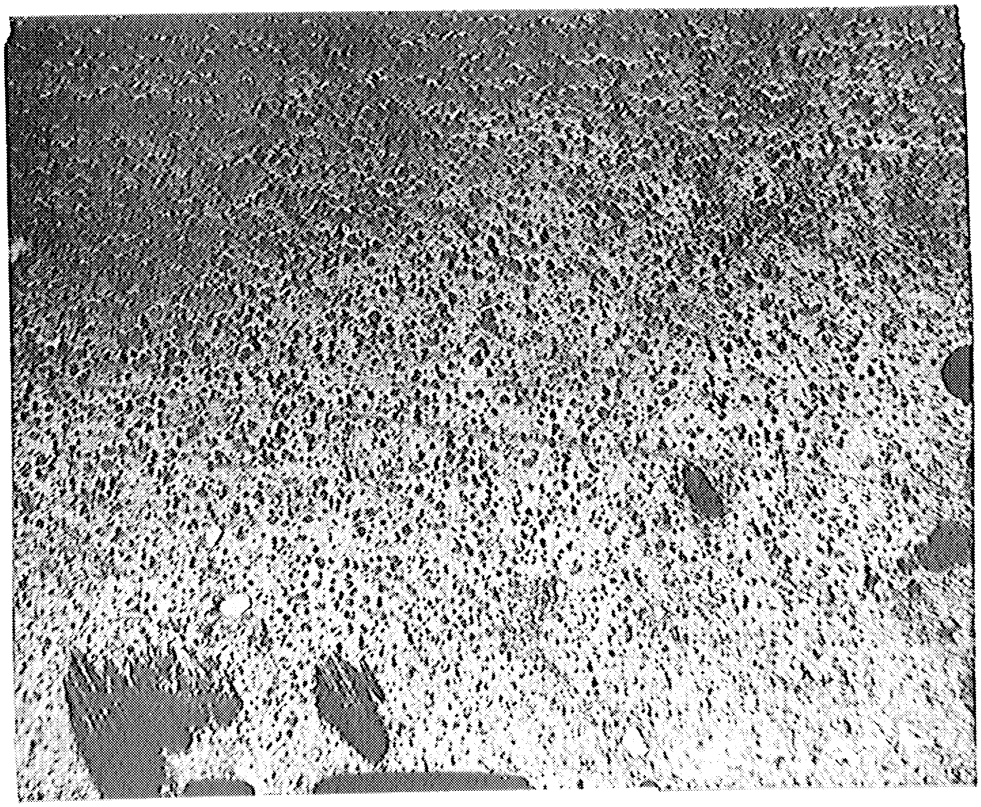

Figure 10. Cavitation damage on 1100-0(2S0) aluminum. After 5 minutes in test section, standard cavitation, throat velocity 65 ft/sec, (X100).

(a)

(b)

Figure 11. Development of cavitation damage. Two locations on type 302 stainless steel specimen number 3-5, standard cavitation condition, throat velocity = 64.7 ft/sec, after 15 hours, (X100).

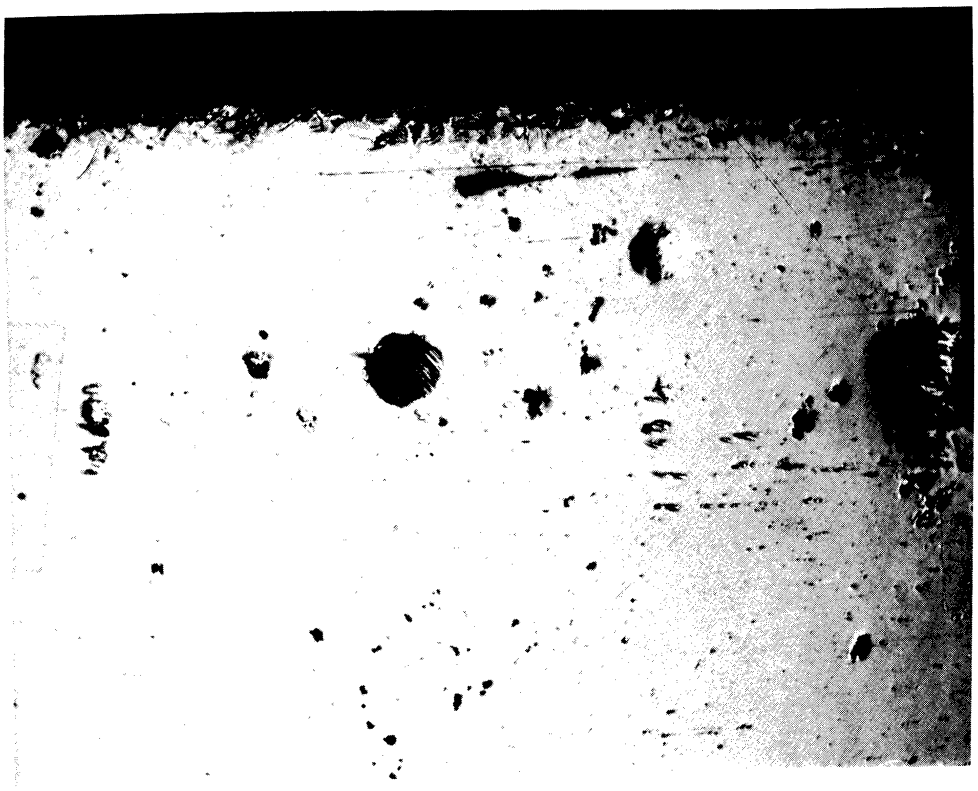

(a)

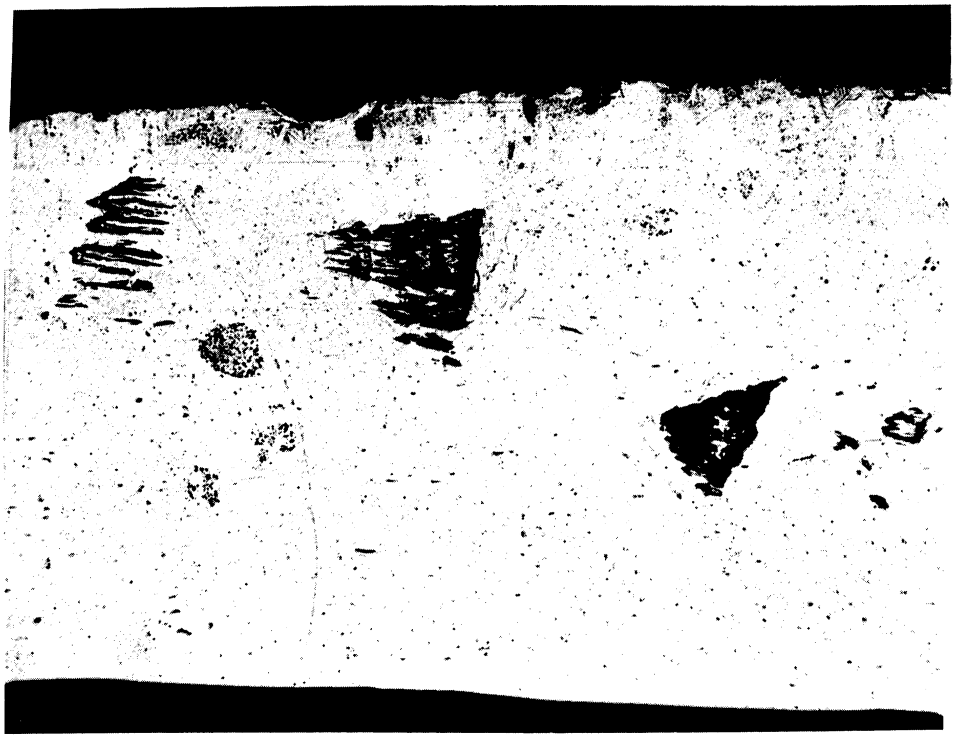

(b)

Figure 12. Development of cavitation damage. Two locations on type 302 stainless steel specimen number 3-5, standard cavitation condition, throat velocity = 64.7 ft/sec, after 30 hours, (X100).

(a)

(b)

Figure 13. Development of cavitation damage. Two locations on type 302 stainless steel specimen number 3-5, standard cavitation condition, throat velocity = 64.7 ft/sec, after 45 hours, (X100).

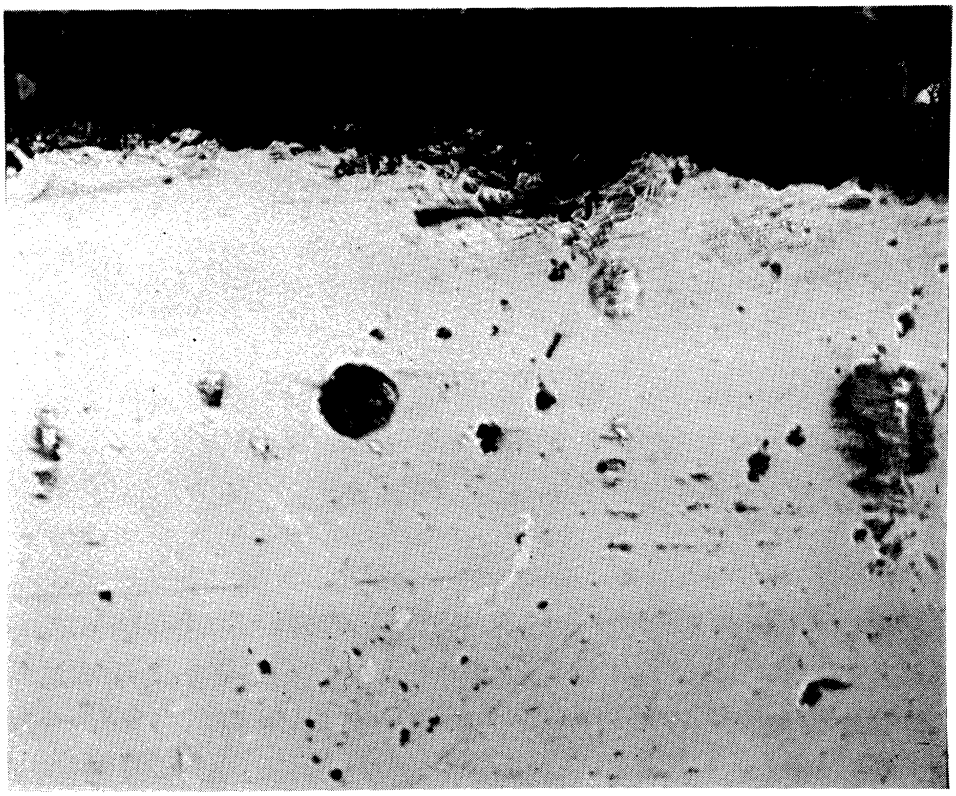

(a)

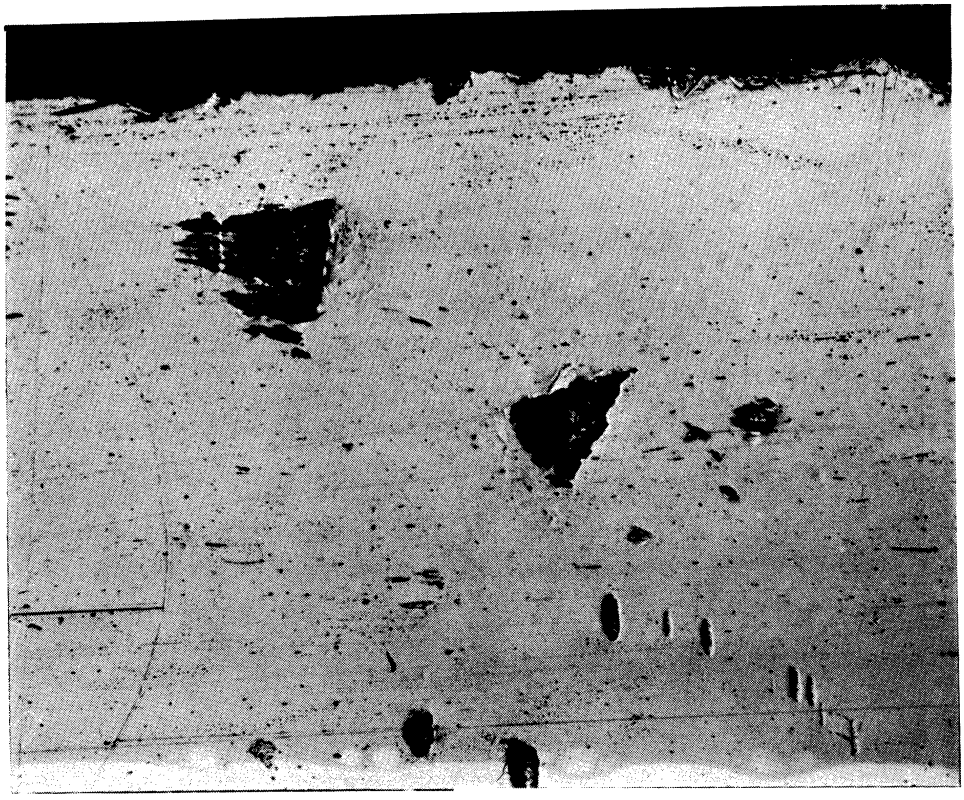

(b)

Figure 14. Development of cavitation damage. Two locations on type 302 stainless steel specimen number 3-5, standard cavitation condition, throat velocity = 64.7 ft/sec, after 75 hours, (X100).

(a)

(b)

Figure 15. Development of cavitation damage. Two locations on type 302 stainless steel specimen number 3-5 standard cavitation condition, throat velocity = 64.7 ft/sec, after 110 hours, (X100).

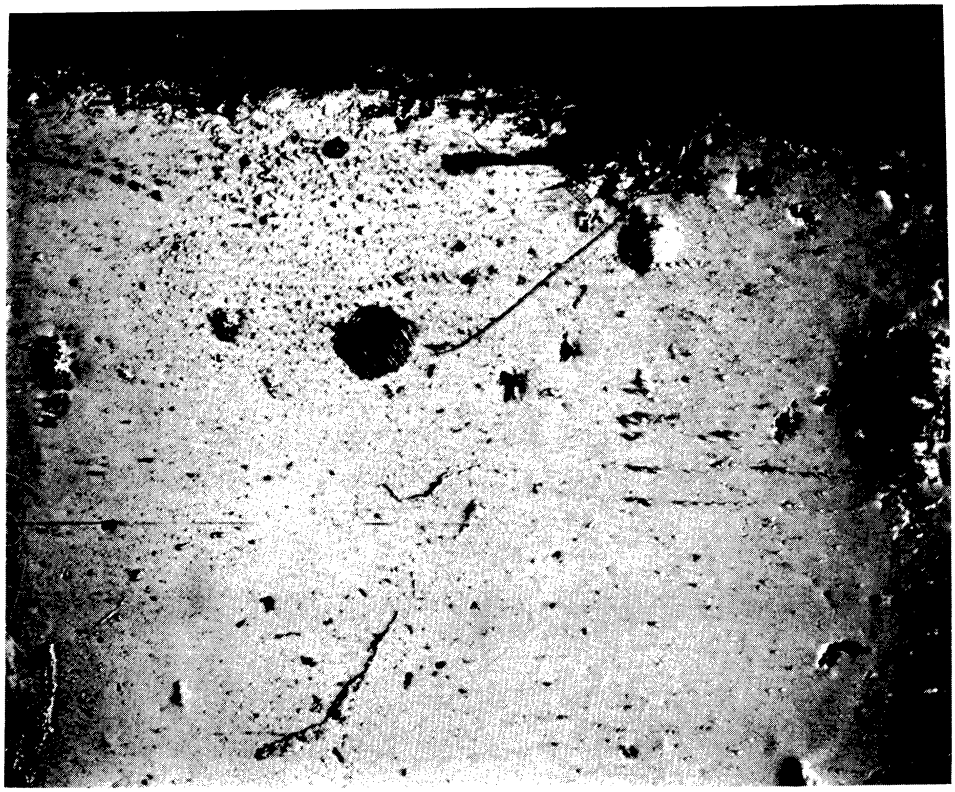

(a)

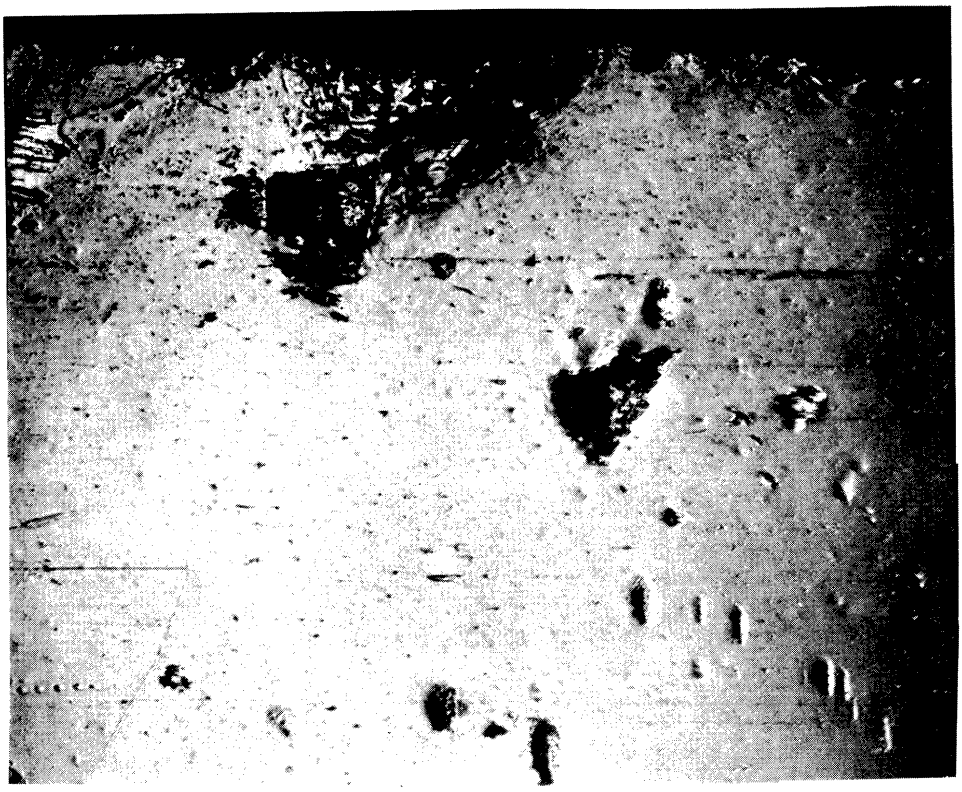

(b)

Figure 16. Development of cavitation damage. Two locations on type 302 stainless steel specimen number 3-5, standard cavitation condition, throat velocity = 54.7 ft/sec, after 150 hours, (X100).

Figure 17. Rust cluster on type 1010 carbon steel specimen. Carbon steel specimen number 1-36, standard cavitation condition, throat velocity = 97.2 ft/sec, after one hour in test section, (X100).

mean or characteristic diameter for purposes of pit tabulation. Upon careful examination of approximately 50 typical pits (stainless steel only) with a proficorder, it was noted that the depth of the pits is only of the order of 5 - 10% of the average diameter.[4,44] The vertical cross-section of the pit is quite irregular in detail, but overall it generally resembles a segment of a sphere.

It will be further noted from Figures 8 through 17, that the cavitation pits fall into two distinct categories:

i) Virtually symmetrical craters*

ii) Pits of irregular contour

A detailed visual examination of two pairs of specimens (i.e.: from two distinct runs with different cavitation conditions and durations) showed that about 10 - 15% of all pits were of the symmetrical crater type, the remainder having irregular contours. The proportion was 8.75% for the largest category of pits, and about 14% for all other sizes. It varied considerably between specimens, but was generally between the limits specified (Table III).

The relatively small vertical variations in the pit contours are difficult to distinguish in the photomicrographs. However, from the proficorder studies,[4,44] generally there is a ridge of raised material adjacent to the pits, but not surrounding them entirely. In fact, it exists primarily only on the downstream side in about 90% of the pits examined.[44] However, no (symmetrical) crater-type pits have as yet been examined.

---

* See upper photo, Figure 11, for example.

TABLE III

PIT COUNT TABULATIONS*

Tabulation A
Pit Count and Various Sizes

| | | Pit Size (mils) VVL (10 > D > 5) | | VL (5 > D > 2-1/2) | | L (2-1/2 > D > 1) | | S (1 > D > .4) | |
|---|---|---|---|---|---|---|---|---|---|
| | | % Cir. | Total | % Cir. | Total | % Cir. | Total | % Cir. | Total |
| Sample No. .....4-3 | Polished Surface | 10.0 | 10 | 23.4 | 17 | 17.33 | 75 | 12.5 | 400 |
| Sample Position.....Front | Numbered Side | 21.75 | 23 | 18.7 | 48 | 16.05 | 81 | 15.1 | 325 |
| Standard Cavitation | Opposite Side | 18.75 | 16 | 21.1 | 19 | 14.55 | 55 | 4.9 | 465 |
| Throat Velocity.....64.5fps | Subtotal (2 sides) | 20.5 | 39 | 19.4 | 67 | 15.45 | 136 | 9.1 | 790 |
| Duration of Run.....150 hrs. | Total All Surfaces | 18.4 | 49 | 21.4 | 84 | 16.1 | 211 | 10.3 | 1190 |
| Sample No. .....5-3 | Polished Surface | 15.4 | 13 | 22.2 | 18 | 25.4 | 110 | 25.8 | 480 |
| Sample Position.....Back | Numbered Side | 11.1 | 9 | 21.1 | 19 | 15.9 | 63 | 16.3 | 320 |
| Standard Cavitation | Opposite Side | 6.3 | 32 | 7.2 | 14 | 10.2 | 49 | 12.9 | 350 |
| Throat Velocity.....64.5fps | Subtotal (2 sides) | 7.4 | 41 | 15.2 | 33 | 13.4 | 112 | 14.5 | 670 |
| Duration of Run.....150 hrs. | Total All Surfaces | 9.3 | 54 | 17.7 | 51 | 19.4 | 222 | 19.2 | 1150 |
| Sample No. .....18-3 | Polished Surface | 0 | 11 | 4.5 | 23 | 6.8 | 74 | 15.0 | 320 |
| Sample Position.....Front | Numbered Side | 0 | 29 | 5.0 | 40 | 5.9 | 51 | 13.5 | 200 |
| Cavitation to Nose | Opposite Side | 0 | 13 | 9.1 | 11 | 9.1 | 33 | 12.3 | 130 |
| Throat Velocity.....64.5fps | Subtotal (2 sides) | 0 | 42 | 5.9 | 51 | 7.2 | 84 | 13.1 | 330 |
| Duration of Run.....50 hrs. | Total All Surfaces | 0 | 53 | 5.4 | 74 | 7.0 | 158 | 14.0 | 650 |
| Sample No. .....19-3 | Polished Surface | 9.1 | 33 | 17.2 | 64 | 15.0 | 100 | 10.2 | 365 |
| Sample Position.....Back | Numbered Side | 5.3 | 19 | 0 | 14 | 9.3 | 43 | 18.7 | 150 |
| Cavitation to Nose | Opposite Side | 11.1 | 9 | 0 | 16 | 7.7 | 26 | 8.6 | 105 |
| Throat Velocity.....64.5fps | Subtotal (2 sides) | 7.1 | 28 | 0 | 30 | 8.7 | 69 | 14.5 | 255 |
| Duration of Run.....50 hrs. | Total All Surfaces | 8.2 | 61 | 11.7 | 94 | 12.4 | 169 | 11.9 | 620 |
| TOTAL ALL 4 SAMPLES | | 8.75 | 217 | 13.9 | 303 | 14.3 | 760 | 14.1 | 3610 |

Tabulation B
Pitting Intensity

| | | | | | Total pits/in.$^2$ - hr. VVL (10 > D > 5) | | VL (5 > D > 2.5) | | L (2.5 > D > 1) | | S (1 > D > .4) | |
|---|---|---|---|---|---|---|---|---|---|---|---|---|
| No. | Pos. | Cav. Condition | Vel. | Duration | Pol. | Side | Pol. | Side | Pol. | Side | Pol. | Side |
| 4-3 | Front | Standard | 64.5fps | 150 hrs. | 1.79 | 0.87 | 3.05 | 1.49 | 13.44 | 3.04 | 71.7 | 19.6 |
| 5-3 | Back | Standard | 64.5fps | 150 hrs. | 2.33 | 0.915 | 3.22 | 0.74 | 19.7 | 2.50 | 86.0 | 14.9 |
| 18-3 | Front | Cav. to Nose | 64.5fps | 50 hrs. | 5.91 | 2.81 | 12.38 | 3.41 | 39.8 | 5.62 | 172.0 | 22.1 |
| 19-3 | Back | Cav. to Nose | 64.5fps | 50 hrs. | 17.75 | 1.87 | 34.4 | 2.01 | 53.8 | 4.62 | 196.0 | 17.1 |

Tabulation C
Summary

| | | VVL | | VL | | L | | S | |
|---|---|---|---|---|---|---|---|---|---|
| | | % Cir. | Total | % Cir. | Total | % Cir. | Total | % Cir. | Total |
| 4-3 | Total All Surfaces | 18.40 | 49 | 21.40 | 84 | 16.10 | 211 | 10.26 | 1190 |
| 5-3 | Total All Surfaces | 9.26 | 54 | 17.65 | 51 | 19.4 | 222 | 19.2 | 1150 |
| 4-3 & 5-3 | Total All Surfaces | 13.6 | 103 | 20.0 | 135 | 17.8 | 433 | 14.67 | 2340 |
| 18-3 | Total All Surfaces | 0 | 53 | 5.4 | 74 | 6.96 | 158 | 14.0 | 650 |
| 19-3 | Total All Surfaces | 8.2 | 61 | 11.7 | 94 | 12.4 | 169 | 11.9 | 620 |
| 18-3 & 19-3 | Total All Surfaces | 4.39 | 114 | 8.94 | 108 | 9.8 | 327 | 13.0 | 1270 |
| 4-3 & 5-3 + 18-3 & 19-3 | Total | 8.75 | 217 | 13.87 | 303 | 14.34 | 760 | 14.07 | 3610 |

* Memo, L. Barinka, Nov., 1961.

It is suggested by the preceding observations that:

i) The craters are the result of a single, very intense, blow.

ii) The irregular pits are more likely the result of many weaker blows which eventually result in a fatigue-type failure of a portion of the surface, (perhaps in some cases the location of a non-metallic inclusion). Thus their shape is determined more by the microscopic characteristics of the material than by the details of the bubble dynamics. Since their shape does not change with subsequent testing (discussed later), it is presumed that the material is removed from the surface in a single event, and probably in a single piece.

iii) The mechanism of failure of the irregular pits may well be the peeling-off of a slab of material. (As has been mentioned previously, the pits are generally proportionately very shallow.) In this case, such a slab would tend to peel off in the downstream direction because of the fluid-dynamic drag force of the through-velocity. This pivoting-back and tearing-away could leave a raised portion in the remaining material on the downstream edge. A picture of such a slab, apparently almost ready to leave the surface, was shown by Boetcher.[3] The photograph is reproduced here for convenience (Figure 18).

iv) The facts that there are perhaps 7 - 8 times as many irregular pits as craters, and that presumably many blows

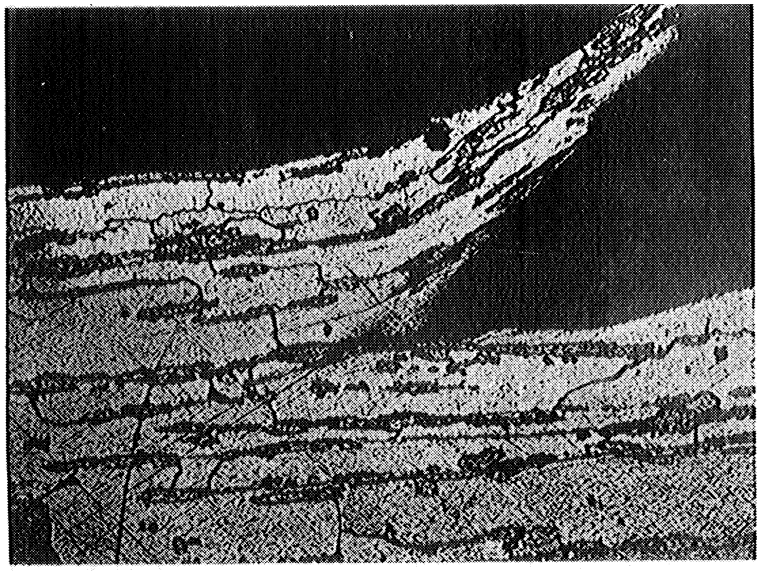

Figure 18. Flake at surface of hot-rolled high-chromium iron, (X100).(3)

are required to form a single pit of the irregular type, strongly indicate that the fluid energy from bubble collapse, available on the solid surface to cause damage, is much more frequently available in small quanta than in large. This is further confirmed by the fact that small pits of all types are much more numerous than large (discussed later). These observations suggest an energy quanta spectrum, perhaps as indicated in Figure 19. Such a curve would apply only to a single cavitating flow regime, and a particular fluid. A family of curves would thus be required to represent the various fluids, cavitation and fluid conditions. For a given test material, only bubbles capable of delivering quanta of energy above a fixed threshold would be capable of causing crater-type damage, while smaller quanta, with repeated application, would cause the fatigue-type irregular contour pits. It is hoped that in the future, as data become available with different fluids and materials, it may be possible to verify this hypothetical model.

2. Pit Size and Location Distribution

The smallest pits which were tabulated, corresponding to the lower limit of observation and counting with the present method, have a diameter of about 0.25 mils. However, pits down to almost any arbitrarily small diameter are observed if higher magnification is used. The largest pits observed so far (up to 150 hour runs) have a mean diameter of about

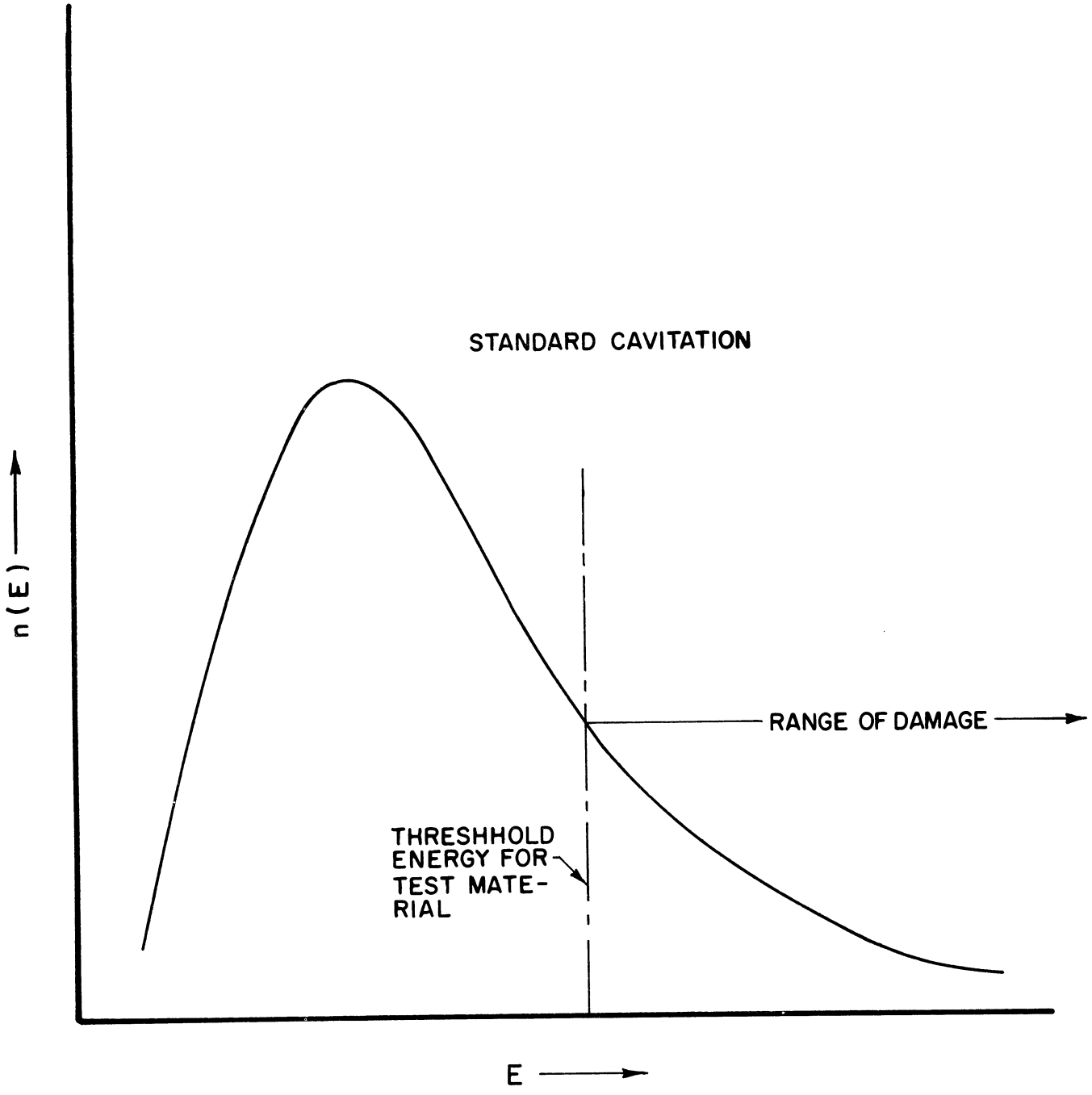


Figure 19. Hypothesized bubble energy spectrum, where $n(E)$ = number of bubbles from those "in vicinity of" damage specimen which deliver an energy quantum, $E$, to the surface of the specimen; $E$ = energy delivered by an individual bubble to the surface of the specimen.

10 mils. The frequency of the occurrence of small pits is very much greater than that of large pits. For all specimens, both large and small pits are formed in each test. Generally the pits are located distinctly; i.e.: they do not tend to overlap until the overall pitting density becomes such that most of the surface is covered. However, in a few cases, particularly, but not exclusively, with aluminum, clusters or families of small pits have been observed, which contain in some cases hundreds of very small circular pits, and are generally surrounded by undamaged areas. The darkened areas of Figure 9 represent such clusters on an aluminum sample, and one is apparently shown on stainless steel in the lower photo of Figure 12. However, this latter cluster can not be seen in the subsequent pictures of the same area (lower photos, Figures 13 - 16), taken after further exposure to cavitation, indicating possibly a difference in the lighting, the actual disappearance of these pits, or the fact that foreign particles were mistaken for pits.

The location of pits on the test specimens is not much affected by the cavitation condition, at least within the reproducibility limits of the data. Generally, the damage appears to be more or less concentrated in the leading and trailing third of the area, with the damage intensity in the central portion only about 1/3 to 1/4 that at the ends. Also, there is considerably more pitting along and near the side edges than along the longitudinal centerline. The above statements apply for all cavitation conditions. Hence, it appears that local cavitation, induced by the test specimen itself, over and above the general cavitation

pattern, may be most significant in determining the damage distribution. However, as will be discussed later, the quantity of damage is very definitely a strong function of the overall cavitation condition.

The fact that the pitting is concentrated along the edges of the specimens (in some cases perhaps 50% of the pitting will be found in the 10% of the surface area adjacent to the edges), can be partially explained by local cavitation induced by "end effects" from the test specimen, and partially by the fact that the failure of the material in the vicinity of the edges could be induced by a smaller applied stress than for material more centrally located.

The detailed examination of the two pairs of specimens previously mentioned indicated that the pitting intensity (pits/area-time) was considerably greater (factor of 3 and 15) on the polished surfaces than on the sides, and differed considerably between the apparently symmetrical front and back positions in the venturi. The applicable pit counts are listed in Table III.

The pit sizes are divided into four categories: VVL, VL, L, and S, which correspond to the mean diameter limits, in mils, given in the table. The first tabulation, A, shows the percent of pits out of the total which are approximately circular, as well as the total number of pits, in each condition and category.

The second tabulation, B, shows the pitting intensities (pits/$in^2$/hr) encountered on the polished face and on the sides in the various categories. Tabulation C summarizes the results of A.

The difference in pitting intensity between polished surface and sides probably involves effects due to the surface treatment and

the different localized flow regimes. These effects cannot be separated at the present time, and it is planned to conduct a test to compare the weight losses for specimens polished all over and not polished at all.

The large differences in volume removed (Table I) between the supposedly symmetrical holder positions, i.e., "front" and "back" position in the venturi, and also between the two sides of a given specimen as sometimes occur, are probably due to two factors. Firstly, there may be insufficient numbers of pits for good statistical distribution, and secondly, there may be some lack of homogeneity in the material in spite of the fact that all specimens of a given material were cut from the same sheet and with the same orientation with respect to direction of rolling. However, a summation of volume losses from all runs indicates that the overall difference between the volume lost from samples in the front, and in the back holders is only about 3-1/4% of the total volume removed in all runs. Further, the average of the differences between the front and the back holder for each pair of samples is about 27-1/2% of the average volume loss per pair, and in one run there is a factor of 50 between the volume losses at the two holder positions.

Thus, there seems to be little or no difference between the positions which influence the averaged results. The damage process does appear to be very sensitive to small inhomogeneities between specimens or to temporal differences in the flow pattern, so that large differences in the damage rates appear for a single pair of specimens. Hence, the prediction of the damage rate to be expected in a given test could be in error by several hundred percent.

3. Test Duration

Figures 11-16 show the development of surface damage on a stainless steel specimen under "standard cavitation" for a duration of 150 hours at two different locations. From these photomicrographs, it is noted that the number of pits increases with time, but the size and shape of the pits, once formed, remains unchanged. It was verified in the proficorder study[4] that the depth contours also were unchanged. This can be explained by the fact that the probability of a second pit forming at a fixed spot where a pit has already formed is small, considering that the portion of surface actually pitted is relatively small even after long duration tests. (Only about 3-1/2% for the 150 hour test.) Thus the probability of superposition of pits is small if it is assumed that there is no significant perturbation of the stream (in a direction to increase pitting at that point) or weakening of the surface by an existing pit,* and thus the location of new pits is quite random. From the experimental evidence, such is apparently the case. There are exceptions, as for example shown in Figures 15 and 16 (lower series of photos) where a new damage spot was formed along the upper edge of the specimen, covering all the small pits formed previously in this area.

---

* Actually the effects may be such that the formation of new pits in an already pitted location may be retarded beyond a purely random process because:
  a) The ridge raised around most pits may deflect the stream in such a way as to prevent the approach of a bubble; and,
  b) the material in the vicinity of an existing pit may be strengthened by the cold-work involved in the formation of the pit.

At the lower right corner of Figure 13 there is a chain of small pits forming a line of about 20 mils (approximately 2 inches on the picture). This type of damage is seen quite often on all the specimens. From the orientation and general similarity of these pits, one might speculate that a bubble had collapsed and rebounded several times with a very high frequency in this region, forming a string of pits. Such rebounds have been previously observed experimentally and are predicted theoretically.[17,43]

4. Materials

The duration of the tests on carbon steel and aluminum is much shorter than it is for stainless steel. In the case of carbon steel, this is because of the corrosion of the surface encountered shortly after exposure to the cavitation field, so that a meaningful pit count is impossible. Apparently, the damage mechanism involves substantial chemical as well as mechanical effects in this case. In one run, preferential corrosion around the pits was noted. Thus a two-fold mechanism was apparently involved; i.e.: mechanical pitting followed by stress-corrosion, weakening the material for additional mechanical pitting. The longest run for carbon steel was 17 hours, after which the surface was so badly rusted that the pits and the rust clusters are practically indistinguishable. Figure 17 shows the rust formation after only one hour of test under standard cavitation condition and at a velocity of 97.2 fps. A typical pitted surface for carbon steel before corrosion becomes important, can be seen in Figure 8. It is similar to the stainless steel surfaces.

The testing time for aluminum was only five minutes since pitting was so rapid (Figures 9 and 10). Figure 9 shows results for 61-ST6 aluminum with a hardness of 57 $R_B$ and Figure 10 for 2S0 (fully annealed) aluminum. From an examination of Figure 10, wherein the specimen was exposed to static water for about 15 minutes after a five minute cavitation run, it is not clear whether there is pitting or a build-up of a spongy oxide (see patch of apparently fresh, shiny surface perhaps below an oxide coating). In tests on the harder aluminum (Figure 9) the specimen was removed from the facility immediately after the five minute cavitation run so that corrosion was presumably more limited. These specimens show pitting similar to that of the steel, but occurring much more rapidly than the steel. However, the rate of pitting of the soft aluminum (Figure 10) is many times that of the harder (Figure 9).*

Both of these tests may indicate (as did carbon steel) an interplay of chemical and mechanical effects, wherein oxide formation may be greatly accelerated by mechanical scouring. Approximately the saturation quantity of air was dissolved in the water. Hence, in the cavitation region, air as well as water vapor presumably exists within the cavities. Thus an oxidizing reaction may have proceeded at a very high rate as fresh surface was continuously exposed by the cavitation.

---

* Unfortunately no detailed pit counts were made on the soft samples as these tests were conducted before a standard pit-counting technique was developed. Hence no direct comparison is possible.

5. Surface Blueing

It was noted in several runs (early specimens with aluminum and later stainless steel), that a surface discoloration developed in regions of relatively severe cavitation damage. (In the case of the aluminum, this was the region directly downstream from a small pin used to trigger cavitation on specimens used in the early part of the investigation which were flush with the venturi wall.) As examined under a low-power microscope, the discoloration was in the form of "rainbow" - colored strips, perhaps the order of 10 mils across.

The explanation of this phenomenon is not known at present. However, it has been noted in subsequent tests with mercury on carbon steel and stainless steel (to be described in a future report), and has also been reported by previous investigators,[23,32,46] by whom it was called "temper blueing".

6. Microstructural Examination of Cavitation Damage on Stainless Steel

a) Slip Lines in Vicinity of Pits

Microscopic examination of pits in stainless steel caused by exposure to a cavitating stream of water has revealed plastic deformation in the region surrounding a pit.

The sample (3-26) had been run for eleven hours at standard cavitation conditions ( i.e., to the midpoint of the sample) and a throat velocity of 95 feet per second (see Table I).

The damaged surface of the sample selected for observation of structure in the region of pitting is shown in Figure 20-a. The results of observations on one irregularly-shaped pit (i.e., not crater-type)

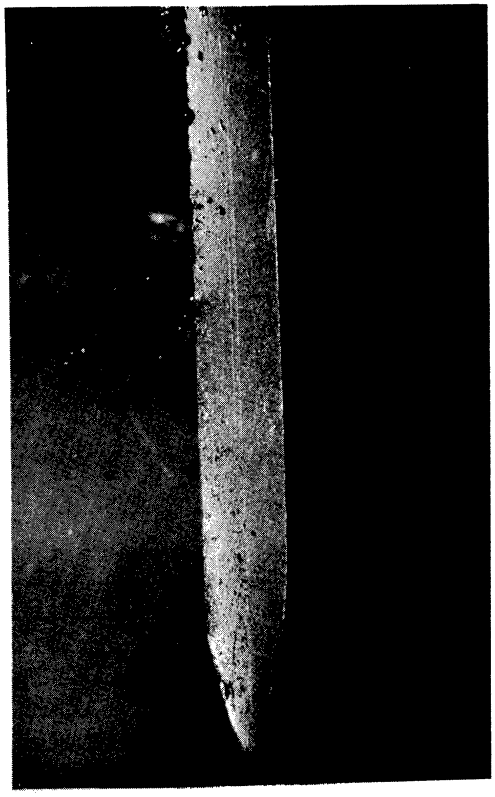

20-a

Photograph through mount-7X

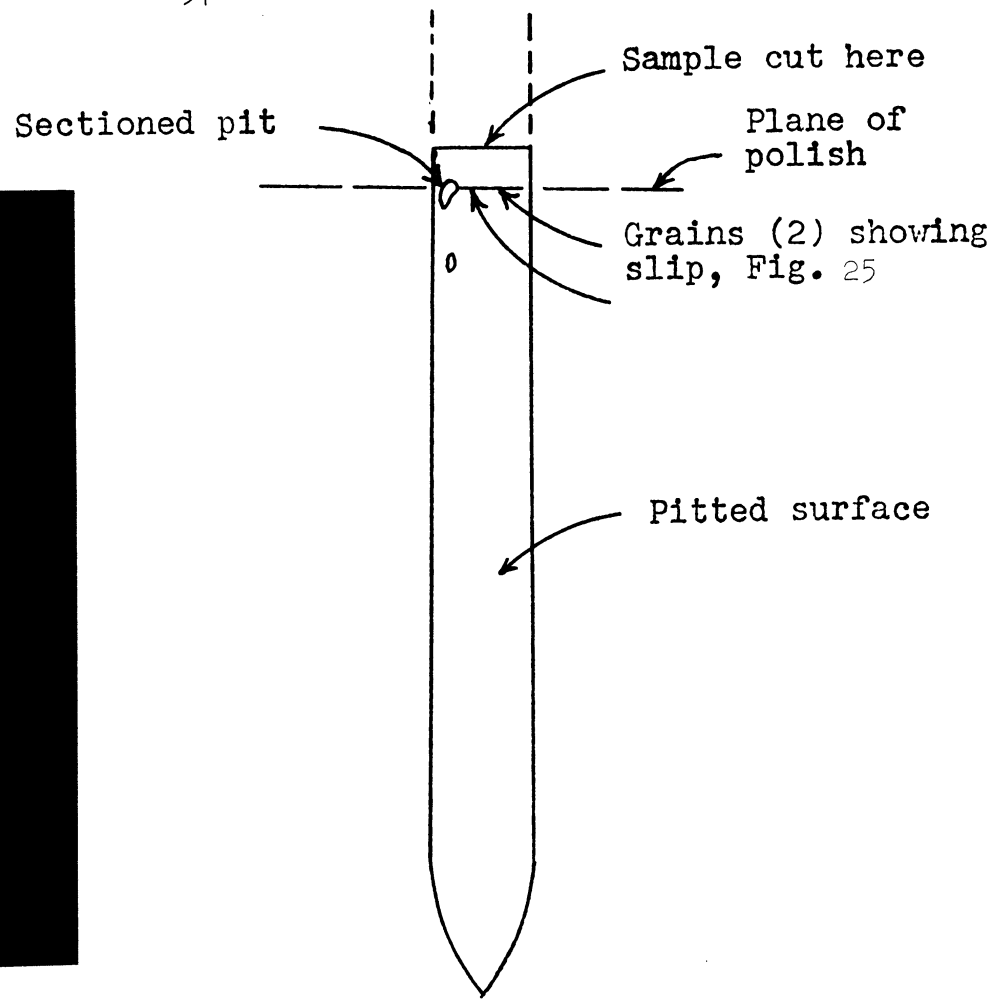


20-b

Schematic of Fig. 20-a

Figure 20. Photograph of pitted surface of test specimen.

are presented. Figure 20-b indicates the particular pit selected. Figure 21 is a 75X enlargement of the pitted surface in the region of the pit selected for observation. The particular pit examined is that in the upper left-hand corner of the photograph. It is noted (Figure 23) that the pit is about 2 mils across, and about 0.2 mils deep which gives an approximate width to depth ratio for the pits which have been observed.

The sample was cut just ahead of the pit as indicated in Figure 20-b and in a cold-setting polyester mount. The schematic diagram of orientation is shown in Figure 22 which indicates how the sample was photographed through the transparent mount in Figure 20-a and also that the photomicrographs were taken of the structure in a plane perpendicular to the pitted surface.

The exposed surface of the sample was ground down to the pit selected for microscopic examination on wet silicon carbide polishing papers No. 400 and 600. Fine polishing was accomplished with 6 micron diamond abrasive, and Linde A abrasive using the Syntron. The sample was then etched electrolytically with a 60% nitric acid in water solution.

Slip lines were clearly observed in the immediate vicinity of the pit as shown in Figure 23-a. Slip is not observable in every grain which borders on the region of the pit. This is expected since slip is strongly a function of crystal orientation, and deformation should occur only in those crystals whose lattice structures are properly oriented with respect to the stress field.

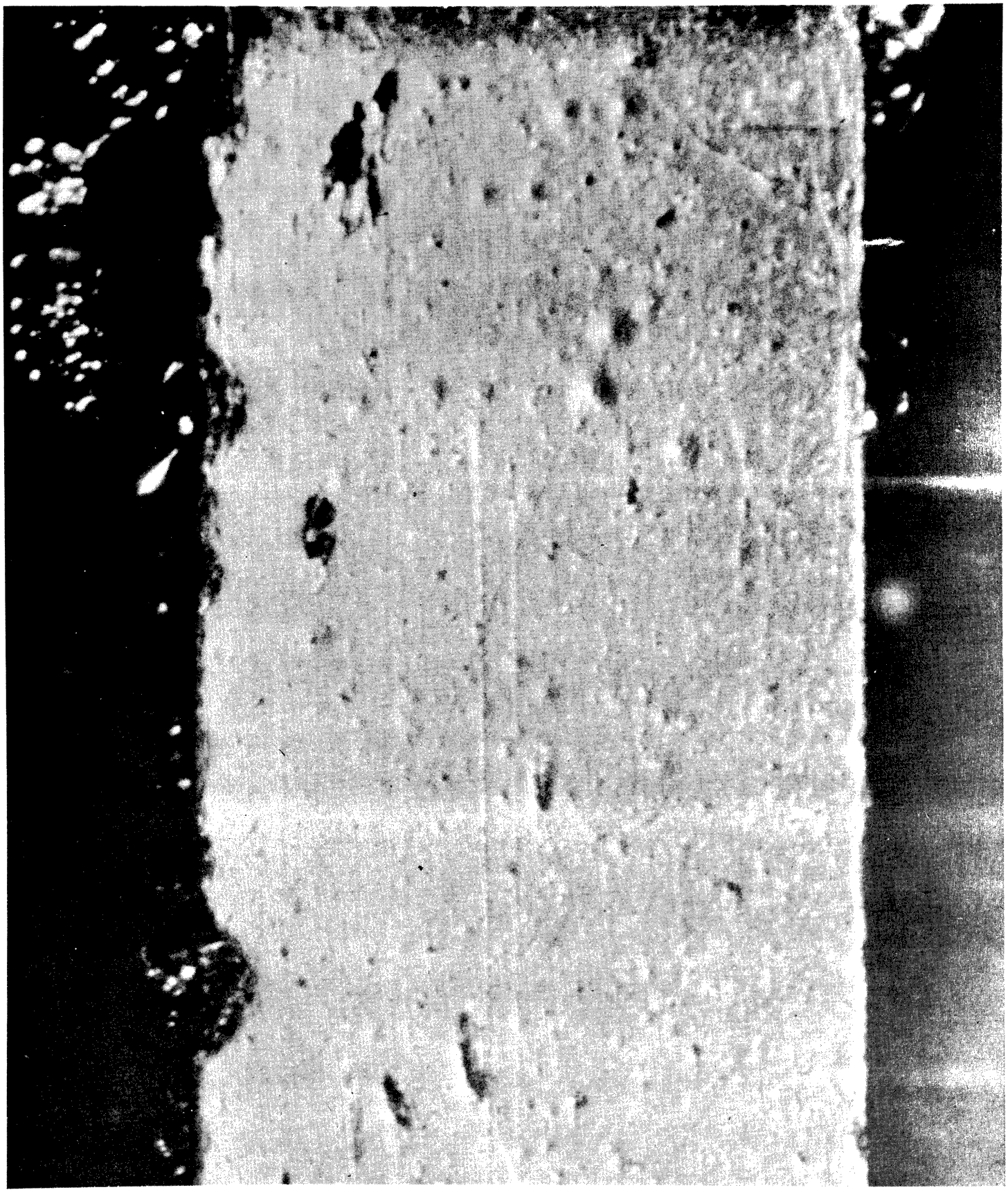

Figure 21. Photograph of pitted surface of specimen - 75X.
(Pit examined is shown in upper left hand corner.)

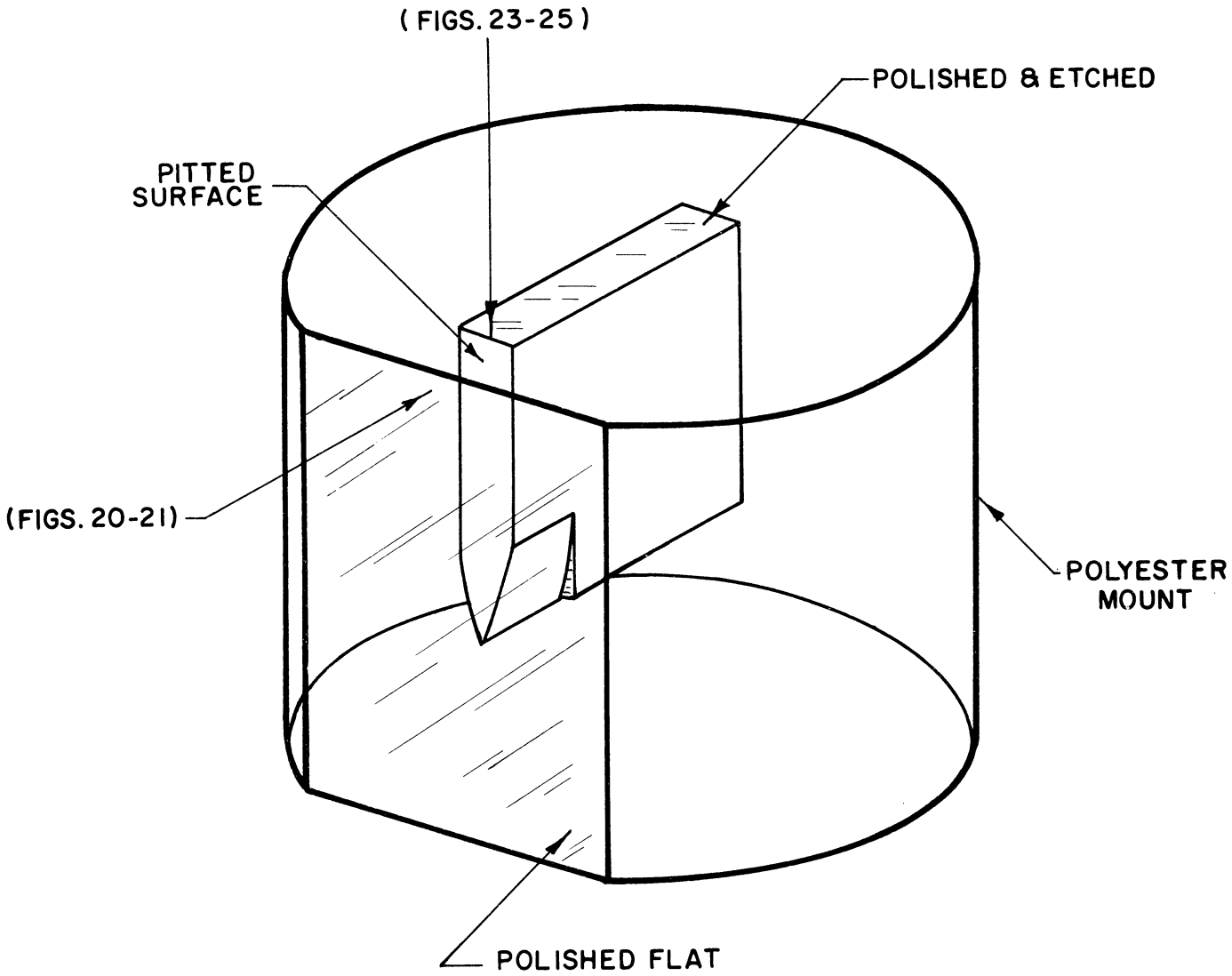


Figure 22. Schematic diagram of sample orientation in polyester mount.

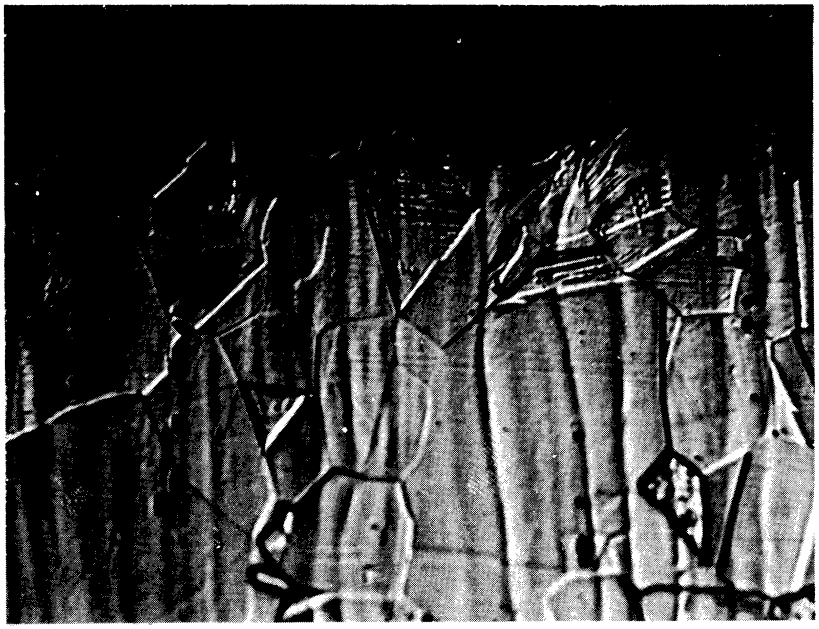

(a)

(b)

Figure 23. Typical sections through irregular shaped pit showing slip lines. (Magnification 1000X, oil immersion, oblique illumination.) Figure 23-b is the same pit as Figure 23-a, but after additional polishing to show slip bands exist in 3 dimensions.

The fact that the slip bands exist in three dimensions is shown by Figures 23-b and 24 which are photomicrographs of the same pit section after polishing to a greater depth into the pit and re-etching.

b) Slip Lines Elsewhere in the Structure

From the observations on the sectioning of this pit, and of other pits in this sample, it can be concluded that the observed slip lines are unique to cavitation pits. The interior of the sample is completely free of any evidence of plastic deformation. Grains near the exposed surface have been observed to be completely free of slip lines except near a pit, with two exceptions. Two isolated grains, both on the surface of the specimen, were found to contain microstructural evidence of crystallographic slip. The microstructures of these grains are shown in Figure 25-a and 25-b. Their location on the sample surface is indicated in Figure 20-b.

Both of these grains are on the surface of the sample which was exposed to the cavitating fluid. Although there was no optically observable pitting or surface deformation, the presence of slip lines may indicate that some initial damage to the metal structure had already occurred. Indications of such initial damage prior to pitting was observed by Ellis[5] using an x-ray diffraction technique.

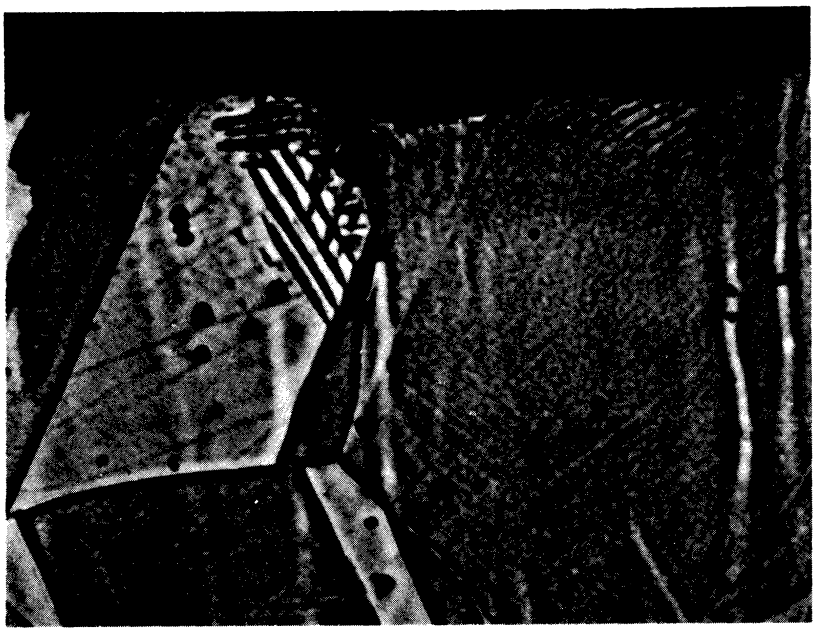

Figure 24. Typical section through irregular pit showing same slip lines as in Figure 23-b. (Magnification 2000X, oil immersion, slightly oblique illumination.)

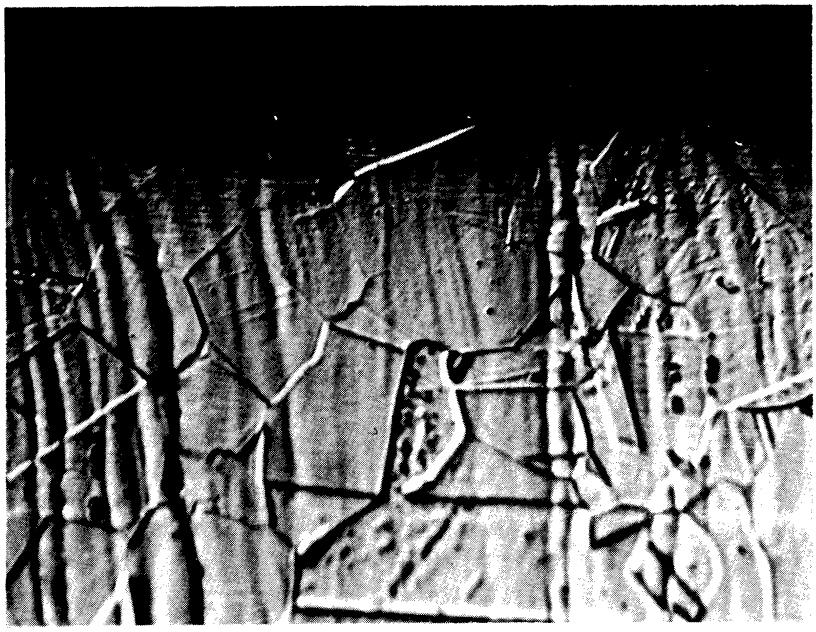

(a)

(b)

Figure 25. Evidence of crystallographic slip in two different isolated grains away from pits. (Magnification 1000X, oil immersion, a) oblique illumination, b) slightly oblique illumination.)

## V. CORRELATION OF CAVITATION DAMAGE WITH TEST PARAMETERS

### A. Calculation of Volume Loss and Area Damaged

#### 1. Selection of Parameters

To delineate the effect of the various test parameters it is desirable to have a parameter which is given by a single number to represent the cavitation damage incurred. A logical choice for such a parameter, and one that has been used widely in the past, is the volume (or weight) of material removed. This has obvious disadvantages in that a given volume loss does not correspond to a given impairment of function unless the specified distribution exists. However, coupled with knowledge of the type of damage (i.e.: general shape and distribution of pits), this disadvantage is largely obviated. The total number of pits, or simply the number of pits in any one of the size categories is not adequate and no single alternative parameter is known. Hence, to describe the effect of the various test parameters volume (or weight) loss has been used, realizing that the pitting characteristics are also available.

In most previous investigations, weight or volume loss has been determined by direct weighing. However, this has proven impractical for the water tests herein described. For the durations so far attained, the weight or volume losses have not been great enough as a proportion of the test specimen weight for accurate measurement by any direct technique. As an alternative, volume losses have been computed from the pit counts.* It is realized that the absolute numbers so attained will not

---

* These are presented in terms of volume loss per unit area with units of cm. It is noted that numerically this is equal to the average depth of material removal if the damage were spread uniformly over the exposed surface.

by highly accurate. However, they should be reasonably consistent, so that the comparisons between runs under different test conditions should be meaningful. If an eventual comparison to a direct technique can be made, it may be found that multiplication of the results from the pit count calculations by a simple factor will provide accurate, absolute magnitudes.

2. Derivation of Relation

The relation between pit size and number and the volume removed is derived from the results of the proficorder analysis.[4,44] The traces of approximately 50 pits were studied and a close resemblance among them found. From this, "typical" pits were postulated depending on size category. All were assumed composed of a ridge and a well, both cylindrical, (Figure 26). The relation between depth and height of ridge and well, and mean diameter of the pit, was obtained from the proficorder traces. Thus the volume of metal removed from a typical pit can be estimated.

The damaged surface of three stainless steel specimens was studied to get a typical pit-size distribution, which was incorporated with the pit-volume information to give average volumes, based on three visual sizes ($0.3 < D_p < 1.5$ mils, $1.5 < D_p < 3.0$ mils and $3.0 < D_p < 10$ mils; small, large, and very large). These volumes, multiplied by the number of pits in the various classifications, gives the total volume removed. A more detailed description of this method is given in Reference 44.

The total volume loss is not based only on the polished surface, but is extrapolated to cover the entire area (8.689 x polished surface), assuming the pitting intensity on the sides and polished surface is the

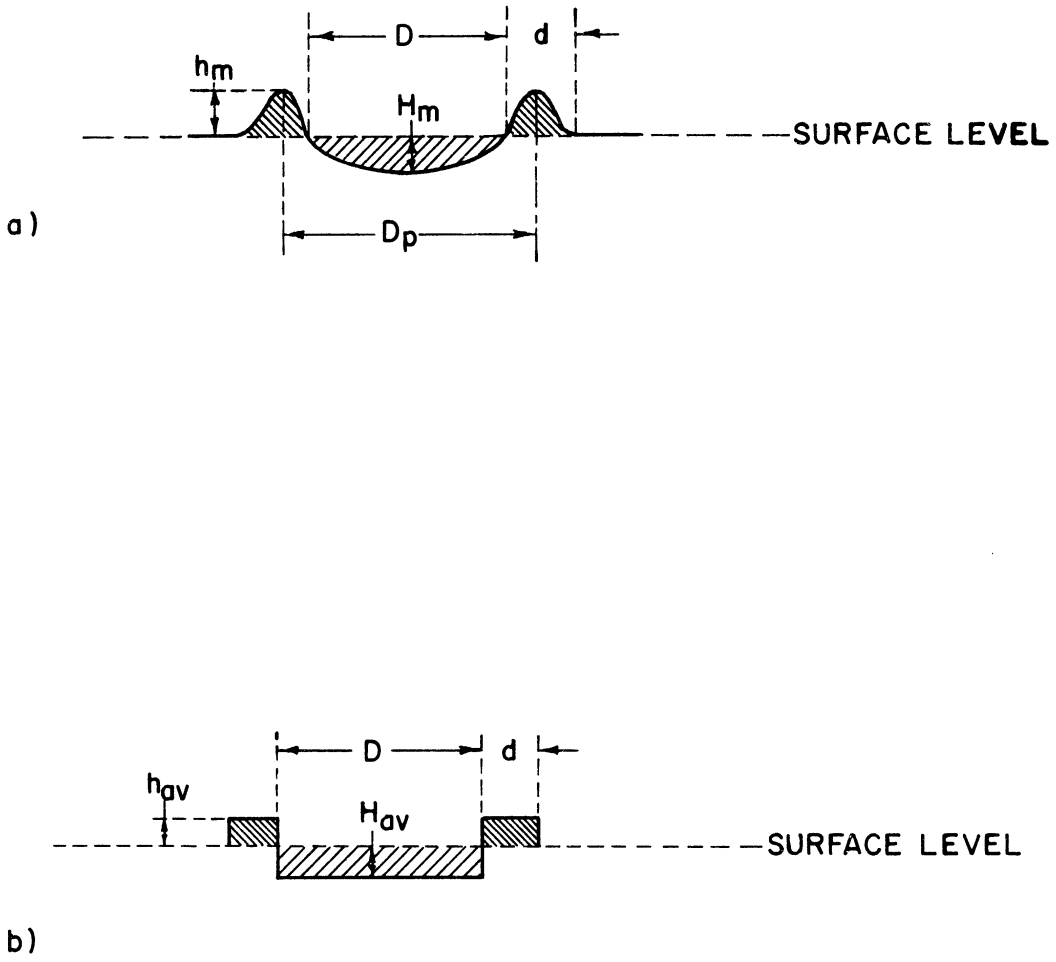


Figure 26. Exaggerated sketch of typical pit, a (upper) and the model assumed for calculating volume loss, b (lower).

same. As mentioned in a previous section, this does not appear to be the case. Instead, based on the detailed examination of 4 specimens, it appears that the pitting intensity on the sides is only about 1/3 to 1/4 that on the polished surface. If it is possible eventually to determine a suitable constant to represent the ratio of pitting intensities between these locations, the present results can be corrected by multiplying by a suitable factor. However, even though an incorrect value of this ratio is used, the results between different runs are still consistent.

## B. Volume Loss as a Function of Various Parameters

### 1. Time

Figures 27, 28, 29 are plots of volume loss per unit area versus test duration for four pairs of specimens - three pairs of stainless steel and one pair of carbon steel - under three different cavitation conditions. The arithmetic mean values of these pairs of data for stainless steel only are summarized on logarithmic coordinates in Figure 30 and on cartesian coordinates in Figure 31, along with two additional points for a fourth and a fifth cavitation condition at a single test duration. All the curves show rapid damage formation in the early stages of the test ( $< 3$ hours, most evident on cartesian coordinate plot, Figure 31), which levels off from perhaps 3 to 20 hours, and then is followed by an accelerating damage rate.

A rapid initial damage rate leads to the assumed existence of "weak spots" (perhaps inclusions) which are quite easily removed. However, apparently these are exhausted relatively quickly, leading to the

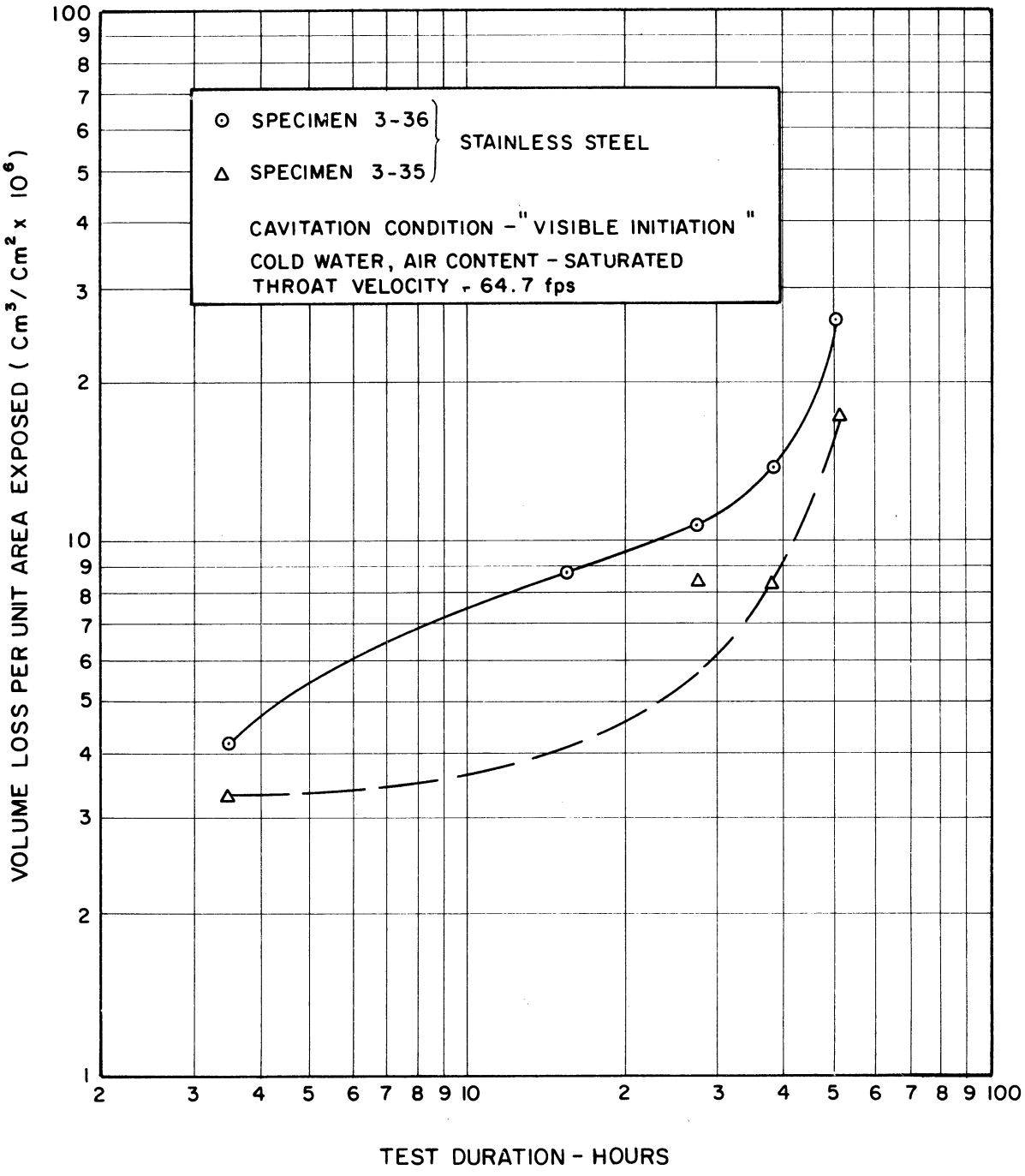


Figure 27. Volume loss from stainless steel specimens per unit area of specimen exposed to fluid vs test duration. (Visible initiation, 64.7 ft/sec).

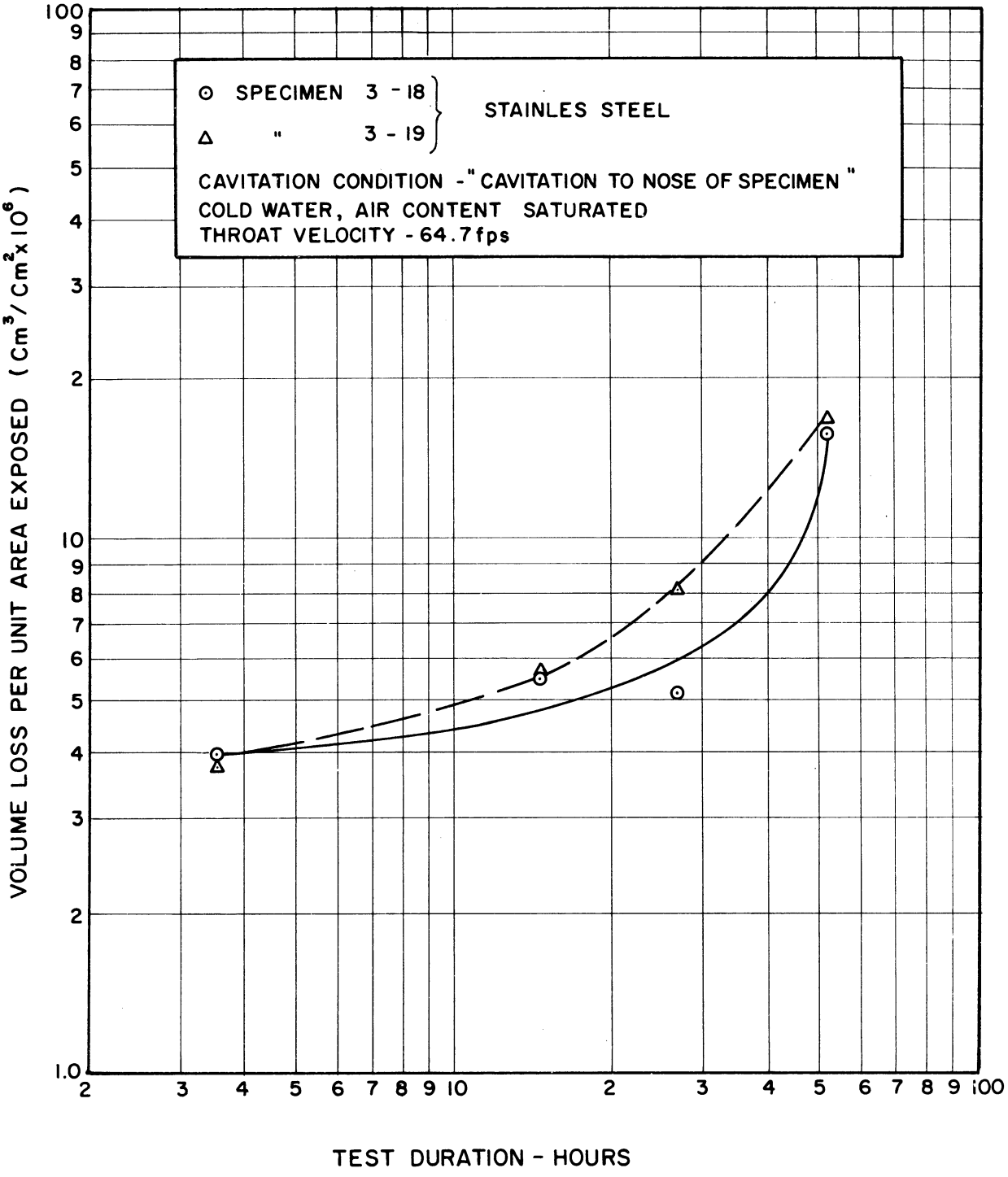


Figure 28. Volume loss from stainless steel specimens per unit area of specimen exposed to fluid vs test duration. (Cavitation to nose, 64.7 ft/sec)

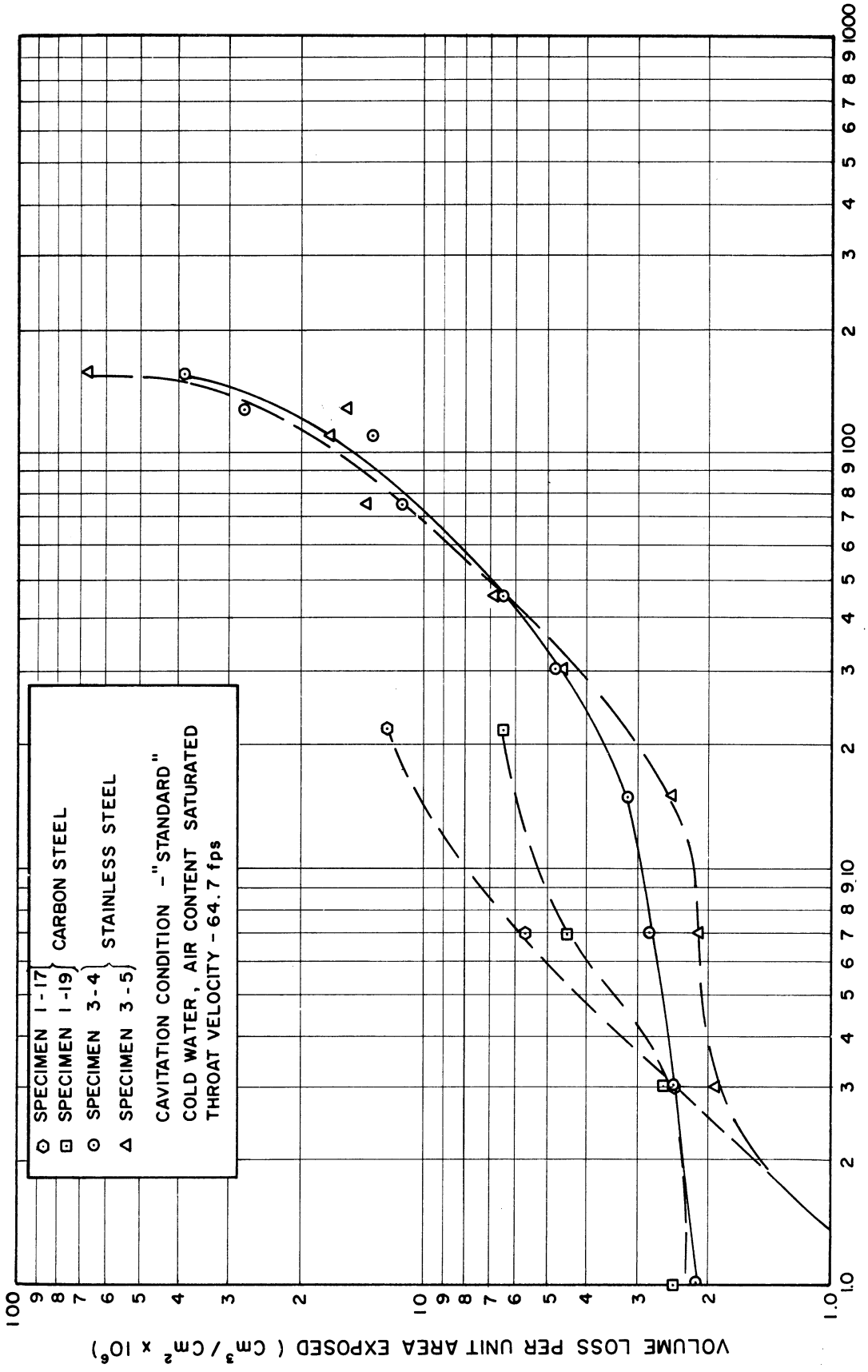


Figure 29. Volume loss from stainless steel and carbon steel specimens per unit area of specimen exposed to fluid vs test duration. (Standard cavitation, 64.7 ft/sec).

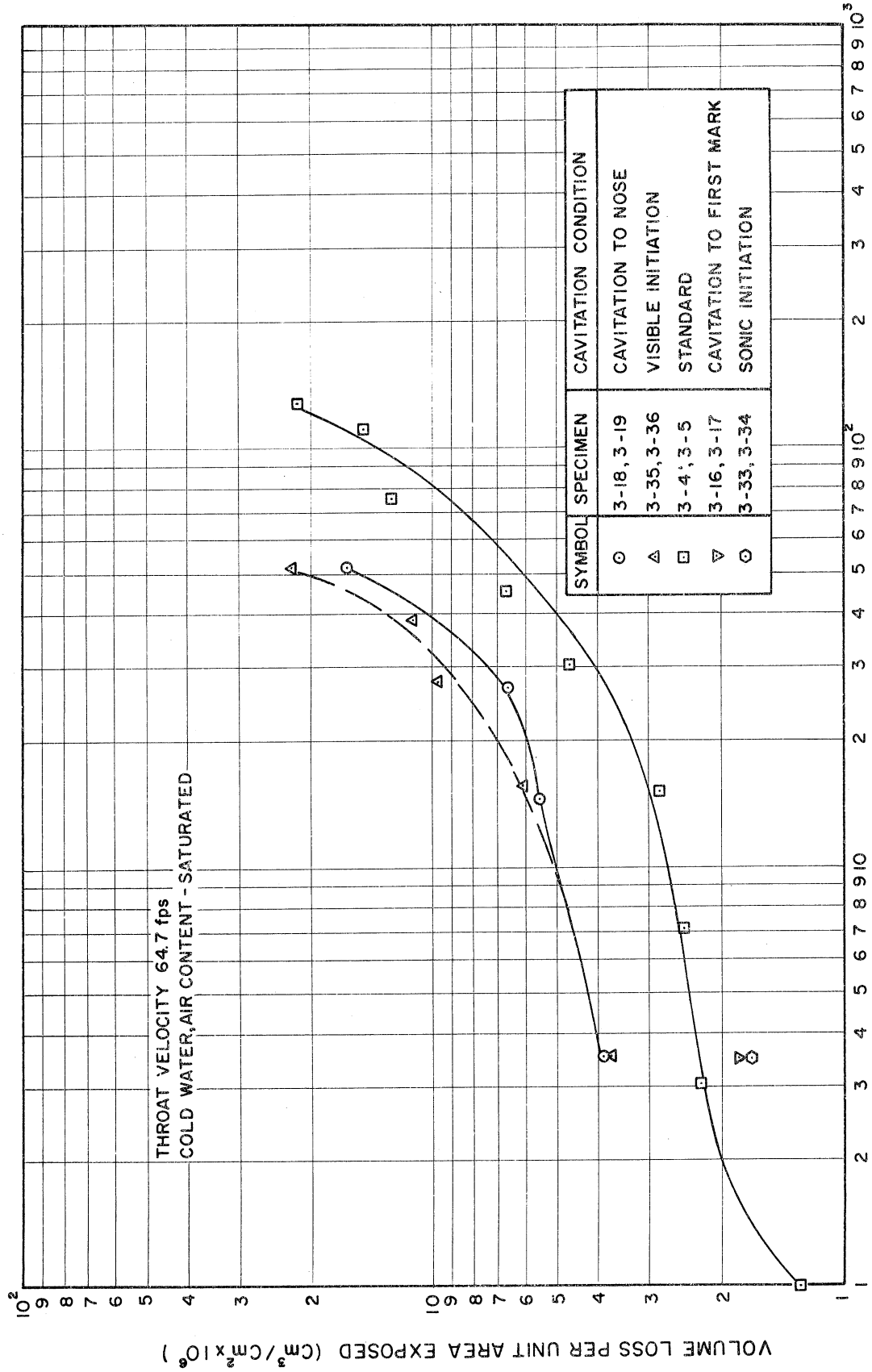


Figure 30. Mean volume loss per unit area of specimen exposed to fluid for pairs of stainless steel specimens vs test duration; for several cavitation conditions. (Logarithmic coordinates).

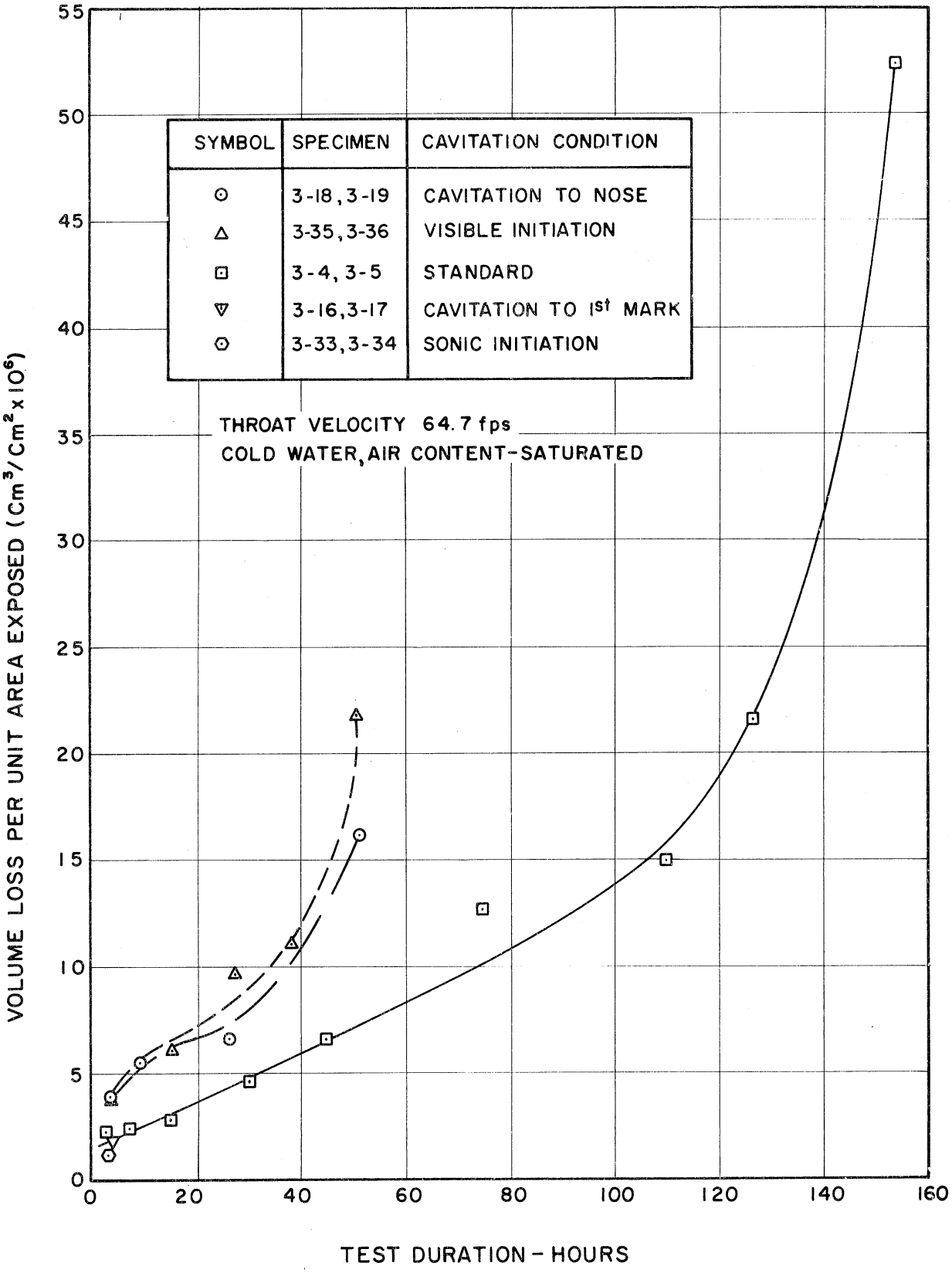


Figure 31. Mean volume loss per unit area of specimen exposed to fluid for pairs of stainless steel specimens vs test duration; for several cavitation conditions. (Cartesian coordinates).

leveling-off of the damage curve. When a specimen is exposed to cavitation for a longer period, even the "good material" is attacked so that a steep portion of the curve appears again with the acceleration of damage rate perhaps due to flow perturbations caused by the roughened surface. A strong similarity to conventional creep curves is evident in the shape of these curves. The possible connection between previously observed "incubation periods" is discussed later (References 4, 11, and 20 for example).

2. Cavitation Condition

Figures 30 and 31 compare the cavitation conditions, summarizing the previous figures as well as presenting single points for sonic initiation and cavitation to "first mark" (which is beyond the downstream end of the test specimen). The data is further illustrated in Figure 32 which is a cross-plot of volume loss versus cavitation condition at various durations. Damage intensity at each test duration is least for sonic initiation, but of the same order as for the well-developed cavitation conditions ("Standard" and "First Mark"). However, the damage intensity is greater by a factor of 2 to 3 for "visible initiation" and "cavitation to the nose" (of the specimen) which are about comparable.

The variation of damage intensity with degree of cavitation (cavitation condition) is believed principally the result of two conflicting trends. As the extent of the cavitating region is increased, the number of bubbles present is increased. However, the general pressure level in the vicinity of the test specimen (Figures 6 and 7) is decreased,

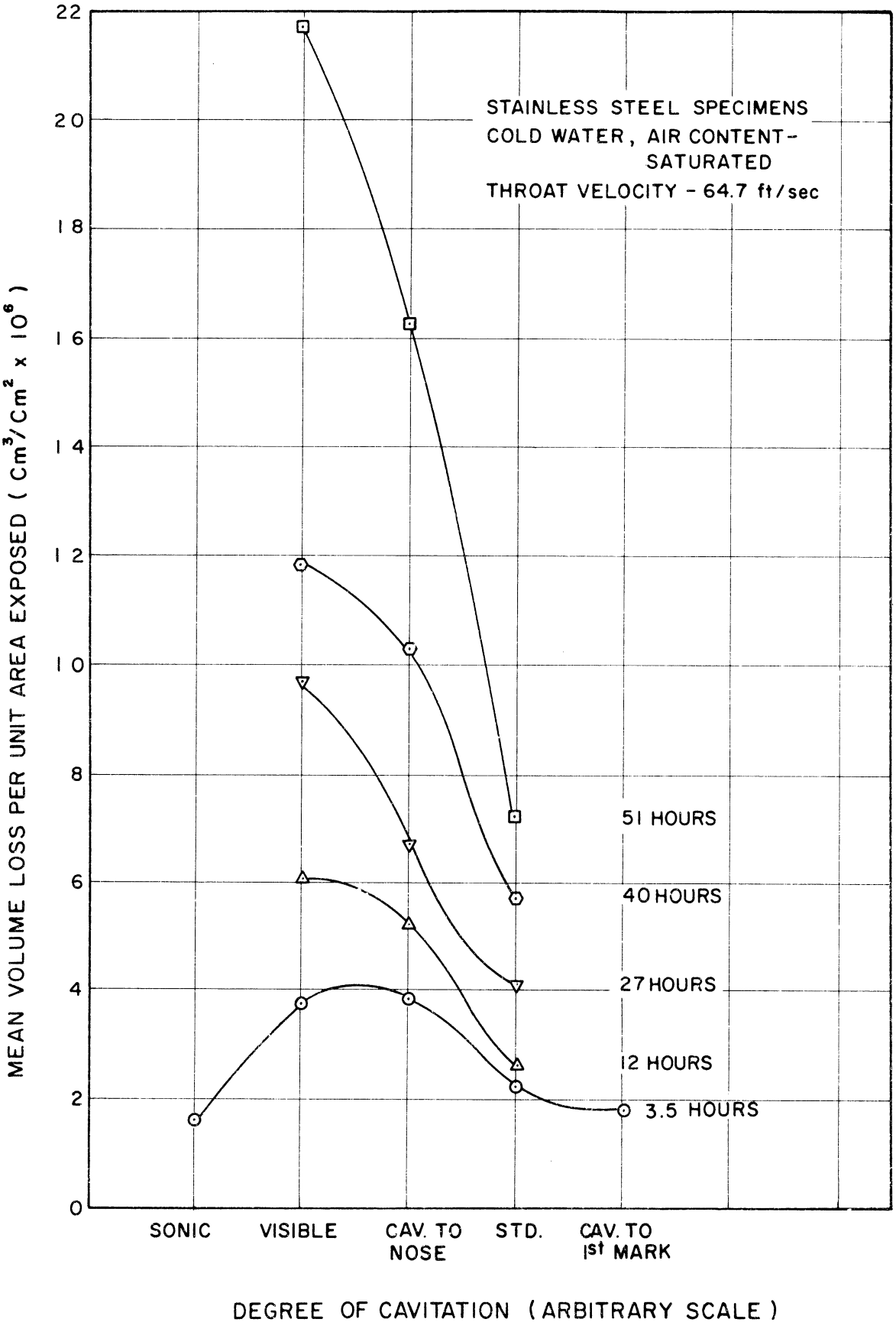


Figure 32. Mean volume loss per unit area of specimen exposed to fluid for pairs of stainless steel specimens vs degree of cavitation; for several test durations.

and thus the driving force available for bubble collapse is decreased. In terms of the "energy spectrum" concept discussed previously (Figure 19), the spectra for these conditions might appear somewhat as shown in Figure 33. The interplay of these conflicting trends results in a maximum in the damage intensity versus degree of cavitation curve between "cavitation to nose" and "visible initiation", and a decrease to either side. The decrease for well-developed cavitation is a result of the fact that the pressure in the vicinity of the test specimens is not much greater than vapor pressure (Figure 7), providing only small collapsing force, even though there are very many bubbles present. Thus, the area under curve (Figure 33) to right of threshold energy is small. On the other hand, for sonic and visible initiation, at the test velocity cited of 64.7 feet per second, the unperturbed pressure at the midsection of the test specimens is about 10 psi above vapor pressure (Figure 6), giving a large driving force for the collapse of whatever bubbles may be present. Apparently in visible initiation there are enough bubbles, probably largely a result of local cavitation from the specimen*, to cause about the same pitting intensity as cavitation to the nose, (thus areas under curve to right of threshold energy for these conditions are about the same), whereas in sonic initiation the number of bubbles (even from local cavitation) has apparently been decreased considerably.

* Although this could not be seen with unaided vision, it is probable that it will be observed in future tests with high speed motion pictures or stroboscopic lighting.

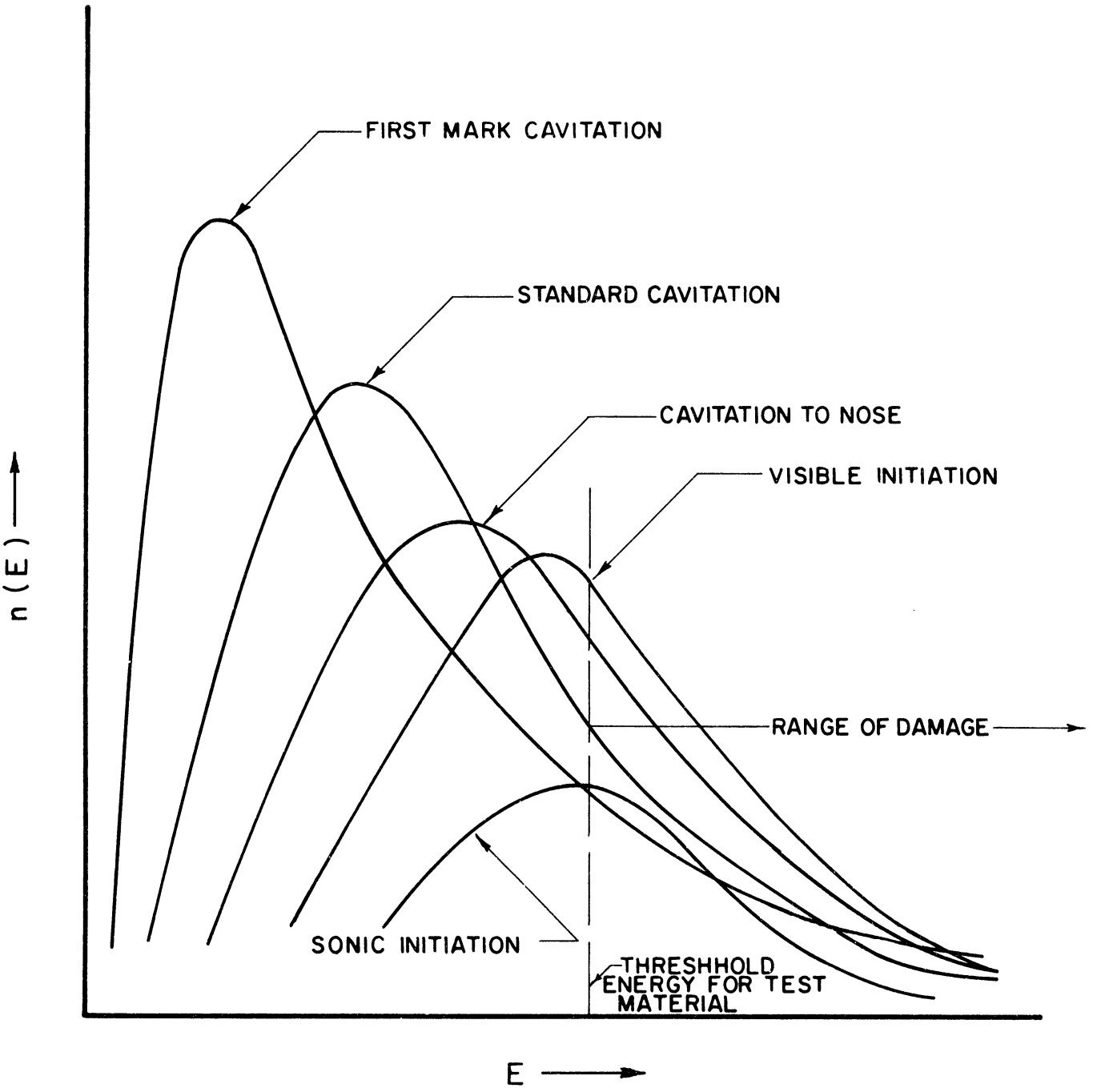


Figure 33. Hypothezised bubble energy spectra for various cavitation conditions at a constant velocity, for a given material. (Presumably, curves at higher velocity are generally similar, but at higher n(E) and E .) n(E) = number of bubbles from those "in vicinity" of damage specimen which deliver an energy quantum, E, to surface of the specimen. E = energy delivered by an individual bubble to the surface of the specimen.

This general type of behavior is also evidenced by tests with magnetostriction devices reported by Nowotny[27] in which the fluid temperature is varied over the range between solidification temperature and boiling temperature at a constant pressure. It is found that the damage reaches a maximum at some temperature well below the boiling temperature (as low as 50° C for atmospheric pressure in some of Nowotny's work). Presumably at temperatures near the boiling temperature there are very many bubbles but the collapse energy is small, so that the damage is small. At lower temperatures there are fewer but more energetic bubbles with resultant increased damage. As the temperature is reduced still further, the energy of the individual bubbles continues to increase, but the number of bubbles becomes extremely small so that the resultant damage decreases.

Tests with still greater pressure in the vicinity of the test specimens were made. The pressure, which was as high as possible and limited only by the facility capability, was 14.0 psi above vapor pressure at the minimum pressure point and 22.6 psi above vapor pressure at the test specimen mid-point for 55.5 ft/sec. These pressures correspond to about 3 and 9 psi above vapor pressure at the same locations respectively for sonic initiation; i.e.: $\sim$1 atmosphere (or $\sim$30 ft. of fluid) above the sonic cavitation initiation condition. In these "zero cavitation" tests under the same contions* the volume removal was only about 7% that for sonic initiation, indicating the continuing presence of a

---

* Concluded by prorating runs at slightly different conditions using approximate relations between known results. Though exact numerical value may not be meaningful, the order of magnitude is significant.

few locally induced cavitation bubbles, and/or that high velocity erosion produces similar pitting but in a substantially smaller amount. The latter is believed to be true to some extent, and has been mentioned by previous investigators.(35)

An additional observation, that appears consistent with the general trend of the previous discussion, is that proportionately more small pits were found on the "visible initiation" specimens that on these from "cavitation to nose". This seems to indicate that the "visible initiation" damage is only slightly affected by the overall cavitation field, which presumably contains relatively large bubbles since a relatively large length of travel is afforded, but instead is markedly influenced by local cavitation induced by the small test specimens. On the other hand, "cavitation to the nose" is largely a result of bubbles from the overall field. It is hoped that a more detailed examination of the specimens, to be made in the future, to detect differences in size distributions, as a function both of degree of cavitation and velocity, may throw more light on the mechanism.

3. Velocity

Figures 34, 35, and 36 show the dependence of damage intensity upon velocity for stainless steel, carbon steel, and aluminum, respectively. In these runs, standard cavitation was used, and the throat velocity was in the range from 55 to 100 feet/second. The water temperature was at about 70°F and it contained about the saturation quantity of air.

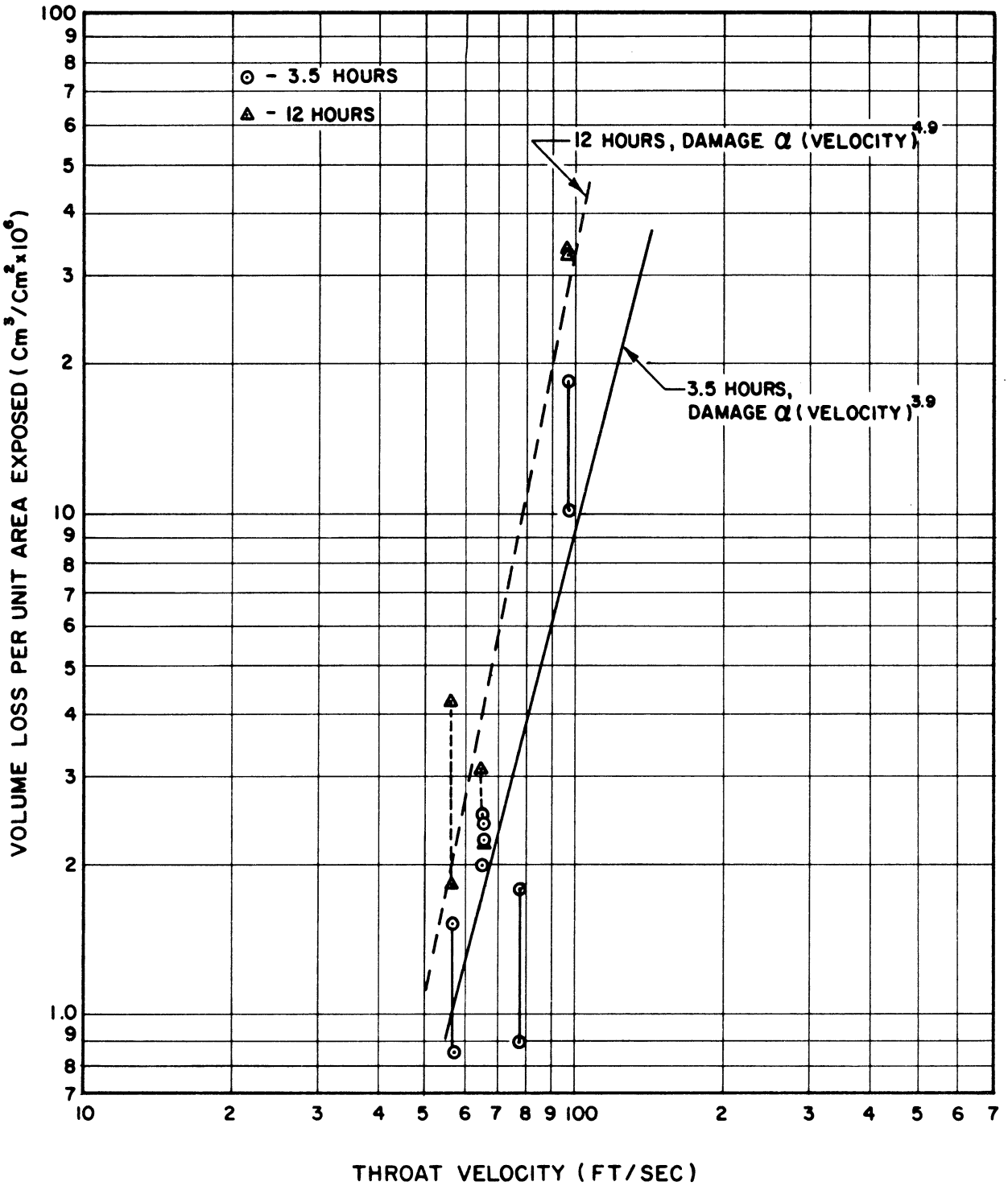


Figure 34. Volume loss per unit area of specimen exposed to fluid for stainless steel specimens vs throat velocity, for two different test durations, under standard cavitation condition.

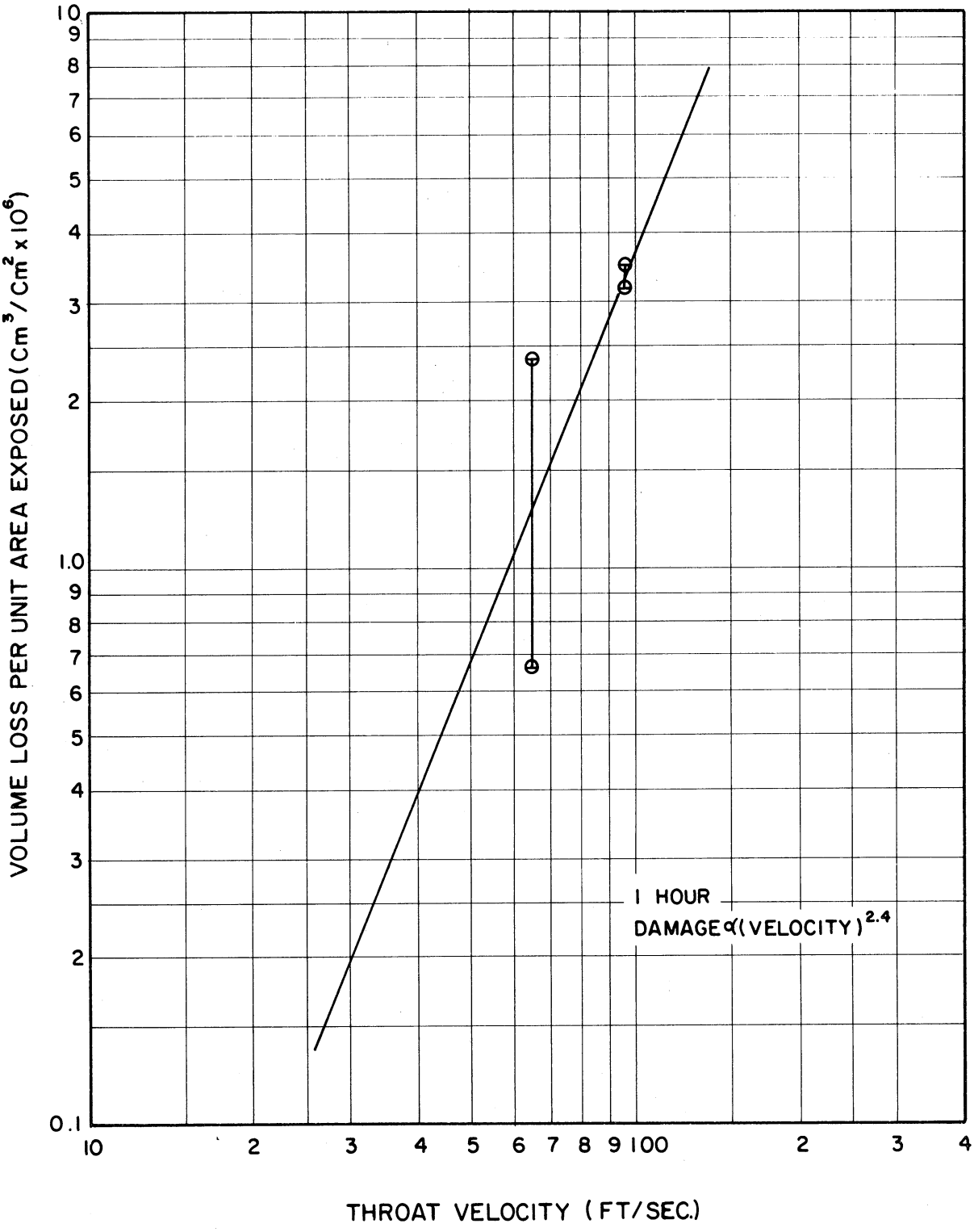


Figure 35. Volume loss per unit area of specimen exposed to fluid for carbon steel specimens vs throat velocity, for one hour test duration under standard cavitation condition.

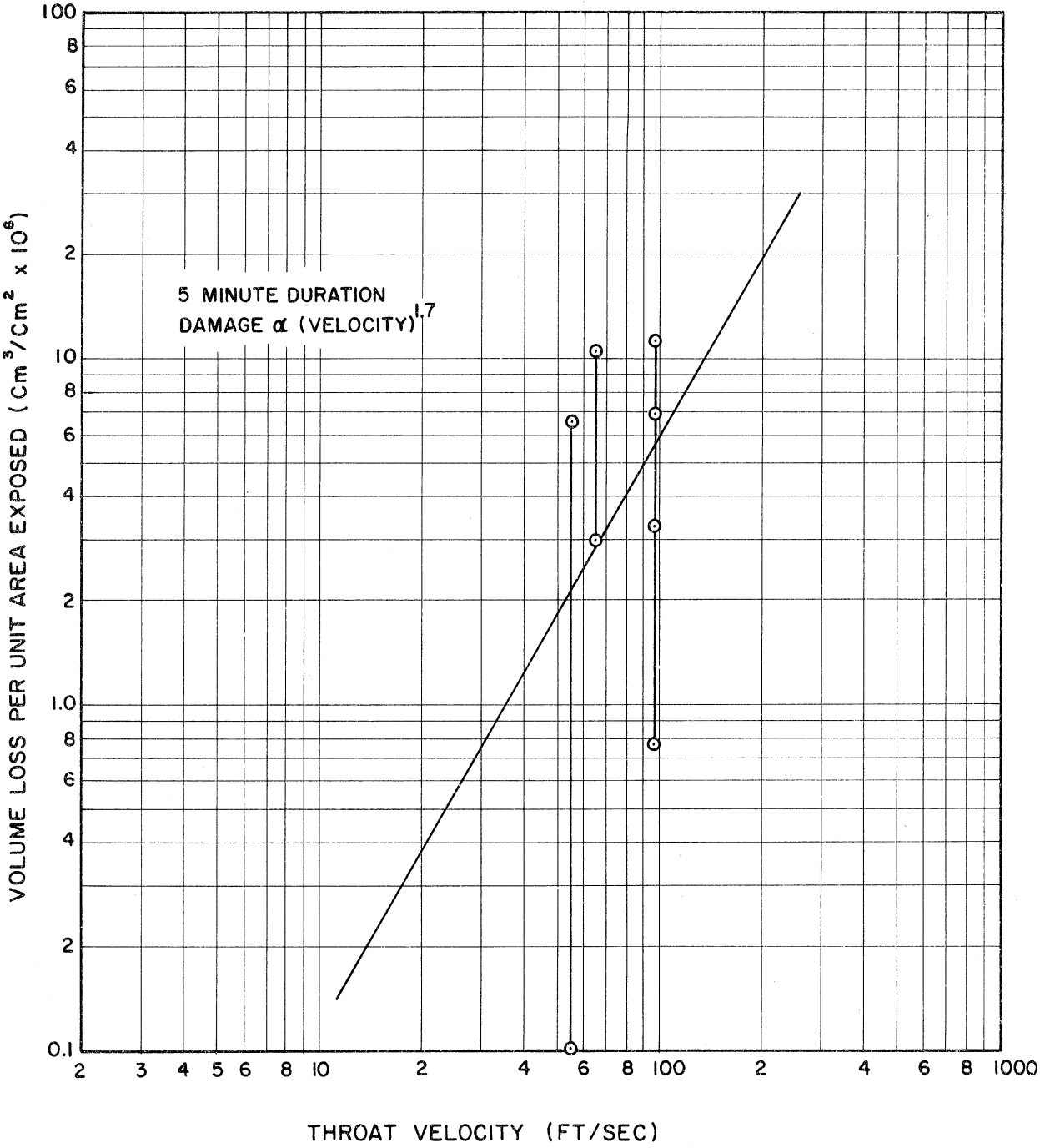


Figure 36. Volume loss per unit area of specimen exposed to fluid for aluminum specimens vs throat velocity, for five minute test duration under standard cavitation condition.

It is noted from these figures that, while cavitation is apparently a positive function of through-velocity the experimental scatter is such that no conclusions regarding the type of function are justified. However, a "best curve" assuming a simple power dependence (Vol $\alpha$ $V^n$) has been shown using a least mean square fit.

Consideration of the mechanism by which velocity is assumed to influence damage indicates that the existence of a simple relation would be surprising. From the viewpoint of bubble dynamics, it is assumed that velocity influences the pressures generated in bubble implosions by translating the bubbles, during their growth and collapse, through regions of changing external pressures. The translational bubble velocity, and hence the pressure gradients with respect to time seen by the bubbles, as well as the magnitudes of the pressures themselves at given locations, depend upon the through-velocity. However, the precise formulation of this dependence is not possible at present, due to the highly complex three-dimensional, two-phase flow in the present cavitating venturi. The large cavitation "scale effects" described in previous reports from this investigation,[9,10] show the inapplicability of dynamic similarity considerations to this type of flow. However, even if the dependence of bubble implosion pressures upon through-velocity were known, the relation between these pressures and the damage intensity would still be a highly complex function of material properties and not at present capable of precise formulation. However, two approximate formulae have been suggested in the past:

i) Damage $\alpha(V-V_{threshold})^{2*}$

This was suggested by Honegger, and is quoted by Ackeret.[1] It was based on tests with a jet-impact type of apparatus on various types of materials. The existence of a threshold velocity below which no damage will be incurred is implied. This implication seems reasonable for tests in flowing systems, where corrosion is negligible, the material has appreciable fatigue and yield strength, and increased through-velocity implies increased stagnation pressure (as in present stainless steel tests) if it were substantially true that all bubbles in a given system delivered approximately the same energy quanta to the surface. However, this latter condition does not appear to be likely. For the present tests, insufficient low velocity data is available to draw conclusion in this matter.

The observation of a threshold velocity has not been uncommon in the past, when test conditions were as previously specified.[7, 11, 22]

ii) Damage $\alpha\ V^n$

Some investigators have not considered a threshold velocity but rather a pure exponential dependence (but with an exponent of the order 5 - 7 rather than 2). Such a relation might in some cases closely approximate the Honegger curve, and might be considered to represent

---

* Based on his own tests, Honegger suggested a value of 380 feet/second for $V_{threshold}$. According to Hobb's data,[11] also from an impact device, a value of about 300 feet/second applies for mild carbon steel, brass, and duraluminum, although the endurance limits of these materials differ significantly. However, the exponent is about 5.5 rather than 2, although the exponential dependence above the threshold velocity is clearly shown.

conditions more closely, if some small damage persisted even at small velocity, perhaps due to corrosion effects or the existence of a small number of sufficiently energetic bubbles even at low velocity. Apparently the pure exponential relation was first suggested by Knapp[17] from observations on soft aluminum in a water tunnel. He reported a value of 6 for the exponent.

The absence of an appreciable threshold velocity in Knapp's case seems reasonable considering the very low fatigue and yield strength of the material, so that even relatively non-energetic bubble implosions could create damage. Subsequent investigators who have presented their data in the framework of such a relation are Hobbs,[11] Kerr and Rosenberg,[15] and Lichtman, et.al.[22] Their values of the exponent were all between 5 and 7. However, Moussons data[24] shows a value of 11.7 for velocities between 200 and 235 feet/second and 3.8 between 235 and 265 feet/second or 9 if taken over the whole range. His tests were on copper for which it seems likely a threshold velocity would exist ( high yield and fatigue strength and low corrosivity). If a threshold velocity for these tests of 168 feet/second is assumed, the Honegger formula applies quite closely for his exponent of 2. However, the assumption of different threshold velocities in this case leads to almost any value for a consistent exponent. Hence, either the Knapp or Honegger-type of formulation could be applied to almost any set of data.

Examination of the present data plotted as previously described for stainless steel, carbon steel, and aluminum (Figures 34, 35, and 36) indicates values of the exponent, n, of 3.9 and 4.9 for

stainless steel after 3.5 hours and 12.0 hours respectively, 2.4 for carbon steel after 1 hour, and 1.7 for aluminum after 5 minutes. Thus all values are considerably less than those of the previous investigators already discussed. However, it is noted that considering all cases together the exponent is increasing with time and approaching the range of the previous investigations. This can be seen from Figure 37 where n is plotted against time. However, a consideration of the actual phenomenon, (previously discussed), as well as the experimental evidence from this and previous investigations indicates that general formulations along the lines of either Honegger or Knapp are likely to be very limited in application. A more meaningful relation must consider the peculiarities of the particular flow system used, as well as the properties of the material tested.

4. Specimen Material

A comparison of damage intensities among the three materials used, stainless steel, carbon steel, and aluminum, in terms of volume loss per unit area per unit time can be made. As previously observed in Figure 31 a plot of volume loss per unit area versus test duration for stainless steel, indicates a very high initial damage rate. The shortest test duration for stainless steel was one hour, for which the volume loss per unit area was comparable to that of aluminum after only a five minute test duration. Assuming a constant damage rate for each material during these shortest initial time intervals for which data is available, the volume loss per unit area per unit time at a velocity of 65 ft/sec., was about 30 times greater for aluminum than for either

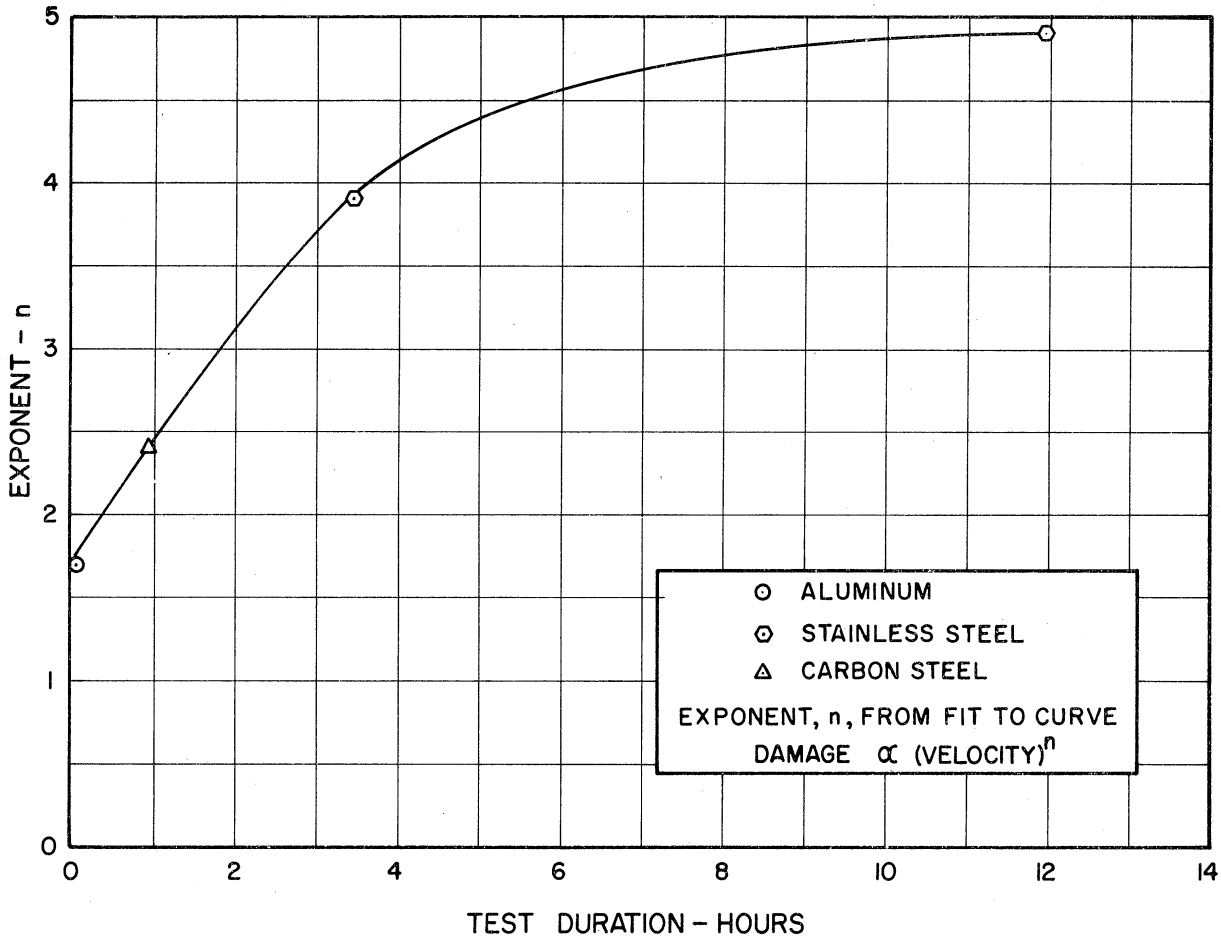


Figure 37. Value of the exponent, n, vs test duration for several specimen materials, where n is obtained by assuming Damage $\propto$ (Velocity)$^n$.

carbon steel or stainless steel, at 95 ft/sec, the damage rate was about 20 times greater for aluminum than for the steels which were about comparable. However, after 22* hours, at 65 ft/sec the total damage for the carbon steel is about three times that for the stainless steel.

A comparison of the physical properties listed in Table II, shows a ratio of approximately 2.6 between the stainless steel and aluminum in fatigue limit, and 0.9 in yield strength (the similar ratios between stainless steel and carbon steel are 1.4 and 1.23, respectively). Referring to the bubble energy spectrum model, Figure 33, the corresponding difference in damage intensities is explained by the considerable difference in threshold energy quanta necessary to be delivered by a bubble. Presumably this threshold would be a positive function of fatigue and/or yield strength. However, the proportionate number of bubbles possessing such quanta is unknown unless the shape of the spectrum curve is known. In addition to the above mechanical effects, it is believed that corrosion (as previously discussed) may play a large role in the damage on aluminum and carbon steel.

As previously indicated the carbon steel and stainless steel (Table II) are fairly close in physical properties, although the strength and hardness of the stainless steel are somewhat greater. However, the major share of the difference in damage between these is attributed to the much greater corrosivity of the carbon steel.

A final material comparison is that between plexiglass and the others. No long-duration test was made; however, in a 3.5 hour test, the

---

* No longer duration carbon steel runs were made. Even at this duration corrosion was becoming significant.

pitting was much less than that in a similar stainless steel test, and apparently almost non-existent. (The tabulation of pits is difficult because of the transparent nature of the material.) The plexiglass data are not included on the curves because of their limited extent. However, the explanation for the excellent cavitation resistance of the plexiglass is believed to involve its low modulus of elasticity (about $4.5 \times 10^5$ psi). The pressure wave assumed to impinge on the surface, due to the implosion of bubbles, is extremely transient and local, and is not capable of application at high intensity to a surface which distorts easily and substantially. A similar effect has long been known in that rubberizing of steel surfaces prevents cavitation damage.(7)

5. Water Condition

Only very limited data has so far been obtained on the effect of water condition. The most obvious variables to be considered are temperature, gas content, and perhaps pH.* It might be expected that the major effect of an increase of temperature would be an increase in corrosion rates. There would also be some effect due to the change in the physical properties of surface tension, viscosity, bulk modulus, saturated vapor density, thermal conductivity, etc. However, until suitable analyses of the bubble collapse are available, no prediction of effects on this basis can be made. Only a single hot-water test of 1.0 hours duration was made with water at 150°F on stainless steel. It was found that the damage intensity was reduced from the comparable cold

* pH in all tests was about 10 which is typical of boiler feed water.

water tests by about 4%. However, the difference is too small to be significant, since an average percent standard deviation of about 23% was calculated for two pairs of repetitive runs (all that are presently available).

The anticipated effect of gas content is such that its reduction should result in increased wear. In fact, it is well known that the injection of air into a cavitating stream will reduce wear. The mechanism involved is believed to be the reduction of collapse violence if bubbles contain a significant portion of non-condensible gas, as well as a reduction in the bulk modulus of the liquid if the gas is not in solution. However, an opposite trend could be caused by increased oxidation in materials subject to corrosion due to the presence of additional air.

A single comparison was made between water with air content somewhat in excess of saturation ( unsettled tap water), and water deaereated to about 50% of saturation, in a 1.0 hour test with stainless steel and cold water. The damage intensity with tap water was less by about 7% as for the hot water test, so that again the difference is not statistically significant.*

It is planned to explore both of these effects in greater detail when the improved water facility becomes available.

---

* Generally, the water used in the damage tests had an air content near saturation, but had been contained in the facility for a long time so that with no free surface exposed, most of the air was in solution and no free air in process of being entrained. This water is generally partially deaereated, as indicated by a Winkler test for oxygen which showed a very low oxygen content after the water had been in the loop for several days, probably due to oxidation of the steel surfaces. However, the nitrogen is still presumably at saturation for 1 atm.

C. Comparison with Irradiated Specimen Test

The most important error in these experiments is probably in the volume loss calculation. Only 50 pits were studied in detail for which a usable proficorder trace was obtained from 14.[4] Statistically, this is a limited sample. Also, there is uncertainty regarding the equality of the visually-determined pit size (effective area of crater) and that actually existing because of the difficulty of differentiating between depressed and raised portions in the microscope. Since the diameter comes into the weight loss calculations to the 3rd power, an error of possible magnitude in this respect would cause a substantial factor in the calculated result. Furthermore, the pit count involves the polished surface alone which is only about 11.5% of the total area exposed. Although it was assumed that the pitting intensity ( pits per unit area-time) on the polished surface is the same as it is on the sides, detailed examination of four specimens (previously discussed) showed that this was probably not the case. These results indicate that the calculated weight losses are too great by a factor of about 2 on this account. However, this "first approximation" assumption will be maintained until more comprehensive data becomes available.

To check the calculated weight losses, and to develop a technique useful for the future, a test was made with an irradiated stainless steel specimen for approximately 14 hours.[45] The radioactivity in the stream, caused by the eroded particles, was measured as a function of time. The results are compared with data calculated from pit counts in Figure 38. The curves are of very similar shape, being separated by an almost constant factor of about 4.0, which is most

encouraging. However, the irradiated tracer results are higher, so that the error generated if the specimen sides do not incur the same pitting intensity as the polished surface increases the discrepancy.

The possible errors in the pit-count approach have been previously discussed. Unfortunately there is also the possibility of large errors in the irradiated tracer technique as it was used. These involve calibration of standard sample, homogeneity of mixture in fluid throughout the facility, possible settling rates, counting techniques, etc. It is hoped that the method can be refined in future tests so that it will be possible to place confidence in the absolute results attained. For the present, it is impossible to state which of the curves presented in Figure 38 is the more precise, and the degree of discrepancy does not seem surprising. However, the shape of the damage versus time curve as indicated by the pit-count calculations is clearly verified by the test.

Another result of the irradiated tracer test was the verification of the hypothesis of single-event particle removal from the test specimens. By the use of accurately graduated filters,[45] it was ascertained that the size spectrum of the irradiated particles in the stream was approximately the same as that visually determined for the pits.

D. Incubation Period for Cavitation Damage

As previously discussed, various previous investigators have reported the existence of an "incubation period" before cavitation damage was incurred. However, the irradiated tracer test and the pit-counts clearly show that, if there is such a period, it must be well less than one hour even for the present tests with their moderate velocity, on

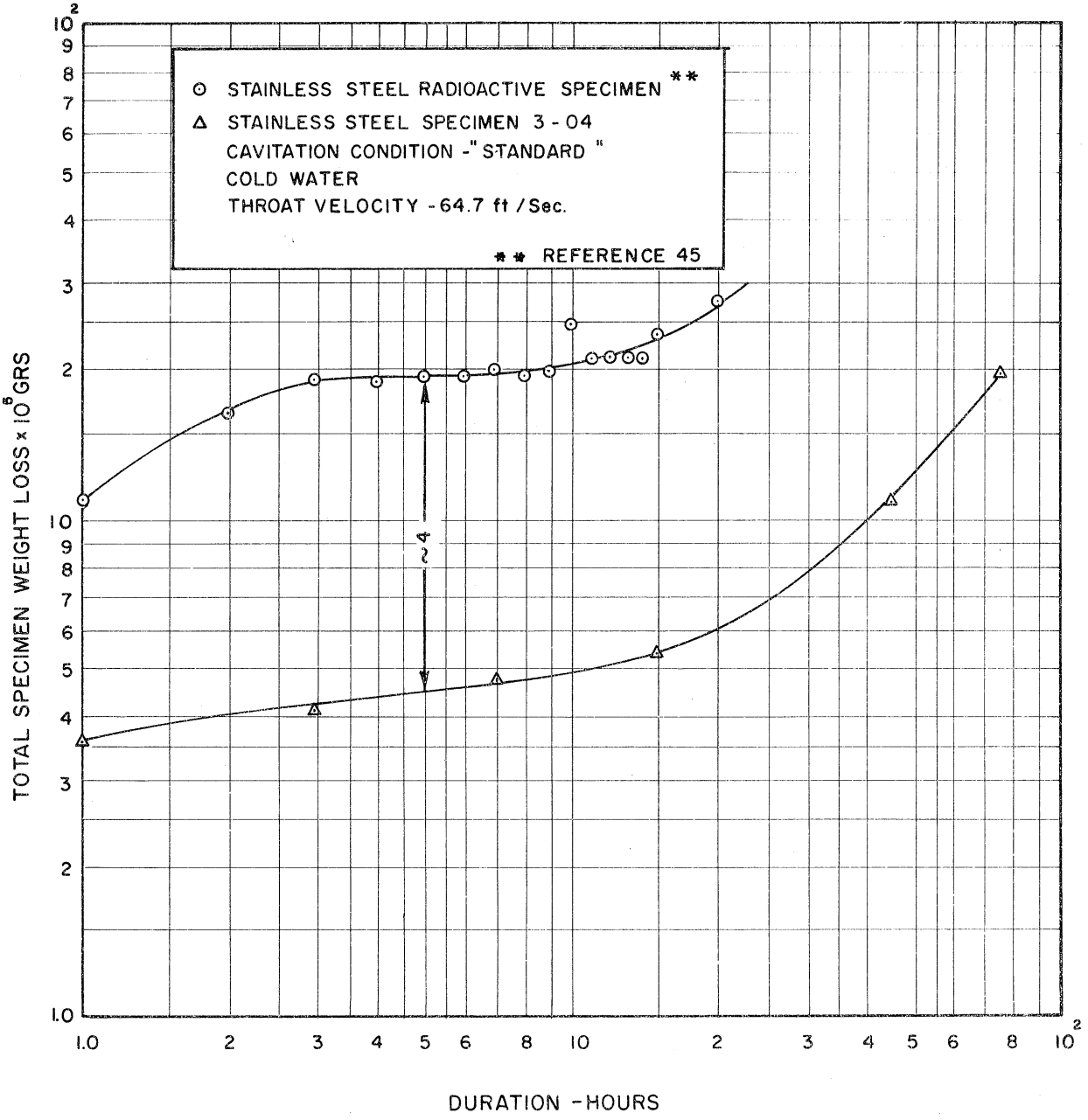


Figure 38. Comparison of the total weight loss from stainless steel specimens as determined by pit counting technique and by radiactive specimen technique.

materials as resistant as stainless steel (usually incubation periods have been reported on the order of minutes to a few hours with magnetostrictive tests where damage is incurred much more rapidly than in flowing systems). The present tests in fact seem to show the opposite trend in that the damage rate is very much greater during the initial portion of the tests than later. However, the absolute quantity of damage during this initial period is small because of its short duration, and, as mentioned previously, it could not be detected by direct weight measurements. This is significant since the previous investigators who reported an incubation period,[4,11,20] relied on such a method of detection. A previous investigation relying on an irradiated paint as tracer[15] did not show an incubation period, nor did that by Knapp and Hollander[16] using pit count data.

It is noted in the damage versus time curves (Figures 27-31) that the initial rapid damage rate is replaced by a much more gradual rate, and finally again by a rapidly accelerating rate. It is believed that the incubation period concept results from a linear extrapolation to zero damage of this second steep portion of the curve. Generally, the damage prior to this period could not have been detected by weight loss, but only by detailed examination of the specimens, or an irradiated tracer method.

## VI. CONCLUSIONS

The major conclusions to be drawn from the investigations described in this report, in the opinion of the authors, are the following:

1. Pits are the result of mechanical action. Two mechanisms are postulated: i) a single event from an extraordinarily strong pressure wave exerted on the surface by bubble implosion; and ii) a fatiguing action resulting from many weaker pressure pulses on the surface. In the present tests the latter mechanism was most important, although the relative importance of these two probably depends upon fluid, material, and test conditions. The mechanical nature of the attack has been proven by the observed presence of slip lines in the matrix of the damaged sample.
2. In some cases, corrosion definitely contributes significantly to the overall damage. The relative contribution of corrosion of course depends upon the material-fluid combination as well as the other cavitation parameters.
3. Microscopic pits (on the order of 10 mils or less in diameter), formed in the early stages of cavitation, do not grow in subsequent testing. Hence, they do not present perferred damage cites. The location of the formation of pits appears, on a microscopic scale, to be entirely random, at least up to that stage where a proportionately small portion of the surface is covered. On a microscopic scale,

the location of fatigue-type pits is probably influenced by surface "weak spots" such as inclusions.

4. Generally, the pits formed in these tests have a width to depth ratio of the order of 10 to 20.

5. Degree of cavitation influences the pitting intensity through two opposing mechanisms:

   i) More developed cavitation means numerically more bubbles in the vicinity of the test specimen.

   ii) Less developed cavitation means higher pressure level in the vicinity of the test section and hence, more driving force for bubble collapse.

6. The damage on the test specimens, located in the venturi, is influenced significantly by local cavitation induced by the test specimens, over and above the general cavitating field.

7. For all the materials tested, the appearance of the cavitation damage is similar.

8. The effect of an increase in throat velocity is to increase the rate of damage. However, no simple formulation seems possible, in view of the actual data and the complexity of the flow phenomenon. In particular, no single approximate value could be assigned to the exponent if a simple exponential dependence were assumed, as it has been by some previous investigators.

   No evidence of a threshold velocity for damage can be deduced from the present tests. However, it is felt that

this is a reasonable hypothesis for cases where the material has appreciable fatigue and yield strength, and corrosion effects are negligible.

9. The non-existence of an incubation period for cavitation damage is clearly indicated in the present tests. Instead, a very rapid damage rate was measured at first (both by irradiated tracer and pit count), followed by a leveling-off period, and then a second accelerating damage rate as the damage begins to cover a substantial portion of the exposed area. It is believed that the linear extrapolation to zero of this second rising portion of the curve has led to previous conclusions of the existence of an incubation period. It is noted that weight losses first become directly measurable at about this point.

10. A surface appearance, similar to that denoted by "temper blueing", is often observed on the steel specimens in regions of severe cavitation pitting.

## VII. BIBLIOGRAPHY ON WORK OF PREVIOUS INVESTIGATORS


1. Ackeret, J. "Experimental and Theoretical Investigations of Cavitation in Water." NACA TM No. 1078, May, 1945.

2. Beeching, R. "Resistance to Cavitation Erosion." Trans. Inst. Engr. and Shipbuilders in Scotland, Vol. 85, April, 1942.

3. Boetcher, H. N. "Failure of Metals Due to Cavitation Under Experimental Conditions." Trans. ASME, Vol. 58, (1936) 355-360.

4. Cramer, V. F. and Hammitt, F. G. Cavitation Pit Diameter-Depth Observation for Stainless Steel in Water. Internal Report No. 9, ORA Project 03424, University of Michigan.

5. Ellis, A. T. "Production of Accelerated Cavitation Damage by Acoustic Field in Cylindrical Cavity." Acoustical Society of America, Journal, Vol. 27, No. 5, (Sept., 1955) 913-921.

6. Gilmore, F. R. "Growth or Collapse of Spherical Bubble in Viscous, Compressible Liquid." Heat Transfer, Fluid Mechanics Institute, Stanford University Press, (1952) 53-64; also CIT Report No. 26-4, April 1, 1952.

7. Godfrey, D. J. "Cavitation Damage - A Review of Present Knowledge." Chemistry and Industry, (June 6, 1959) 686-691.

8. Hammitt, F. G., et. al., Fluid Dynamic Performance of a Cavitating Venturi - Part I. Progress Report 03424-2-T, University of Michigan.

9. Hammitt, F. G. Observation of Cavitation Scale and Thermodynamic Effects in Stationary and Rotating Components. June, 1961, Project 03424 Internal Report No. 7 (To be presented ASME Hydraulics Conference, May, 1962).

10. Hammitt, F. G., Chu, P. T., Cramer, V. F. and Wakamo, C. L. Observations and Measurements of Flow in a Cavitating Venturi. Internal Report No. 6, ORA Project 03424, University of Michigan, April 25, 1961.

11. Hobbs, J. M. Problems of Predicting Cavitation Erosion From Accelerated Tests. ASME Paper No. 61-Hyd-19, 1961.

12. Hunsaker, J. C. "Cavitation Research." Mechanical Engineering, (April, 1935) 211-216.

13. Jones, I. R. and Edwards, D. H. "An Experimental Study of the Forces Generated by the Collapse of Transient Cavities in Water." J. Fluid Mech., Vol. 7, (1960) 596-609.

14. Kerr, S. L. "Determination of the Relative Resistance to Cavitation-Erosion by the Vibratory Method." Trans. ASME, Vol. 59, No. 4, (1937) 373-395.

15. Kerr, S. L. and Rosenberg, K. "An Index of Cavitation Erosion by Means of Radioisotopes." ASME Trans., Vol. 80, (1958) 1308-1314.

16. Knapp, R. T. and Hollander, A. "Laboratory Investigations of Mechanism of Cavitation." Trans. ASME, Vol. 70, No. 5, (July, 1948) 418-35.

17. Knapp, R. T. "Recent Investigations of the Mechanics of Cavitation and Cavitation Damage." Trans. ASME, (Oct., 1955) 1045-1054.

18. Knapp, R. T. "Accelerated Field Tests of Cavitation Intensity." Trans. ASME, Vol. 80, No. 1, (Jan., 1958) 91-102.

19. Kornfeld, M. and Suvorov, L. "On the Destruction Action of Cavitation." J. Appl. Physics, Vol. 15, (June, 1944) 495-506.

20. Leith, E. C. and Thompson, A. L. "Some Corrosion Effects in Accelerated Cavitation Damage." J. Basic Engr., Dec., 1960.

21. Leith, W. C. Cavitation Damage of Metals. Ph.D. Thesis, McGill University, March, 1960.

22. Lichtman, J. Z., Kallas, D. H. and Chatten, C. K. "Study of Damaging Effects of Cavitation Erosion to Ships' Underwater Structures." Trans. ASME, Vol. 80, No. 6, (Aug., 1958) 1325-1339.

23. Morgan, J. H. Discussion on Reference 36.

24. Mousson, J. M. "Pitting Resistance of Metals Under Cavitation Conditions." Trans. ASME, Vol. 59, (1937) 399-408.

25. Naude, C. F. and Ellis, A. T. "On the Mechanism of Cavitation Damage by Non-Hemispherical Cavities Collapsing in Contact with a Solid Boundary." Trans. ASME, J. Basic Engr., Vol. 83, Series D. No. 4, (Dec., 1961) 648-656.

26. Nechleba, M. "Das Problem der Kavitation." Maschinenbautechnik, Vol. 2, (1955) 81.

27. Nowotny, H. Werkstoffzerstorung durch Kavitation. published by V.D.I. - Verlag Gimbh, Berlin, NW 7, 1942, English Translation published by Edwards Brothers, Ann Arbor, Michigan, 1946.

28. Parsons, Sir Charles and Cook, S. S. Trans. of Inst. of Naval Arch., Vol. 61, p. 223, Appendix II, 1919 (Reference quoted by Silver[41]).

29. Petracchi, C. "Intorno All Interpetazione del Processo di Corrosione per Cavitazione." La Metallurgia Italiana, Vol. 41, No. 1, (1949) 1-6; Engineer's Digest, Vol. 10, No. 9, (Sept., 1949) 314.

30. Plesset, M. S. "Dynamics of Cavitation Bubbles." ASME Trans. (J. Appl. Mech.), Vol. 16, No. 3, (Sept., 1949) 277-282.

31. Plesset, M. S. and Ellis, A. T. "On Mechanism of Cavitation Damage." ASME Trans., Vol. 77, No. 7, (Oct., 1955) 1055-64.

32. Plesset, M. S. Personal communication to F. G. Hammitt, Dec., 1960.

33. Plesset, M. S. and Michell, T. P. "On the Stability of the Spherical Shape of a Vapor Cavity in a Liquid." Quar. Appl. Math., Vol. XIII, No. 4, (Jan., 1956) 420-430.

34. Poritsky, H. "The Collapse or Growth of a Spherical Bubble or Cavity in a Viscous Fluid." Proc. First U.S., Nat. Cong. Appl. Mech., ASME, (1952) 813-821.

35. Poulter, T. C. "The Mechanism of Cavitation Erosion." Journal Applied Mechanics, (March, 1942) A-31 - A-195.

36. Prieser, H. S. and Tytell, B. H. "The Electrochemical Approach to Cavitation Damage and Its Prevention." Corrosion - National Association of Corrosion Engineers. Vol. 17, (1961) 107-121.

37. Rao, N. S. G., et al. "Prediction of Cavitation Damage." J. Hyd. Div., Proc. ASCE, (Sept., 1961) 37-62.

38. Rayleigh, Lord. "On the Pressure Developed in a Liquid During the Collapse of a Spherical Cavity." Scientific Papers, Vol. 6, p. 504-507.

39. Rheingans, W. J. "Accelerated-Cavitation Research." Trans. ASME, Vol. 72, (1950) 705-724.

40. Schroeter, H. "Werkstoffzerstorung bei Kavitation." Zeitschrift V.D.I., Vol. 78 (March, 1934) 349-351.

41. Silver, R. S. "Theory of Stress Due to Collapse of Vapour Bubbles in a Liquid." Engineering, p. 501-502.

42. Taylor, I. "Cavitation Pitting by Instantaneous Chemical Action From Impacts." ASME Paper No. 54-A-109.

43. Trilling, L. "The Collapse and Rebound of a Gas Bubble." J. Appl. Phys., Vol. 23, No. 1 (Jan., 1952) 14-17.

44. Walsh, W. J. Analysis of Proficorder Data for Cavitation Pits. Internal Report No. 2, ORA Project 03424, University of Michigan.

45. Walsh, W. J. and Hammitt, F. G. Cavitation and Erosion Damage Measurements with Radioisotopes. Internal Report No. 4, ORA Project 03424, Nucl. Eng. Dept., University of Michigan; also Trans. ANS, Vol. 4, No. 2 (Nov., 1961) 247; to be published, Nucl. Sci. and Eng.

46. Wheeler, W. H. "Indentation of Metals by Cavitation." Trans. ASME, J. Basic Engr., (March, 1960) 184-194.

47. Wislicenus, G. F. Fluid Mechanics of Turbo Machinery. McGraw-Hill Book Company, Inc., (1947) 74.

# VIII. APPENDIX

## A. Specification of Cavitation Conditions

The cavitation condition for all tests is defined in terms of "degree of cavitation", referring (except for initiation) to the extent of the cavitating region.

i) Sonic Initiation - First sonic manifestation beyond that of single phase flow. This was detected either by ear or electronically using a piezoelectric crystal. The results of these two methods were approximately the same. In all cases, sonic initiation occurred at a higher throat pressure than visible initiation.

ii) Visible Initiation - First appearance of a more or less complete ring of cavitation. This always appears first at the throat exit.

iii) Cavitation to Nose - The approximate location of the termination of the cavitation region is at the upstream nose of the test specimen.

iv) Standard - The approximate location of the termination of the cavitation region is at the center of the test specimen.

v) First Mark - The approximate location of the termination of the cavitation region is about 1-3/4 inches from the throat outlet.

The location of these termination points is shown to scale in Figure 1. Although the termination is not sharp, the cavitation conditions can be quite precisely reproduced.

B. Standard Deviation of Volume Loss Per Unit Surface Area

The standard deviation is given by

$$\sigma^2 = \sum_{i=1}^{n} \frac{(\bar{V} - V_i)^2}{n - 1}$$

where:

$\sigma$ = standard deviation

$V_i$ = volume loss per unit area for the i-th specimen

$n$ = number of specimens under identical conditions

$\bar{V}$ = average of $V_i = \sum_{i=1}^{n} V_i/n$

Stainless Steel

Standard Cavitation Condition

Velocity = 64.7 ft/sec

Duration = 3.5 hours

| Specimen Number | $V_i$ ($cm^3/cm^2 \times 10^6$) |
|---|---|
| 3-14 | 2.44 |
| 3-15 | 2.24 |
| 3-04 | 2.50 |
| 3-05 | 1.95 |

$\bar{V} = 2.28 \times 10^{-6}$ $cm^3/cm^2$

$\sigma = 0.248 \times 10^{-6}$ $cm^3/cm^2$

% Std. Deviation $= \frac{24.8}{2.28} = 10.9\%$

Aluminum

Standard Cavitation Condition

Velocity = 96.2 ft/sec

Duration = 5 minutes

| Specimen Number | $V_i$ ($cm^3/cm^2 \times 10^6$) |
|---|---|
| 2-04 | 3.35 |
| 2-07 | 7.03 |
| 2-10 | 11.19 |
| 2-13 | 0.784 |

$\overline{V} = 5.59 \times 10^{-6}$ $cm^3/cm^2$

$\sigma = 2.04 \times 10^{-6}$ $cm^3/cm^2$

% Std. Deviation $= \frac{204.}{5.59} = 36.6\%$